NASA TECHNICAL NOTE

NASA TN D-8234 c.1

LOAN COPY: TO
AFWL TECHNIC
KIRTLAND A

TECH LIBRARY KAFB, NM
0133764

NASA TN D-8234

AN ANALYTICAL STUDY AND WIND-TUNNEL TESTS OF AN AEROMECHANICAL GUST-ALLEVIATION SYSTEM FOR A LIGHT AIRPLANE

Eric C. Stewart

Langley Research Center
Hampton, Va. 23665

21 SEP 1976
Technical Library
AF Weapons
Laboratory

NATIONAL AERONAUTICS AND SPACE ADMINISTRATION • WASHINGTON, D. C. • AUGUST 1976

TECH LIBRARY KAFB, NM
0133964

1. Report No.	2. Government Accession No.	3. Recipient's Catalog No.
NASA TN D-8234		

4. Title and Subtitle	5. Report Date
AN ANALYTICAL STUDY AND WIND-TUNNEL TESTS OF AN AEROMECHANICAL GUST-ALLEVIATION SYSTEM FOR A LIGHT AIRPLANE	August 1976
	6. Performing Organization Code

7. Author(s)	8. Performing Organization Report No.
Eric C. Stewart	L-10635
	10. Work Unit No.
9. Performing Organization Name and Address	505-10-11-02
NASA Langley Research Center Hampton, Va. 23665	11. Contract or Grant No.
	13. Type of Report and Period Covered
12. Sponsoring Agency Name and Address	Technical Note
National Aeronautics and Space Administration Washington, D.C. 20546	14. Sponsoring Agency Code

15. Supplementary Notes

16. Abstract

An aeromechanical gust-alleviation system to reduce the normal accelerations of light airplanes in turbulent air has been proposed. This report gives the results of an analytical study of such a system using stability derivatives determined in static wind-tunnel tests of a 1/6-scale model of a popular, high-wing, light airplane equipped with the gust-alleviation system. The results of the wind-tunnel tests, including static measurements of the effects of the alleviation system, are presented. The analysis concentrates on the longitudinal short-period mode dynamics of the system and includes root loci, airplane frequency responses to vertical gusts, power spectra of the airplane responses in a von Karman gust spectrum, time-history responses to vertical gusts, and handling characteristics. The system reduces the airplane's normal acceleration response to vertical gusts while simultaneously increasing the pitching response and reducing the damping of the longitudinal short-period mode. The normal acceleration response can be minimized by using the proper amount of static alleviation and a fast response system with a moderate amount of damping. The addition of a flap-elevator interconnect or a pitch damper system further increases the alleviation while moderating the simultaneous increase in pitching response. The system provides direct lift control and may reduce the stick-fixed longitudinal static stability.

17. Key Words (Suggested by Author(s))	18. Distribution Statement
Gust alleviation Light airplane Gust response Turbulence	Unclassified – Unlimited Subject Category 01

19. Security Classif. (of this report)	20. Security Classif. (of this page)	21. No. of Pages	22. Price*
Unclassified	Unclassified	80	$4.75

*For sale by the National Technical Information Service, Springfield, Virginia 22161

AN ANALYTICAL STUDY AND WIND-TUNNEL TESTS OF AN AEROMECHANICAL GUST-ALLEVIATION SYSTEM FOR A LIGHT AIRPLANE

Eric C. Stewart
Langley Research Center

SUMMARY

An aeromechanical gust-alleviation system to reduce the normal acceleration of light airplanes in turbulent air has been proposed. The proposed system uses auxiliary aerodynamic surfaces to drive the trailing-edge flaps and keep the lift constant. This report gives the results of an analytical study of the system using stability derivatives determined in static wind-tunnel tests on a 1/6-scale model of a popular high-wing light airplane equipped with the gust-alleviation system. The results of the wind-tunnel tests, including static measurements of the effects of the alleviation system and hinge moments produced by the auxiliary surfaces, are presented. The analysis concentrates on the longitudinal short-period mode dynamics of the system and includes root loci, airplane frequency response to vertical gusts, power spectra of the airplane response in a von Karman gust spectrum, time-history responses to vertical gusts, and handling characteristics. Also included is a short analysis of unsteady lift effects. The uncertainty in the analytical results due to experimental error in the parameters determined in the wind-tunnel tests is determined. The system reduces the airplane's normal acceleration response to vertical gusts while simultaneously increasing the pitching response and reducing the damping of the longitudinal short-period mode. The normal acceleration response can be minimized by using the proper amount of static alleviation and a fast response system with a moderate amount of damping. The addition of a flap-elevator interconnect or a pitch rate damper system further increases the alleviation while reducing the simultaneous increase in pitching response. The alleviation system provides direct lift control and may reduce the stick-fixed longitudinal static stability.

INTRODUCTION

The ride of a light airplane is often rough in windy weather due to the airplane's excessive responsiveness to turbulence. The normal acceleration responses are especially large because of the low wing loadings of light airplanes. One possible solution

for this problem would be to use wings which have a higher loading at cruise as suggested in reference 1. However, the wing loading would have to be increased by at least the same amount as the desired decrease in average normal acceleration, and full-span flaps would be required to maintain the low landing speeds characteristic of light airplanes. Another method which theoretically can decrease the vertical gust response to zero (ref. 2) is to drive control surfaces on the wing (for example, flaps) as a function of the gusts to negate the changes in lift on the wing. Such a system requires a gust sensor, powered actuators, and possibly a feedback control system. The actuators not only have to be powerful enough to overcome the hinge moments of the control surfaces, but also fast enough to follow the rapidly changing gusts. Alternatively, an aeromechanical gust-alleviation system was developed and successfully tested some years ago. (See ref. 3.) That system used modified horizontal-tail surfaces to drive the flaps mechanically and thus used the energy in the gusts themselves as the power source. Recently, a variation of this approach has been proposed for light airplanes. This variation uses two auxiliary aerodynamic surfaces mounted on either side of the fuselage to drive the flaps. Thus, the system does not require modification to the horizontal-tail surfaces while retaining the fundamental advantages of simplicity and easy maintenance.

An analysis of the proposed system on a popular high-wing light airplane has been performed in reference 4. That analysis used stability derivatives determined by methods described in reference 5 and devoted much effort to the phugoid response. The system was also described briefly and preliminary results were presented in reference 6. The present analysis, while ignoring the phugoid response, uses stability derivatives determined from static wind-tunnel tests and studies several other areas in greater detail. The static wind-tunnel tests were conducted on a 1/6-scale model of the subject light airplane equipped with the proposed alleviation system.

Tests were conducted to (1) determine the parameters necessary for the analytical study, (2) demonstrate the static effectiveness of the system in maintaining constant lift as the angle of attack changed, and (3) determine the hinge-moment characteristics of the alleviation system's aerodynamic surfaces. A determination of the experimental uncertainty in the parameters used in the analytical study was made.

The analytical study employed several different types of calculations including (1) root locus, (2) frequency response of the airplane to both vertical gusts and elevator control inputs, (3) power spectra of the airplane's response by assuming a von Karman gust spectrum, (4) time-history responses to step vertical gusts and step elevator inputs, and (5) the elevator position required for trimmed flight at different lift coefficients. One or more of these types of calculations were used to study several different subjects related to an evaluation of the performance of the gust-alleviation system. The different subjects were as follows: (1) unsteady lift effects, (2) the impact of experimental

uncertainty in the aerodynamic parameters, (3) variation of the static vertical alleviation factor, (4) variation of the flap natural frequency and damping ratio, (5) variation of center-of-gravity location, (6) passenger location relative to airplane center of gravity, (7) the addition of a flap-elevator interconnect or a pitch damper, and (8) the airplane's handling characteristics.

SYMBOLS

$A, B, C,$
a, ϕ, ω_n, ζ — unsteady lift transfer function parameters (appendix B)

a — pitch damper gain, sec^2

b_f — span of flap, m

b_v — span of vane, m

C_D — drag coefficient, $\frac{D}{\frac{1}{2}\rho V^2 S}$

C_h — hinge-moment coefficient referred to flap hinge line, $\frac{H}{\frac{1}{2}\rho V^2 S_f c_f}$

C_L — lift coefficient, $\frac{L}{\frac{1}{2}\rho V^2 S}$

C_m — pitching-moment coefficient, $\frac{M}{\frac{1}{2}\rho V^2 Sc}$

C_Z — vertical-force coefficient, $\frac{Z}{\frac{1}{2}\rho V^2 S}$

c — mean aerodynamic chord, m

c_f — flap chord, m

D — drag, N-m

g — acceleration of gravity, 9.81 m/sec^2

H — hinge moment, N-m

I_f flap inertia about flap axis, kg-m^2

I_v vane inertia about vane hinge line, kg-m^2

i incidence of vane relative to local angle of attack due to trim control, rad (see accompanying definitions for eq. (A1))

i_r ratio of flap inertia to flap plus reflected vane inertia (see eq. (A13))

K negative of ratio of flap-deflection change to angle-of-attack change, $-\frac{\Delta\delta_f}{\Delta\alpha}$

K_H static horizontal gust-alleviation factor

K_o loading spring torque at zero flap deflection, N-m

K_s loading spring gradient, N-m/rad

K_V static vertical alleviation factor (see appendix A)

K_y ratio of radius of gyration to mean aerodynamic chord, $\frac{k_y}{c}$

k_y radius of gyration in pitch, m

L lift, N

ℓ scale of turbulence, m

l ratio of tail length to mean aerodynamic chord of wing

l_n effective vane length (see eq. (A13))

l_p longitudinal distance behind center of gravity, m

l_v longitudinal distance from airplane center of gravity to vane quarter chord (vane length), m

M pitching moment, N-m

m	mass of airplane, kg; also ratio of change in flap deflection to change in elevator deflection in steady state (see eq. (A13))
m'	ratio of vane incidence change to elevator deflection change (see accompanying definitions for eq. (A1))
n	normal acceleration, positive downward, g units
q	pitching velocity, rad/sec; also dynamic pressure, N/m^2
q_f	flap equation factor, $\frac{1}{2}\rho V^2 S_f c_f$, N-m
S	area of wing, m^2
S_f	area of flap, m^2
s	Laplace variable, sec^{-1}
t	time, sec
$u_s(t)$	unit step function (appendix B)
V	true velocity with respect to undisturbed air mass, m/sec
w_o	increment in vertical velocity with respect to undisturbed air mass, m/sec
Z	vertical force, positive downward, N
α	angle of attack, rad or deg
α_o	increment in angle of attack with respect to undisturbed air, $\frac{w_o}{V}$, rad
γ	gearing ratio, $\frac{\Delta\delta_v}{\Delta\delta_f}$
γ_m	gearing ratio, $\frac{\delta_e}{\delta_f}$
$\delta(t)$	unit impulse function (appendix B)
δ_e	elevator deflection assuming trim position is zero, positive when trailing edge is down, rad or deg

δ_f flap deflection, positive when trailing edge is down, rad or deg

δ_v vane dihedral deflection angle, positive when outboard end is down, rad

ϵ downwash angle, positive downward, rad

ζ flap-vane damping ratio

θ increment in pitch angle, positive nose up, rad

μ relative density factor, $\frac{m}{\rho Sc}$

ρ density of air, kg/m^3

σ real part of characteristic root, rad/sec; also root-mean-square gust velocity, 2.83 m/sec

$\Phi_n(\omega)$ normal acceleration power spectral density, $(g/rad)^2/rad/sec$

$\Phi_q(\omega)$ pitch-rate power spectral density, $(rad/sec/rad)^2/rad/sec$

ϕ total incidence of vane relative to local angle of attack (see eq. (A3)), rad

ω imaginary part of characteristic root, rad/sec; also frequency, rad/sec

ω_n natural frequency, rad/sec

Subscripts:

f flap

g gust

pd pitch damper

t tail

w wing fuselage

A bar over a symbol denotes the Laplace transform of a variable. Primes denote an alleviated parameter. Dots over symbols denote derivatives with respect to time.

Stability derivatives are indicated by subscript notation; for example,

$$C_{Z_\alpha} = \frac{\partial C_Z}{\partial \alpha}, \quad C_{m_q} = \frac{\partial C_m}{\partial\left(\frac{qc}{2V}\right)}.$$

DESCRIPTION OF SYSTEM

A sketch of the basic components of the system is presented in figure 1. Two auxiliary aerodynamic surfaces, or vanes, are mounted on either side of the fuselage near the wing. These vanes are hinged about a chordwise axis adjacent to the fuselage and change their dihedral angle in response to gusts as shown in the front view of figure 1. The vanes are also hinged about a spanwise axis (side view of fig. 1) to change their angle of incidence as a function of stick position in order to provide pilot control. As the vanes move upward (increase their dihedral) in response to an upgust, the flaps are deflected upward by the flap-vane linkage. The flaps decrease the lift on the wing by an amount almost equal to the increase in lift on the wing due to the gust which caused the vane dihedral deflection. In this way the lift on the airplane is maintained relatively constant regardless of the gust encountered by the airplane. Both vanes and both flaps are interconnected so that they deflect together symmetrically to prevent the system from producing rolling moments.

This gust-alleviation system achieves its alleviation by reducing the lift-curve slope of the airplane to a small value so that there are small changes in lift due to gust-induced angles of attack. This low response to changes in angle of attack practically eliminates the pilot's ability to change the flight path by using the elevator unless some sort of compensation is provided. The spanwise pivot axis for changing vane incidence and the pilot's control linkage shown in the side view of figure 1 are provided for this purpose. As the elevator is deflected, the vane is rotated about its quarter chord line by an angle equal to, but in the opposite direction from, the change in angle of attack commanded by the elevator deflection. The steady-state angle of attack of the vane is, therefore, constant; and, except for transients, the flap does not respond to changes in angle of attack due to elevator control inputs. However, the flaps still respond to changes in angle of attack due to gusts.

A loading spring is provided so that the vanes do not have to operate at a near zero angle of attack in order to maintain the flap equilibrium position at zero deflection. At a zero vane angle of attack the vane will be generating drag but no lift and will therefore unnecessarily penalize the airplane's performance. The lift on the vane at a positive

vane angle of attack must be balanced by the loading spring in order to keep the flap deflection at the center zero position for the trimmed flight condition in the absence of gusts. If the flight condition changes, either the spring preload or the vane incidence relative to the airplane must be readjusted to reposition the flap to zero deflection for the new angle of attack of the airplane. A positive vane angle of attack results in the system alleviating horizontal gusts as well as vertical gusts since the lift on the vanes will change with airspeed. However, horizontal gusts are of much less importance than vertical gusts except for low-speed approaches.

EQUATIONS OF MOTION

Basic Equations

The following equations are based primarily on the mathematical model of reference 2 with a different flap equation to account for the response of the flap-vane system. The equations are perturbation equations in which α_o, θ, δ_f, α_g, and δ_e are assumed to be zero at the equilibrium condition.

Z-force equation:

$$\left[\frac{c}{V}s\left(-2\mu + \frac{\partial\epsilon}{\partial\alpha}lC_{Z_{\alpha_t}}\right) + C_{Z_{\alpha_w}} + C_{Z_{\alpha_t}} - \frac{\partial\epsilon}{\partial\alpha}C_{Z_{\alpha_t}}\right]\bar{\alpha}_o + \left[s\frac{c}{V}\left(2\mu + lC_{Z_{\alpha_t}}\right)\right]\bar{\theta}$$

$$+ \left\{s\frac{c}{V}\left(\frac{\partial\epsilon}{\partial\delta_f}C_{Z_{\alpha_t}}l\right) + \left[-\frac{\partial\epsilon}{\partial\delta_f}C_{Z_{\alpha_t}} + \left(C_{Z_{\delta_f}}\right)_w\right]\right\}\bar{\delta}_f$$

$$= \left[\frac{c}{V}s\left(lC_{Z_{\alpha_t}} - \frac{\partial\epsilon}{\partial\alpha}lC_{Z_{\alpha_t}}\right) + \left(-C_{Z_{\alpha_w}} - C_{Z_{\alpha_t}} + \frac{\partial\epsilon}{\partial\alpha}C_{Z_{\alpha_t}}\right)\right]\bar{\alpha}_g + \left[-\left(C_{Z_{\delta_e}}\right)_t\right]\bar{\delta}_e \qquad (1a)$$

Pitching-moment equation:

$$\left[\frac{c}{V}s\left(\frac{\partial\epsilon}{\partial\alpha}lC_{m_{\alpha_t}}\right) + \left(C_{m_{\alpha_w}} + C_{m_{\alpha_t}} - \frac{\partial\epsilon}{\partial\alpha}C_{m_{\alpha_t}}\right)\right]\bar{\alpha}_o + \left[\left(\frac{c}{V}\right)^2 s^2\left(-2\mu K_y^2\right)\right.$$

$$\left. + \frac{c}{V}s\left(lC_{m_{\alpha_t}}\right)\right]\bar{\theta} + \left\{\frac{c}{V}s\left(\frac{\partial\epsilon}{\partial\delta_f}lC_{m_{\alpha_t}}\right) + \left[-\frac{\partial\epsilon}{\partial\delta_f}C_{m_{\alpha_t}} + \left(C_{m_{\delta_f}}\right)_w\right]\right\}\bar{\delta}_f$$

$$= \left[\frac{c}{V}s\left(lC_{m_{\alpha_t}} - \frac{\partial\epsilon}{\partial\alpha}lC_{m_{\alpha_t}}\right) + \left(-C_{m_{\alpha_w}} - C_{m_{\alpha_t}} + \frac{\partial\epsilon}{\partial\alpha}C_{m_{\alpha_t}}\right)\right]\bar{\alpha}_g + \left[-\left(C_{m_{\delta_e}}\right)_t\right]\bar{\delta}_e \qquad (1b)$$

Flap hinge-moment equation:

$$\left(K\omega_n^2\right)\bar{\alpha}_o + \left(i_r s^2 - K\omega_n^2 \frac{l_n}{V} s\right)\bar{\theta} + \left(s^2 + 2\zeta\omega_n s + \omega_n^2\right)\bar{\delta}_f = \left(-K\omega_n^2\right)\bar{\alpha}_g + \left(\omega_n^2 m\right)\bar{\delta}_e \qquad (1c)$$

The flap equation (eq. (1c)) is developed fully in appendix A (eq. (A13)). The natural frequency and damping ratio of the flap-vane system are designated ω_n and ζ, respectively. Also shown in appendix A is the static alleviation factor K_V which is related to K as follows:

$$-\frac{\Delta\delta_f}{\Delta\alpha} = K = K_V\left(\frac{C_{L_\alpha}}{C_{L_{\delta_f}}}\right) \qquad (2)$$

The results which are presented herein will be in terms of the static alleviation factor K_V. When $K_V = 0$, there is no alleviation; and when $K_V = 1.0$, the static lift-curve slope is zero.

Two equations are added to calculate the pitching rate and normal acceleration,

$$\bar{q} = s\bar{\theta}$$

$$\bar{n} = \frac{V}{g} s\left(\bar{\alpha}_o - \bar{\theta}\right) - \frac{l_p s\bar{q}}{g}$$

where l_p is the longitudinal distance between the center of gravity and the passenger location. In all but one case l_p is equal to zero so that $\bar{n}$ is the acceleration at the center of gravity.

Equations (1) and these two equations were solved on a high-speed digital computer to produce (1) the roots of the characteristic equation, (2) the frequency response of the airplane with respect to gust and elevator forcing functions, and (3) time-history responses to step inputs of gust and the elevator.

Power spectra of the normal acceleration and pitching responses were calculated by using the von Karman gust representation as follows:

$$\Phi_n(\omega) = \left|\frac{n}{\alpha_g}(\omega)\right|^2 \frac{\sigma^2 \ell}{2\pi V^3} \frac{1 + \frac{8}{3}\left(1.339\ell\frac{\omega}{V}\right)^2}{\left[1 + \left(1.339\ell\frac{\omega}{V}\right)^2\right]^{11/6}}$$

and

$$\Phi_q(\omega) = \left|\frac{q}{\alpha_g}(\omega)\right|^2 \frac{\sigma^2 \ell}{2\pi V^3} \frac{1 + \frac{8}{3}\left(1.339\ell\frac{\omega}{V}\right)^2}{\left[1 + \left(1.339\ell\frac{\omega}{V}\right)^2\right]^{11/6}}$$

where

σ = 2.83 m/sec

ℓ = 300 m

V = 59 m/sec

In this analysis the square root of the power spectrum rather than the power spectrum is used in order to get the values proportional to the acceleration or pitching rate. Values proportional to the acceleration or pitching rate are thought to be more appropriate because the acceleration and pitching rate have more intuitive meaning to a passenger than acceleration squared or pitching rate squared.

The square root of the area under the power spectrum curve up to a frequency of 20 rad/sec is taken to be the root-mean-square response of the airplane herein. Theoretically, the area should be determined for frequencies to infinity. However, the truncated area described above is used because of limitations of the mathematical model which are described next.

Unsteady Lift Effects

Equations (1) do not represent the motions of the airplane well for high frequencies because they assume that lift is generated instantaneously and that part of the lift is proportional to the frequency. In reality, it takes some time for lift to be generated after the angle of attack or flap deflection changes, and the terms which are proportional to frequency are a crude approximation for the lift due to the lag in the wing and flap downwash on the tail. In appendix B these time-dependent effects are approximated more accurately by some simple combinations of first-order and second-order functions. These functions make the lift build up to its full value over the time it takes to transverse a few chord lengths and eliminate the terms proportional to the frequency while maintaining a linear set of equations. The lift due to the lag in the downwash on the tail is approximated by a short-time-constant first-order function combined with a long-response-time second-order function. The first-order function has a sign opposite that of the second-order function and is used to represent the upwash due to the vortex shed off the trailing edge

of the wing after an angle-of-attack or flap-deflection change. The second-order function is used (in conjunction with the final value of the first-order function) to represent the final value of the downwash angle.

Flap-Elevator Interconnect and Pitch Rate Damper

Two possible methods of increasing the effectiveness of the alleviation and reducing the pitch responses were investigated. The first was a flap-elevator interconnect to change the flap pitching-moment characteristics, and the second was a pitch rate damper. (See fig. 2.) The flap-elevator interconnect was assumed to make the elevator deflection a function of the flap deflection by a mechanical link so that

$$\delta_e = \gamma_m \delta_f$$

where γ_m was the gearing ratio. When the flap-elevator interconnect is investigated, it is assumed that the vane incidence does not change with an elevator deflection caused by a flap deflection. This assumption can be realized physically by holding the control stick fixed. The pilot will be able to feel the reaction of the forces in the linkages. These forces may be objectionable; in which case, a separate aerodynamic surface instead of the elevator may be required. The elevator was used herein only because its aerodynamic effectiveness was already known.

When the pitch rate damper was used, it was assumed to act through the simple control law

$$\frac{\bar{\delta}_e}{\bar{q}} = \frac{0.125a\omega_{n_{pd}}^2}{s^2 + 1.4\omega_{n_{pd}}s + \omega_{n_{pd}}^2}$$

where a and $\omega_{n_{pd}}$, the gain and natural frequency, were variable. The constant in front of a was inserted so that when $a = 1$, the steady-state elevator position for a given pitch rate produced the same pitching moment as that produced by the airplane's basic pitch rate damping. As with the flap-elevator interconnect, it was assumed that an elevator deflection caused by the pitch rate damper does not change the vane incidence.

Static Stability Equations

The effective C_{m_α} of the airplane with the system active (designated C'_{m_α}) is a function of the C_{m_α} of the unalleviated airplane and the pitching-moment coefficient of the flap. It can be determined from equations 1(b) and 1(c) by assuming $\bar{\delta}_e = \bar{\theta} = 0$, dropping the dynamic terms (terms including the Laplace variable s), and eliminating $\bar{\delta}_f$,

$$C'_{m_\alpha} = \left[C_{m_{\alpha_w}} + C_{m_{\alpha_t}} - \frac{\partial \epsilon}{\partial \alpha} C_{m_{\alpha_t}}\right] - K\left[\left(C_{m_{\delta_f}}\right)_w - \frac{\partial \epsilon}{\partial \delta_f} C_{m_{\alpha_t}}\right] \tag{3a}$$

or

$$C'_{m_\alpha} = C_{m_\alpha} - KC_{m_{\delta_f}} \tag{3b}$$

where the terms in the brackets have been replaced with C_{m_α} and $C_{m_{\delta_f}}$, respectively. When the flap-elevator interconnect was used, the effective pitching-moment coefficient of the flap was modified so that the equation was

$$C'_{m_\alpha} = C_{m_\alpha} - K\left[C_{m_{\delta_f}} + \gamma_m\left(C_{m_{\delta_e}}\right)_t\right] \tag{4}$$

Stick-Fixed Handling Characteristics

Satisfactory static stability of an airplane does not insure that the stick-fixed handling characteristics will also be satisfactory. That is, a negative (stable) C'_{m_α} does not insure that the slope of the curve of trimmed elevator position against lift coefficient will be negative (stable). The slope of the curve for elevator position against lift coefficient (called the stick-fixed handling characteristic herein) must be determined separately from the static stability. This determination was made by (1) eliminating the dynamic terms in equations (1), (2) dropping the Laplace transform notation for α, δ_f, and δ_e, (3) adding a term to the lift equation to account for the weight of the airplane, (4) reinserting the total angle of attack in place of the perturbation angle of attack, and (5) adding a term C_{m_o} to the pitching-moment equation to provide equilibrium with the new reference angle of attack. In addition, the flap equation had to be modified to account for the critical fact that the hinge moment produced by the loading spring did not vary with velocity or dynamic pressure. (See appendix A (eq. (A3)).) The resulting equations were

$$\left[C_{Z_{\alpha_w}} + \left(1 - \frac{\partial \epsilon}{\partial \alpha}\right)C_{Z_{\alpha_t}}\right]\alpha + \left[\left(C_{Z_{\delta_f}}\right)_w - \frac{\partial \epsilon}{\partial \delta_f} C_{Z_{\alpha_t}}\right]\delta_f + \left[\left(C_{Z_{\delta_e}}\right)_t\right]\delta_e = -C_L \tag{5a}$$

$$\left[C_{m_{\alpha_w}} + \left(1 - \frac{\partial \epsilon}{\partial \alpha}\right)C_{m_{\alpha_t}}\right]\alpha + \left[\left(C_{m_{\delta_f}}\right)_w - \frac{\partial \epsilon}{\partial \delta_f} C_{m_{\alpha_t}}\right]\delta_f + \left[\left(C_{m_{\delta_e}}\right)_t\right]\delta_e = -C_{m_o} \tag{5b}$$

$$\left(q_f C_{h_\alpha}\right)\alpha + \left(q_f C_{h_{\delta_f}} + K_s\right)\delta_f + \left(q_f m' C_{h_\alpha}\right)\delta_e = \left(-K_o - q_f C_{h_\alpha} i\right) \tag{5c}$$

where

$$q_f = \frac{1}{2}\rho V^2 S_f c_f$$

These three equations were solved simultaneously for different velocities or lift coefficients to produce the trimmed angle of attack, flap position, and elevator position.

It will be shown that the stick-fixed handling characteristics are influenced by the static horizontal alleviation factor K_H. It is shown in appendix A (eqs. (A11) and (A12)) that

$$K_H = K_V\left(\frac{\alpha_V}{\alpha}\right)$$

or

$$K_H = K_V\left(\frac{K_o}{K_o + q_f C_{h_\alpha} i}\right)$$

where the quantities in parentheses are evaluated at the trimmed flight conditions with $\delta_f = \delta_e = 0$.

STATIC WIND-TUNNEL TESTS

Static wind-tunnel tests were run to determine as many of the aerodynamic parameters in equations (1) and equation (5c) as possible. A 1/6-scale model was built of a popular high-wing, single-engine, light airplane. The model had a removable horizontal tail and wing so that the contributions of the individual components could be measured and the downwash parameters, $\partial\epsilon/\partial\alpha$ and $\partial\epsilon/\partial\delta_f$, calculated. The model was equipped with the gust-alleviation system which permitted measurement of the static hinge-moment characteristics used in equations (5). The inertias of the vanes, flaps, and linkages were not truly representative of those for a full-scale airplane, and the friction levels in the vane and flaps were higher than that which could be achieved in a full-scale airplane. Therefore, the dynamic flap parameters used in equation (1c) were estimated for a full-scale airplane rather than by using values measured for the model. Additional tests were made to demonstrate the effects of the system on static lift, drag, and pitching moment, and to determine the effect of vane location on hinge moment.

Model

The main dimensions of the model are given in figure 3(a), and a photograph of the model mounted in the tunnel test section is presented in figure 4. The model was equipped

with plain flaps (see fig. 3(b)) (the ratio of flap chord to wing chord was 0.25 and the ratio of flap length to wing semispan was 0.37) that could deflect upward as well as downward. A pair of gust vanes (see fig. 3(b)) were mounted on either side of the fuselage and connected to the flaps with rigid mechanical linkages. The linkages were adjustable (see fig. 5) and provided a range of ratios of vane to flap deflection γ of 0.2 to 10.0. Both the vanes and the flaps were provided with mechanical stops to limit the travel of the system. The model had an adjustable elevator; however, no aileron or rudder surfaces were incorporated on the model.

Equipment

The model was tested in a low-speed tunnel with a 12-foot (3.66-meter) octagonal test section at the Langley Research Center. The model was mounted on a three-component balance which measured the normal force, axial force, and pitching moment. A hinge-moment balance and a potentiometer were also installed on the model's flap axis.

Conditions

The tests were run at a tunnel speed of 13.7 m/sec $\left(q = 1.65\ N/cm^2\right)$ which gave a Reynolds number of approximately 2.3×10^5 based on the model wing chord. The range of angle of attack tested was from -4° to 16°. Both the flaps and the elevator were tested through a range of $\pm 20^\circ$. The reference center-of-gravity position was 0.28c.

Model Component Test Results

The model was tested in four different configurations, and the results of these tests are presented in the following figures:

Configuration	Figure
Fuselage + Wing + Tail (Basic model)	6 and 7
Wing + Fuselage	8
Fuselage + Tail	9
Fuselage	10

The aerodynamic parameters needed in equations (1a) and (1b) were calculated from these data as follows. The parameters $\left(C_{L_{\delta_e}}\right)_t$ and $\left(C_{m_{\delta_e}}\right)_t$ were calculated from the data for the basic model. The wing-fuselage data are used to calculate the parameters $C_{L_{\alpha_w}}$ and $C_{m_{\alpha_w}}$ for each of the five tested flap positions and the parameters $\left(C_{L_{\delta_f}}\right)_w$ and $\left(C_{m_{\delta_f}}\right)_w$ for five different angles of attack. In each case a least-squares slope (of C_L

or C_m against δ_e, or of C_L or C_m against α, or of C_L or C_m against δ_f) and a standard deviation of the least-squares slope were claculated by using standard statistical formulas. (See ref. 7.) The parameters $C_{L_{\alpha_t}}$ and $C_{m_{\alpha_t}}$ were calculated by subtracting the slope determined for the fuselage data from the slope determined for the fuselage plus tail data. Since each of these slopes had a calculated standard deviation, the error propagated to the final answer was also calculated by using standard statistical techniques. (See ref. 7.)

The downwash parameters, $\partial\epsilon/\partial\alpha$ and $\partial\epsilon/\partial\delta_f$, were calculated by using the following relationships:

$$C_{m_\alpha} = C_{m_{\alpha_w}} + \left(1 - \frac{\partial\epsilon}{\partial\alpha}\right)C_{m_{\alpha_t}}$$

$$C_{m_{\delta_f}} = \left(C_{m_{\delta_f}}\right)_w - \frac{\partial\epsilon}{\partial\delta_f} C_{m_{\alpha_t}}$$

The parameters C_{m_α} and $C_{m_{\delta_f}}$ were first determined by using the data for the basic model, and the other parameters, $C_{m_{\alpha_w}}$, $C_{m_{\alpha_t}}$, and $\left(C_{m_{\delta_f}}\right)_w$, were determined from the component tests described previously. The one standard deviation values of these parameters were then used to calculate the propagated uncertainties in the computed values of $\partial\epsilon/\partial\alpha$ and $\partial\epsilon/\partial\delta_f$. The results of all the above calculations are presented in the following figures: $C_{L_{\alpha_w}}$ and $C_{m_{\alpha_w}}$ in figure 11, $\left(C_{L_{\delta_f}}\right)_w$ and $\left(C_{m_{\delta_f}}\right)_w$ in figure 12, $\left(C_{L_{\delta_e}}\right)_t$ and $\left(C_{m_{\delta_e}}\right)_t$ in figure 13, and $\partial\epsilon/\partial\alpha$ and $\partial\epsilon/\partial\delta_f$ in figure 14. Only one value was calculated for each of $C_{L_{\alpha_t}}$ and $C_{m_{\alpha_t}}$ since they were considered to be independent of flap position.

The experimental values for the parameters for $\alpha = 0$ and $\delta_f = 0$ were used in the analytical work since these conditions most nearly approximated the trimmed cruise condition. No Reynolds number corrections were made; the tunnel data were assumed to apply directly to the full-scale airplane. The Z-force derivatives were assumed to be equal to the negative of the lift derivatives determined in the tunnel. The derivatives used in reference 4 and the derivatives determined and used herein in the analysis are included in table I.

A horizontal line at the values used in the analytical work has been drawn in figures 11 to 14 so that the possible deviation from the values used can be easily seen. The deviation due to the experimental uncertainty was generally less than that due to nonlinearities (dependence on α or δ_f).

In order to obtain some evaluation of the effect that experimental uncertainty may have on the analytical results, a few calculations were made by using variations of one

standard deviation from the mean values at $\alpha = 0$, $\delta_f = 0$ for four of the parameters. The four parameters used were $C_{m_{\alpha_w}}$, $\partial\epsilon/\partial\alpha$, $\left(C_{m_{\delta_f}}\right)_w$, and $\partial\epsilon/\partial\delta_f$ since they had some of the largest relative standard deviations. (See table I.) Four different combinations of these parameters taking two parameters at a time were used. The signs of the one standard deviation values of $C_{m_{\alpha_w}}$ and $\partial\epsilon/\partial\alpha$ were selected to maximize the change in the static $\bar{\alpha}_o$ term, and the signs of the one standard deviation values of $\left(C_{m_{\delta_f}}\right)_w$ and $\partial\epsilon/\partial\delta_f$ were selected to maximize the change in the static $\bar{\delta}_f$ term.

Static Effects of the Alleviation System

The variations of lift, drag, pitching moment, and flap deflection for one typical alleviated configuration are shown in figure 15. These variations are compared in the figure with those of the model with the alleviation system fixed. In the active range where the flaps were floating free of the mechanical stops, the lift-curve slope of the alleviated model was reduced to about one-third that of the unalleviated model. The center of active range of the flaps (the point where $\delta_f \approx 0$) could be adjusted to any α or C_L by the proper choice of loading spring preload, vane incidence, and flap-vane gearing ratio. (See eq. (A3).) The slope of the lift curve in the active range of the flaps could be adjusted by using different flap-vane gearing ratios and loading spring gradients. (See eq. (A4).) The pitching moment of the model was practically unaffected by the system because the pitching moment due to change in wing camber $\left(C_{m_{\delta_f}}\right)_w$ was approximately canceled by the pitching moment due to flap downwash on the tail $-\frac{\partial\epsilon}{\partial\delta_f} C_{m_{\alpha_t}}$. Since the pitching-moment characteristics of the model did not change appreciably, the static stability of the model was preserved.

The active angle-of-attack range of the system was approximately $\pm 3^o$. Although the range could be extended a few degrees by moving the mechanical stops of the flap and vane to provide more flap travel, the alleviation system will be able to relieve only a small fraction of the gust levels used for design loading calculations. Even so, the system should be able to relieve most gusts encountered in normal operations since the design gusts are very rarely encountered.

Hinge-Moment Coefficients

The hinge-moment coefficients of the combined flap-vane system for various angles of attack and flap deflections are shown in figure 16. The vane was tested at two longitudinal locations. The quarter chord of the vane was first located at the 0.80c location because it allowed a single, direct, mechanical link between the flap and the vane. The data in figure 16(a) indicated that this location was unsatisfactory since the variation of flap hinge-moment coefficient with flap deflection $C_{h_{\delta_f}}$ was positive or unstable for

some angles of attack. When the vane was moved to the 0.26c position, $C_{h_{\delta_f}}$ was negative throughout the angle-of-attack range. The differences shown in figure 16(a) and figure 16(b) were not due to the different gearing ratio γ used for the two sets of data. Qualitative data for a range of different mechanical gains at the 0.80c location always showed the same unstable flap characteristic, positive $C_{h_{\delta_f}}$. These observations indicated the flap downwash was interfering with the flow over the vane and thus was changing the effective angle of attack of the vane.

The values for C_{h_α} and $C_{h_{\delta_f}}$ used in the analysis of the handling characteristics (eq. 5(c)) were -3.0 and -0.5, respectively. These values are reasonably close to the values which can be obtained from figure 16(b). Since C_{h_α} and K_V are dependent on γ (see eqs. (A3), (A4), and (A8)) and the accompanying definitions, the value of C_{h_α} used in the equation had to be different from that obtained from figure 16(b) in order to produce the desired level of static vertical alleviation.

RESULTS AND DISCUSSION

In the following sections several different types of calculations are presented for many different subjects. A complete list of the combinations used is presented in table II. The words "basic airplane" will refer to the response of the unalleviated airplane, $K_V = 0$, at the center of gravity $(l_p = 0)$, with the derivatives given in table I. The derivatives in table I define a center-of-gravity location of 0.28c. For the alleviated airplane the parameters characterizing the alleviation system will be, except where specified otherwise, as follows: $K_V = 0.75$, $\omega_n = 15$, $\zeta = 0.5$, $l_p = 0$, $\gamma_m = 0$, and $a = 0$. The airplane characteristics are the same as those of the basic airplane.

Unsteady Lift Effects

Root locus.- Four roots of the characteristic equation of the unsteady lift equations are compared with the corresponding roots from equations (1) in figure 17 for different levels of static alleviation. Only the two flap mode and the two short-period mode roots are shown for the unsteady lift equations. There were several other high-frequency roots due to the unsteady lift effects. The unsteady lift short-period roots show a slight shift toward the unstable region and the flap roots show a shift to slightly higher frequencies. However, the differences in the two sets of roots are no larger than the differences due to the experimental error in the aerodynamic parameters which will be shown later.

Frequency response.- The effect of the unsteady lift on the normal acceleration frequency response for the basic airplane and for the alleviated airplane is shown in figure 18. The unsteady lift effects are added first for the Z-force equation, then for the Z-force equation and the pitch equation, and then (for the alleviated airplane) for all three

equations. At high frequencies the Z-force equation makes more difference than the pitch equation for both the basic and alleviated airplane. At the short-period frequency, $\omega \approx 6$ rad/sec, the pitch equation makes the most difference for the alleviated airplane. The increased response is due to the decreased short-period damping noted in the previous section.

Since the differences in the results including unsteady lift effects were thought to be insignificant for the purposes of this study and since equations (1) (without unsteady lift effects) were much more convenient to use than the unsteady lift equations, equations (1) were used for all the following results.

Impact of Experimental Error

Root locus.- The short-period roots for the four combinations of the aerodynamic parameters with the largest standard deviations as explained in the model component test results section are shown in figure 19(a). The short-period roots are most sensitive to changes in the flap parameters $\left(C_{m_{\delta f}}\right)_w$ and $\partial\epsilon/\partial\epsilon_f$. The percentage change in the damping ratio is approximately the same, ±14 percent, as the percentage change in the parameters.

Power spectra.- The normal acceleration power spectra for these same parameters (fig. 19(b)) also show comparable variations, especially at the short-period frequency where the spectra have their peaks. The root-mean-square values are less sensitive to the parameter variation because the spectra with the largest low-frequency responses have the smallest high-frequency responses. It should also be mentioned that the variations of the aerodynamic parameters with flap deflection and angle of attack (nonlinearities) were even larger than the variations due to the experimental uncertainty considered here. Although the propagated uncertainty due to these nonlinearities should not be calculated in the same manner as the experimental uncertainty, the nonlinearities will probably also cause considerable variation in the calculated responses. The absolute values of all the following results are therefore questionable since they are based only on the values of the parameters as given in table I. However, the trends for changes in a given variable, such as K_V, should not be affected as strongly by the uncertainty in the parameters as the absolute values are affected.

Static Alleviation Factor

Root locus.- The short-period roots for different vertical static alleviation factors, flap natural frequency, and flap damping ratio are given in figure 20. Only the roots for the static alleviation factors are discussed here; the roots for the flap natural frequency and damping ratio are discussed later under the sections for those subjects.

Increasing the static alleviation factor K_V decreases the short-period damping sharply. In fact, the damping is decreased below the unsatisfactory limit of 0.25 (for $K_V = 1.0$) suggested in reference 8 from the pilot rating standpoint. The computed damping ratio of the basic airplane is 0.58. This calculated value is much lower than the 0.8 to 1.0 value obtained in unpublished studies by using flight data for this airplane. If the basic airplane's damping is really higher, the damping of the alleviated airplane may also be high enough to insure that the handling qualities will not be excessively degraded.

Flap frequency response.- The frequency responses of the flaps for the corresponding levels of static vertical alleviation are shown in figure 21. The responses have peaks which are much higher than the static ratio of flap deflection to angle of attack. For example, at $K_V = 0.75$, the peak value of δ_f/α_g is about twice that of the static ratio of $\Delta\delta_f/\Delta\alpha$. Thus, the magnitude of the gusts that the system can alleviate without the flaps or the vanes hitting the mechanical stops is even less than that which would be inferred from the static ratio or the static data in figure 15.

Power spectra.- The square roots of the normal acceleration power spectra for various levels of static vertical alleviation are shown in figure 22. The optimum level of vertical alleviation as measured by using the root-mean-square acceleration as a criterion is $K_V = 0.75$ and not as might be expected $K_V = 1.0$ where the lift-curve slope is zero. For comparison, the optimum level of alleviation for this airplane by using the methods of reference 2, with optimum flap downwash and flap response characteristics, is $K_V = 0.85$. The small differences between $K_V = 0.85$ and $K_V = 0.75$ are relatively unimportant and could be attributed to the truncation process in determining the root-mean-square values. However, $K_V = 0.75$ is used as the optimum herein.

The pitching response simply increases with K_V. For the optimum vertical alleviation, $K_V = 0.75$, the pitching response is almost three times as large as that of the basic airplane at the short-period peak, whereas the root-mean-square value for the pitching rate is over two times as large. This relationship is a fundamental problem; lower normal acceleration response is accompanied by a higher pitch response. This relationship is also true for most of the results presented subsequently; therefore, in most cases only the normal acceleration power spectra are presented.

Time history.- The time-history responses to 1^o step gust inputs for increasing levels of static gust alleviation are shown in figure 23. The normal acceleration of the alleviated airplane is initially less than that of the basic airplane, but there is considerably more overshoot. The static alleviation factor of $K_V = 0.75$ appears to give the best compromise between initial response and overshoot – a result which agrees with the results of the power spectra calculations. The pitching response and the flap response simply increase with increasing static alleviation.

Flap-Vane Natural Frequency and Damping Ratio

Root locus.- The flap-vane natural frequency and damping ratio have little effect on the short-period damping although they do affect the short-period frequency. (See fig. 20.) However, reducing the flap-vane damping ratio from the nominal value of 0.5 to the value of 0.1 decreases the damping ratio of the characteristic root for the flapping mode (not shown) from 0.56 to 0.23. The other parameters (K_V and ω_n) do not appreciably affect the damping of the flap mode.

Power spectra.- The effect of the flap-vane natural frequency on the normal acceleration power spectra for $K_V = 0.75$ is shown in figure 24(a). When the flap natural frequency is almost the same as the short-period natural frequency, $\omega_n = 5$ rad/sec, the normal acceleration response is actually greater than that of the basic airplane. As the natural frequency of the flap is raised, the normal acceleration response is reduced so that the higher natural frequencies produce better alleviation. This result agrees with the formulas in reference 2 which would predict optimum conditions with an instantaneous flap response for this particular configuration. (The instantaneous response results from the fact that the vane and the wing are at the same longitudinal location so that the gusts reach both the wing and the vane at the same time.)

The effect of flap-vane damping ratio for $K_V = 0.75$ and $\omega_n = 15$ is shown in figure 24(b). For low damping ratios (0.1 and 0.25), the low-frequency response is attenuated, but there is a resonant peak near the flap natural frequency. For higher damping ratios (0.5 and 0.75), the resonant peak is practically eliminated but the low-frequency response is greater than that for the lower damping ratios. The root-mean-square values indicate that $\zeta = 0.25$ is about optimum.

The flap-vane frequency and damping ratio cannot in practice be varied independently as is done in the preceding analysis. In appendix A (eq. (A22)), it is shown that the designer can produce the desired high natural frequency by using a large span vane and an effective flap with a low hinge moment, short chord, and long span. However, this type of vane and this type of flap produce a system with low damping ratios (eq. (A23)) so that a compromise must be made between frequency response and damping ratio.

Center-of-Gravity Variation

The effect of center-of-gravity position on the alleviation is shown in figure 25 for $K_V = 0.75$. As the center of gravity is moved aft, the response is increased, especially near the short-period frequency. A similar effect was apparent in the response calculations (not shown herein) for the basic airplane.

Normal Acceleration Response for Passenger Location Removed From Center of Gravity

Reference 2 indicated that the high pitching responses of gust-alleviated airplanes could cause the normal acceleration for points removed from the center of gravity to be increased. The results for some calculations made for points 0.20c and 0.40c aft of the center of gravity (representative distances for the passenger compartment in the subject aircraft) are shown in figure 26. These calculations show that the level of acceleration is relatively unaffected by the longitudinal location even though the pitching response is increased significantly as shown earlier. This result is due to the fact that the passenger locations on this airplane are near the center of gravity and not 1 or 2 chord lengths away as is possible on a transport airplane. Although the pitching response does not appreciably affect the normal acceleration, the pitching motion itself may cause ride discomfort and may still be important in the overall ride comfort.

Flap-Elevator Interconnect and Pitch Damper

The basic gust-alleviation system, as investigated above, reduces the root-mean-square normal acceleration response no more than about 50 percent while simultaneously increasing the pitching response. In order to determine whether any further gains in alleviation could be achieved and whether the pitching response could be reduced, a flap-elevator interconnect and a pitch damper were investigated. The results of the calculations for different gearing ratios of the flap-elevator interconnect γ_m are shown in figure 27. The corresponding alleviated static stabilities C'_{m_α} calculated from equation (4) are included in the figure. The overall normal acceleration alleviation effectiveness is increased by increasing γ_m except at low frequencies. (See fig. 27(a).) The pitching response is also attenuated at practically all frequencies and with the higher gearing approaches that of the unalleviated case. (See fig. 27(b).)

These results are for a constant ω_n and K_V which in a practical situation would be impossible to achieve. Connecting the flap to the elevator would reduce ω_n because of the increased inertia of the system whereas K_V would also be reduced because of the increased hinge moment. Further study of these effects is required in order to define the interrelationship.

A damper natural frequency of 10 rad/sec is used initially in order to be faster than the short-period response of the airplane. The pitch damper has very little effect on the root-mean-square normal acceleration even though the power spectral density shape is shifted to slightly higher frequencies for higher gains a. (See fig. 28(a).) The pitch rate response (fig. 27(b)) is reduced by the pitch damper so that the damper may be

useful if the pitching response degrades the ride comfort. A much higher pitch damper natural frequency (1000 rad/sec) increases the alleviation only slightly (fig. 29(a)) and reduces the pitching slightly (fig. 29(b)) over that of the slower responding damper. Therefore, it seems that if the natural frequency of the damper is higher than the short-period frequency of the airplane, the actual value is not a primary consideration.

Handling Characteristics

A gust-alleviation system can have a profound effect on the handling characteristics since it modifies one of the basic aerodynamic characteristics of an airplane – the lift-curve slope. The possible deleterious effect of the lowered short-period damping on the handling characteristics has already been mentioned. Other effects of the alleviation system on the handling characteristics will now be discussed.

In the following discussion, the gearing ratio between the elevator and the vane incidence m' is adjusted to maintain the basic airplane's handling characteristics in steady accelerated flight. That is, the elevator deflection required for a given level of steady normal acceleration is the same for the alleviated airplane as that for the basic airplane. The only way the two responses can be the same is for the flap deflection in steady accelerated flight to be zero for the alleviated airplane. This result is accomplished by making the change in vane incidence for a given elevator deflection equal to, but opposite, the change in angle of attack of the vane that would result from the same elevator input. This arrangement will keep the flap deflection zero because the lift on the vane will remain at the original trimmed levels in steady accelerated flight even though the angle of attack (and lift) of the airplane changes in response to elevator control.

With a gearing ratio m' an elevator deflection causes a change in vane incidence which in turn causes a flap deflection since the vane lift changes. The steady-state ratio of flap deflection to elevator deflection if the angle of attack and θ are held constant is designated m. (See eqs. (1c) and (A13).) The relationship between the ratio m and gearing ratio m' is given in the definition accompanying equation (A13). The value of m is proportional to K_V since K_V in turn is proportional to the change in flap deflection for an angle-of-attack (or vane incidence) change. The parameter m rather than m' is used in the following analysis.

Normal acceleration frequency response to elevator inputs.- The results of these frequency response calculations are shown in figure 30 for different levels of static alleviation (and the corresponding m values). At low frequencies the responses are the same as that of the basic airplane since the gearing ratio was selected for the steady-state case. At higher frequencies the alleviated responses are increasingly different from that of the basic airplane, especially for higher levels of alleviation. For $K_V = 1.0$ ($m = -3.21$), there was a relatively large peak at the short-period frequency as a result of the lowered

damping noted earlier for the short-period mode. However, at $K_V = 0.75$, the airplane response to the elevator is not much different from that of the basic airplane, and thus it seems that this response would probably be acceptable to a pilot.

Time history.- The time-history response to a 1^o step elevator input for $K_V = 0.75$ and $m = 2.41$ is compared with that of the basic airplane in figure 31. The fast initial normal acceleration response of the alleviated airplane is like a direct lift control system because the airplane did not have to pitch to produce the normal acceleration. The flaps are producing the normal acceleration in this initial time period. Then as the airplane's angle of attack changes in response to the elevator deflection, the flaps are driven back to zero; and the steady-state normal acceleration is produced by the new angle of attack of the airplane.

Static stability.- The static stability is discussed in this section because it is ordinarily associated with the stick-fixed handling characteristics. Substituting equation (2) into equations (3) and using the numerical values for the various derivatives results in

$$C'_{m_\alpha} = -1.21 - 0.14K_V$$

Since K_V of less than one is desirable, the static stability is not appreciably affected by the gust-alleviation system. This result is a consequence of the near zero value of $C_{m_{\delta_f}}$ and agrees with the tunnel results of figure 15 which shows no appreciable change in C_m with α for the alleviated model.

Stick-fixed handling characteristics.- The results of the calculations using equations (5) are presented in figure 32 for four different levels of the static horizontal gust-alleviation factor K_H and one value of the elevator-vane incidence gearing ratio m'. The elevator-vane incidence gearing ratio was selected to retain the handling characteristics of the basic airplane in steady accelerated flight. The values of the parameters used in equation (5c) are summarized in table III, whereas the values of the parameters in equations (5a) and (5b) are the same as those in table I.

For no horizontal alleviation, $K_H = 0.0$, the handling characteristics $d\delta_e/dC_L$ are practically the same as that of the basic airplane since the flap deflection changes very little with C_L. For higher levels of static alleviation, the stick-fixed handling characteristics are degraded (that is, $d\delta_e/dC_L$ becomes less negative) so that for values of K_H between 0.75 and 1.00, the slope becomes positive. A positive slope represents an unstable equilibrium condition because a change in the elevator position would cause the velocity to diverge rather than stabilize at a new velocity or lift coefficient. A positive elevator deflection (stick forward), for example, would cause the airplane to pitch downward (see fig. 31) and eventually pick up speed. However, for this unstable condition the airplane would never stabilize at a higher speed because a negative deflection (stick

back) from the initial trim is required to trim at a higher speed (lower C_L) (fig. 32). In order to trim or stabilize at a new velocity, the pilot would have to provide the stability by making several elevator inputs rather than a single input. The flap deflection at the new stabilized conditions will be positive for lift coefficients higher than the original trim lift coefficient while the angle of attack will be about the same. This response is different from that of an unalleviated airplane, in which case a change in lift coefficient is accomplished by a change in angle of attack rather than a change in flap deflection.

In order to have the slope of the trimmed elevator position as a function of lift coefficient of the alleviated airplane the same as that of the basic airplane, the lift on the vane must be constant for all airplane lift coefficients. That is, the product of the dynamic pressure and the angle of attack of the vane must be constant. This relationship between the angle of attack of the vane and the dynamic pressure puts additional constraints of the values of m' and i that can be used. However, these values have already been specified on the basis of the desired handling characteristics in steady accelerated flight and the static horizontal alleviation factor. A real-time simulation of the system with a pilot in the loop is needed to determine the best compromise between these conflicting requirements on m' and i.

CONCLUSIONS

An aeromechanical gust-alleviation system for a high-wing light airplane has been investigated analytically by using tunnel-determined values for the airplane aerodynamic characteristics and estimates for the flap response characteristics. The tunnel-determined values were measured by using a 1/6-scale model in the Langley 12-foot (3.66-meter) low-speed tunnel. Even though experimental error in the tunnel-determined characteristics have significant impact on the absolute values of the analytical results, definite relationships or trends could be established and some conclusions can be made.

The conclusions which can be made are as follows:

1. The system does not appreciably affect the static stability.

2. The system reduces the short-period damping significantly.

3. A static vertical alleviation factor of 0.75 appears to be optimum for reducing the normal acceleration response.

4. By using assumed flap response characteristics, the normal acceleration response to a von Karman gust spectrum is reduced about one-half from the unalleviated airplane whereas the pitching response is doubled.

5. Increasing the flap natural frequency increases the amount of alleviation.

6. A higher flap natural frequency can be obtained by using a long span, short chord, highly effective flap with a low hinge moment and a large span vane.

7. A finite flap damping ratio considerably less than critical damping provides the most alleviation.

8. A flap-vane system with the characteristics described in conclusion 6 produces low flap damping ratios so that a compromise between high natural frequency and too low a damping ratio is necessary.

9. A flap-elevator interconnect (which does not affect the flap-vane response characteristics) or a pitch rate damper system improves the normal acceleration alleviation while simultaneously reducing the pitching response.

10. The system produces direct lift control.

11. Although the system did not appreciably affect the static stability, the stick-fixed handling characteristics may be significantly affected. The impact of these effects should be investigated by using a real-time simulation of the system with a pilot in the loop.

Langley Research Center
National Aeronautics and Space Administration
Hampton, Va. 23665
April 28, 1976

APPENDIX A

FLAP AND VANE CHARACTERISTICS

Flap Equation of Motion

In order to understand how the system works, a thorough understanding of the equation which governs the motion of the flap is needed. Therefore, a generalized flap equation is written below. As the discussion progresses, the equation will be simplified for specific applications.

Flap equation:

$$H = \underset{①}{\ddot{\delta}_f\left(I_f + \gamma^2 I_v\right)} = \underset{②}{\dot{\delta}_f\left[\left(\frac{1}{2}\rho V^2 S_f c_f\right)\left(\frac{c}{2V}\right)\left(\gamma^2 C_{h_{\dot{\delta}_v}} + C_{h_{\dot{\delta}_f}}\right)\right]}$$

$$+ \underset{③}{\delta_f\left(\frac{1}{2}\rho V^2 S_f c_f C_{h_{\delta_f}} + K_s\right)} + \underset{④}{\left(\frac{1}{2}\rho V^2 S_f c_f \gamma C_{h_{\alpha_v}}\right)\alpha_v}$$

$$+ \underset{⑤}{\left(\frac{1}{2}\rho V^2 S_f c_f C_{h_{\alpha_f}}\right)\alpha} + \underset{⑥}{\left(-I_f\right)\ddot{\theta}} + \underset{⑦}{K_o} \qquad \text{(A1)}$$

where

$$\alpha = \alpha_{trim} + \alpha_o + \alpha_g$$

$$\alpha_v = \alpha + \frac{l_v \dot{\theta}}{V} + m'\delta_e + i$$

The terms are numbered for reference in the following discussion.

The first term is the inertia term. It is made up of the flap inertia and the vane inertia reflected back to the flap axis by the square of the gearing ratio. The second term is the damping term which is made up of a flap term and a reflected vane term. The third term is the stiffness term. It is assumed here that the vane does not contribute to the stiffness and that a loading spring with gradient K_s adds to the flap deflection hinge moment.

The fourth term is the hinge moment due to changes in angle of attack at the vane. This hinge moment is reflected back to the flap axis by the first power of the gearing ratio. The fifth term is the hinge moment due to the angle of attack at the flap (or the angle of attack of the airplane). The sixth term is the inertial term due to the pitching

acceleration of the airplane. This term was not included in the analysis of reference 4, probably because of its small influence. It should be noted that this term arises even though the flaps (as well as the vanes) were assumed to be mass balanced. The fact that the flaps and vanes were mass balanced explains the absence of any terms proportional to the normal acceleration of the airplane. The seventh term is due to the loading spring being stretched when the flap is at zero deflection. For a constant torque spring (that is, one with a zero gradient but with a constant torque independent of flap position), this term remains but the K_s term in the stiffness term goes to zero. The constant torque spring was the case considered in reference 4.

The angle of attack at the wing α is equal to the trimmed angle of attack of the airplane plus the perturbation angle of attack due to motion of the airplane plus the gust-induced angle of attack. The angle of attack at the vane was assumed to be equal to the angle of attack of the airplane plus three terms. The first added term was an induced angle of attack due to the pitching rate of the airplane and the fact that the vane may not be on the airplane's center of gravity. The distance from the vane to the center of gravity was l_v. The second added term was due to the pilot's control linkage which changes the incidence of the vane so he can change the airplane's flight-path angle by using the elevator. The constant m' was the gearing ratio between the elevator deflection and the vane incidence. The third added term was a term by which the pilot trimmed the whole system to zero hinge moment. It follows that at the trimmed flight condition, $\delta_e = \delta_f = 0$; thus,

$$\left(\frac{1}{2}\rho V^2 S_f c_f \gamma C_{h_{\alpha_v}}\right)(\alpha_{trim} + i) + \left(\frac{1}{2}\rho V^2 S_f c_f C_{h_{\alpha_f}}\right)\alpha_{trim} + K_o = 0 \qquad \text{(A2)}$$

Static Alleviation Factors

The static alleviation factors are a measure of the amount of alleviation produced by the system as the angle of attack or velocity changes slowly (quasi-static changes) about the trimmed flight condition. These factors ignore the dynamic response characteristics of the flap-vane system and the airplane. By using equation (A1) the $\ddot{\delta}_f$, $\dot{\delta}_f$, and $\ddot{\theta}$ terms are dropped. Also, by considering a control-fixed situation, the δ_e and i terms can be combined so that equation (A1) reduces to

$$\left(\frac{1}{2}\rho V^2 S_f c_f C_{h_{\delta_f}} + K_s\right)\delta_f + \left(\frac{1}{2}\rho V^2 S_f c_f C_{h_\alpha}\right)\alpha + \left(\frac{1}{2}\rho V^2 S_f c_f \gamma C_{h_{\alpha_v}}\right)\phi + K_o = 0 \qquad \text{(A3)}$$

where

$$C_{h_\alpha} = \gamma C_{h_{\alpha_v}} + C_{h_{\alpha_f}}$$

$$\phi = m'\delta_e + i$$

$$\alpha = \alpha_{trim}$$

Solving for the flap deflection

$$\delta_f = \frac{-\left(\frac{1}{2}\rho V^2 S_f c_f C_{h_\alpha}\right)\alpha - \left(\frac{1}{2}\rho V^2 S_f c_f \gamma C_{h_{\alpha_v}}\right)\phi - K_o}{\frac{1}{2}\rho V^2 S_f c_f C_{h_{\delta_f}} + K_s}$$

Taking the partial derivatives yields

$$\frac{\partial \delta_f}{\partial \alpha} = \frac{-\frac{1}{2}\rho V^2 S_f c_f C_{h_\alpha}}{\frac{1}{2}\rho V^2 S_f c_f C_{h_{\delta_f}} + K_s} \tag{A4}$$

$$\frac{\partial \delta_f}{\partial V} = \frac{K_s\left[-\left(\rho V S_f c_f C_{h_\alpha}\right)\alpha - \left(\rho V S_f c_f \gamma C_{h_{\alpha_v}}\right)\phi\right] + K_o\left(\rho V S_f c_f C_{h_{\delta_f}}\right)}{\left(\frac{1}{2}\rho V^2 S_f c_f C_{h_{\delta_f}} + K_s\right)^2} \tag{A5}$$

To determine the amount of quasi-static alleviation, these derivatives must be compared with those that would be necessary to maintain the lift constant. The derivatives for the constant lift conditions can be derived from the lift equation as follows:

$$L = \frac{1}{2}\rho V^2 S\left(C_{L_\alpha}\alpha + C_{L_{\delta_f}}\delta_f\right)$$

$$\delta_f = \frac{\frac{L}{\frac{1}{2}\rho V^2 S} - C_{L_\alpha}\alpha}{C_{L_{\delta_f}}}$$

If lift is a constant,

$$\left.\frac{\partial \delta_f}{\partial \alpha}\right|_{L=Constant} = -\frac{C_{L_\alpha}}{C_{L_{\delta_f}}} \tag{A6}$$

APPENDIX A

$$\left.\frac{\partial \delta_f}{\partial V}\right|_{L=\text{Constant}} = \frac{-\dfrac{2L}{\frac{1}{2}\rho V^3 S}}{C_{L_{\delta_f}}}$$

But $C_L = \dfrac{L}{\frac{1}{2}\rho V^2 S}$; thus,

$$\left.\frac{\partial \delta_f}{\partial V}\right|_{L=\text{Constant}} = \frac{-2C_L}{VC_{L_{\delta_f}}} \tag{A7}$$

The static alleviation factors are defined as the ratios of the actual changes in flap deflection given in equations (A4) and (A5) to the changes which would be required to maintain constant lift as given in equations (A6) and (A7):

$$K_V = \frac{\dfrac{\partial \delta_f}{\partial \alpha}}{\left.\dfrac{\partial \delta_f}{\partial \alpha}\right|_{L=\text{Constant}}} = \frac{C_{L_{\delta_f}}\left(\frac{1}{2}\rho V^2 S_f c_f C_{h_\alpha}\right)}{C_{L_\alpha}\left(\frac{1}{2}\rho V^2 S_f c_f C_{h_{\delta_f}} + K_s\right)} \tag{A8}$$

$$K_H = \frac{\dfrac{\partial \delta_f}{\partial V}}{\left.\dfrac{\partial \delta_f}{\partial V}\right|_{L=\text{Constant}}} = \frac{K_s C_{L_{\delta_f}}\left(\frac{1}{2}\rho V^2 S_f c_f\right)\left(C_{h_\alpha}\alpha + \gamma C_{h_{\alpha_v}}\phi - K_o C_{h_{\delta_f}}\right)}{C_L\left(\frac{1}{2}\rho V^2 S_f c_f C_{h_{\delta_f}} + K_s\right)^2} \tag{A9}$$

It should be noted that K as used in equation (1c) is equal to $-\delta_f/\alpha$ in the steady-state controls-fixed situation where $\alpha = \alpha_o + \alpha_g$. Since δ_f is assumed to be zero when α is zero, $-\delta_f/\alpha$ is equivalent to the definition for K, $-\Delta\delta_f/\Delta\alpha$. The latter expression, $-\Delta\delta_f/\Delta\alpha$, is in turn equivalent to the partial derivative $-\partial\delta_f/\partial\alpha$ since δ_f is a linear, first-power function of α. This last equivalency along with equation (A8) determines the relationship between K_V and K

$$-\frac{\partial \delta_f}{\partial \alpha} = -\frac{\Delta \delta_f}{\Delta \alpha} \equiv K = K_V\left(\frac{C_{L_\alpha}}{C_{L_{\delta_f}}}\right) \tag{A10}$$

When $K_V = 1$, the alleviated lift-curve slope is zero whereas at a value of zero the alleviated lift-curve slope is the same as the unalleviated case. Thus, K_V is a convenient normalized measure of the quasi-static alleviation.

It can be shown by algebraic manipulation of equations (A8) and (A9) using the substituted values for $\partial\delta_f/\partial\alpha$, etc., that

$$K_H = K_V\left(\frac{\alpha_v}{\alpha}\right) \tag{A11}$$

or

$$K_H = K_V\left(\frac{K_o}{K_o + q_f C_{h_\alpha} i}\right) \tag{A12}$$

by assuming trimmed flight conditions, $\delta_e = \delta_f = 0$, and that

$$C_L = C_{L_\alpha}\alpha$$

$$C_{h_\alpha} = \gamma C_{h_{\alpha_v}}$$

The first assumptions are not restrictive, and the last assumption merely states that the vane contributes more of the hinge moment due to angle of attack than the flap. The latter assumption, where the small $C_{h_{\alpha_f}}$ term has been omitted, should lead to no more than an error of a few percent.

The physical interpretation of equation (A11) is as follows. First, there can be no horizontal alleviation unless there is vertical alleviation. Secondly, the horizontal alleviation will be exactly equal to the vertical alleviation if the angle of attack of the vane is equal to the angle of attack of the airplane. This case was treated in reference 9 for a spring with zero gradient. Thirdly, the horizontal alleviation is zero (even when K_V is not) if the angle of attack of the vane is zero. If the angle of attack of the vane is not zero, the resultant hinge moment due to lift on the vane must be balanced by a spring in order to maintain the flap deflection at zero. As can be seen from equation (A12) this spring force K_o leads to the horizontal alleviation capability. It is interesting to note that whether the spring has a zero gradient or not is not important because K_s does not appear in equation (A11) or (A12).

APPENDIX A

Flap Dynamics

An alternate, simplified form (used in eq. (1c)) of equation (A1) is

$$\left(K\omega_n^2\right)\bar{\alpha}_o + \left(i_r s^2 - sK\omega_n^2 \frac{l_n}{V}\right)\bar{\theta} + \left[\left(s^2 + 2\zeta\omega_n s + \omega_n^2\right)\right]\bar{\delta}_f = \left(-K\omega_n^2\right)\bar{\alpha}_g + \left(\omega_n^2 m\right)\bar{\delta}_e \qquad \text{(A13)}$$

where the Laplace transform variable has been introduced and the velocity has been assumed to be constant. Trimmed conditions (eq. (A2)) are used to eliminate the static term and the following definitions are used:

$$\omega_n = \sqrt{\frac{-\left(\frac{1}{2}\rho V^2 S_f c_f C_{h_{\delta_f}} + K_s\right)}{I_f + I_v\gamma^2}}$$

$$\zeta = -\left(\gamma^2 C_{h_{\dot{\delta}_v}} + C_{h_{\dot{\delta}_f}}\right)\left(\frac{c}{2V}\right)\frac{\left(\frac{\frac{1}{2}\rho V^2 S_f c_f}{I_f + \gamma^2 I_v}\right)}{2\omega_n}$$

$$i_r = \frac{I_f}{I_f + \gamma^2 I_v}$$

$$m = \frac{m'\left(\frac{1}{2}\rho V^2 S_f c_f \gamma C_{h_{\alpha_v}}\right)}{\frac{1}{2}\rho V^2 S_f c_f C_{h_{\delta_f}} + K_s}$$

$$l_n = \frac{l_v}{\left(\frac{\gamma C_{h_{\alpha_v}} + C_{h_{\alpha_f}}}{\gamma C_{h_{\alpha_v}}}\right)}$$

and the term K has already been defined (eq. (A10)).

APPENDIX A

Parameter Influence on Flap-Vane Response Characteristics

As shown in the text, the amount of alleviation can be greatly increased by raising the natural frequency of the flap-vane system. The obvious way to increase the frequency is to reduce the inertia of the flap, linkages, and vanes. The question was, then, how could the flap natural frequency be increased if it is assumed that the inertia of the system has already been minimized subject to structural limitations. A short analysis was, therefore, made to determine the relationship between some fundamental flap and vane parameters and the resulting natural frequency. The damping ratio of the flap-vane system must be considered simultaneously since a low damping ratio accentuates the airplane response at the flapping mode frequency because of the reduced damping of the characteristic roots for the flap mode.

The natural frequency and damping ratio of the flap-vane system are given by the following formulas:

$$\omega_n = \sqrt{\frac{\text{Stiffness}}{\text{Inertia}}} \tag{A14}$$

$$\zeta = \frac{\left(\frac{\text{Damping}}{\text{Inertia}}\right)}{2\omega_n} \tag{A15}$$

These response characteristics were determined subject to the constraint that the static vertical gust-alleviation factor remained constant. A simplified form of K_V was taken to be

$$K_V \propto \frac{\left(\frac{\text{Vane effectiveness}}{\text{Stiffness}}\right)}{\left(\frac{C_{L_\alpha}}{\text{Flap effectiveness}}\right)} \tag{A16}$$

where the vane effectiveness is the amount of lift or hinge moment produced by the vane for a given increment in angle of attack, and flap effectiveness is the amount of lift produced by the flap for a given flap deflection. In order to determine some general relationships between the response characteristics and certain flap-vane parameters, a number of simplifying assumptions were made. First, it was assumed that the stiffness of the system was due entirely to the flap aerodynamic hinge moment (no loading spring) and that the hinge moment varied with flap span and flap chord squared,

$$\text{Stiffness} \propto C_{h_{\delta_f}} b_f c_f^2 \tag{A17}$$

where $C_{h_{\delta_f}}$ is dependent on gap sealing, hinge location, and other factors. The variation with flap chord squared approximately matches the experimental data (ref. 10). The second assumption was that the inertia was due entirely to the vane and that the vane inertia varied as the fifth power of the vane span

$$\text{Inertia} \propto \gamma^2 b_v^5 \tag{A18}$$

The square of the gearing ratio appears because the vane inertia was reflected back to the flap axis through the gearing ratio. The fifth power of the span appears as a result of assuming that the aspect ratio is constant and that the thickness of the vane skin increases in such a way as to maintain constant fiber stress.

The third assumption was that the damping was due entirely to the vane's motion. The resulting theoretical damping for a constant aspect ratio using simple strip theory was

$$\text{Damping} \propto \gamma^2 b_v^4 \tag{A19}$$

The fourth assumption was that the vane effectiveness was proportional to the third power of the vane span; that is,

$$\text{Vane effectiveness} \propto \gamma b_v^3 \tag{A20}$$

The formula γb_v^3 is also a consequence of the constant vane aspect ratio assumption. The last assumption was that the flap effectiveness varied as follows:

$$\text{Flap effectiveness} \propto C_{L_{\delta_f}} b_f \sqrt{c_f} \tag{A21}$$

The assumption that flap effectiveness varies with the square root of flap chord approximates experimental data (ref. 10).

By substituting equations (A17), (A20), and (A21) into equation (A16), a relationship for the variation of the gearing ratio γ required to maintain constant static alleviation can be determined

$$\gamma \propto \frac{C_{h_{\delta_f}} c_f^{3/2}}{C_{L_{\delta_f}} b_v^3} \tag{A22}$$

where C_{L_α} and K_V have been absorbed in the proportionality. Substituting equations (A17) and (A18) into equation (A14) yields

$$\omega_n \propto \sqrt{\frac{C_{h_{\delta_f}} b_f c_f^2}{\gamma^2 b_v^5}}$$

Substituting equation (A22) to maintain constant static alleviation results in the final desired result

$$\omega_n \propto C_{L_{\delta_f}} \sqrt{\frac{b_v b_f}{C_{h_{\delta_f}} c_f}} \tag{A23}$$

It, therefore, seemed that an effective flap with a low hinge moment, short chord, and a long span would produce the highest response system. A vane with as large a span as possible would also increase the overall response. Substituting equations (A18), (A19), and (A23) into equation (A15) yields the damping ratio relationship

$$\zeta \propto \frac{1}{C_{L_{\delta_f}}} \sqrt{\frac{C_{h_{\delta_f}} c_f}{b_v^3 b_f}} \tag{A24}$$

Comparison of these last two equations shows that some compromise must be made between damping ratio and frequency response since all the parameters are inverted in the second equation; that is, the higher the natural frequency, the lower the damping ratio. This relationship is especially true for the vane span which appears to the third power under the radical for the damping ratio. Another consideration in the design besides natural frequency and damping ratio is the gearing ratio. It must be near unity to limit the stress in the linkage.

APPENDIX B

UNSTEADY LIFT EFFECTS

The unsteady lift representation used herein is described. The functions used approximate the curves shown in references 11 and 12 and are given for comparison with equations (1). The Z-force equation is considered first. The symbols used in this appendix (ω_n, ζ, a, etc.) apply only to the unsteady lift functions and have no relation to the corresponding symbols in the main text.

$\bar{\alpha}_o$ Terms

The $\bar{\alpha}_o$ terms in equations (1) were

$$C_{Z_{\alpha_w}} + C_{Z_{\alpha_t}}\left[1 - \frac{\partial \epsilon}{\partial \alpha}\left(1 - 1\,\frac{c}{V}\,s\right)\right]$$

whereas those for the unsteady lift representation were

$$\frac{0.64C_{Z_{\alpha_w}}\left(\frac{3c}{2V}\right)s + C_{Z_{\alpha_w}}}{\left(\frac{3c}{2V}\right)s + 1.0} + \frac{s^2(C) + s^2\left[(C - A)a + C2\zeta\omega_n\right] + s\left[B\omega_n{}^2 + C\omega_n{}^2 + (C - A)2\zeta\omega_n a\right] + \left[B\omega_n{}^2 a + (C - A)\omega_n{}^2 a\right]}{\left(s^2 + 2\zeta\omega_n s + \omega_n{}^2\right)(s + a)}$$

The first term is the lift on the wing due to the plunging motion. A sketch of the time-history response of this term for a step input of unit magnitude is given so that characteristics of the function will be more apparent. The mathematical equations for this response are also given.

Equations (1)

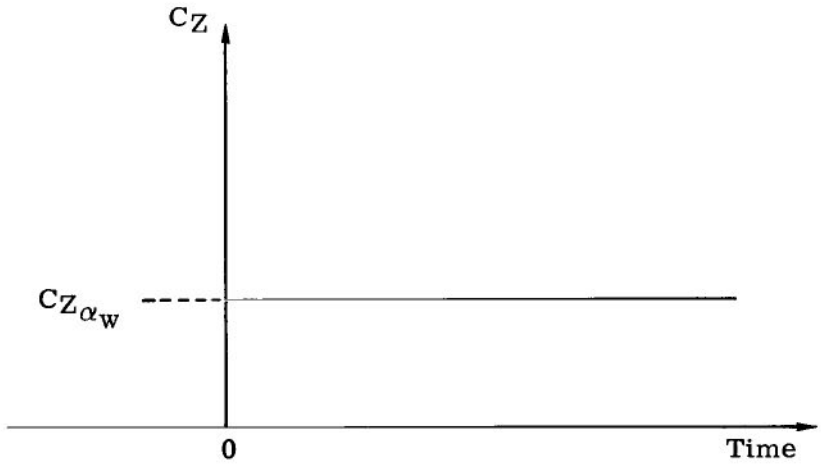

$$C_Z(t) = C_{Z_{\alpha_w}} u_s(t)$$

APPENDIX B

Unsteady lift

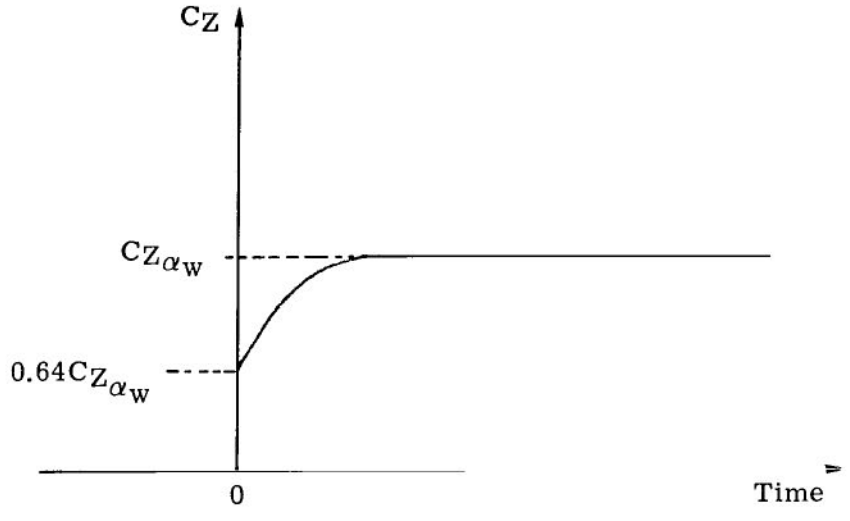

$$C_Z(t) = \left[1 - 0.36e^{-\left(\frac{2V}{3c}\right)t}\right] C_{Z_{\alpha_w}} u_s(t)$$

where $u_s(t)$ is the unit step function defined by

$$u_s(t) = 1 \qquad (t \geq 0)$$

$$u_s(t) = 0 \qquad (t < 0)$$

The second $\bar{\alpha}_o$ term is the lift on the tail due to plunging motion of the airplane. It consists of a lift due to plunging motion of the tail and lift due to downwash from the wing which arrives at a time $\ell c/V$ later. Before the downwash is established, however, an upwash due to the shed vortex from the wing produces a lift in the opposite direction of the downwash (same direction as lift due to plunging motion of tail). The response of the second term in the model of equations (1) has an infinite pulse at time zero for a step input due to the s term. The time-domain representations are

APPENDIX B

Equations (1)

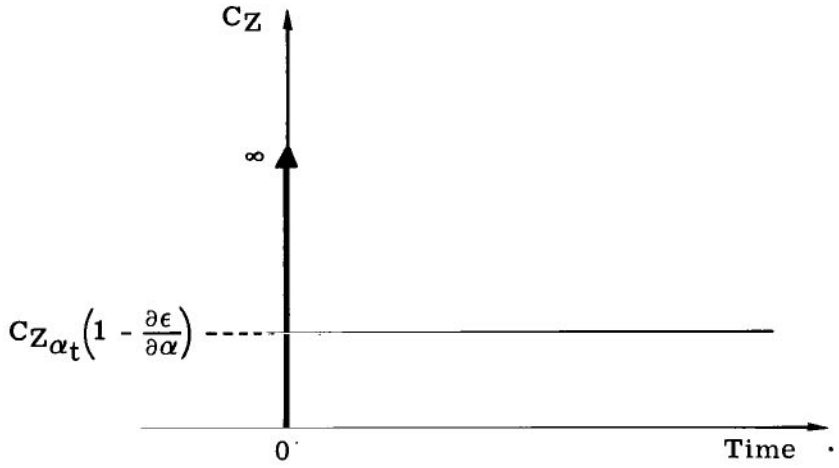

$$C_Z(t) = C_{Z_{\alpha_t}} \frac{\partial\epsilon}{\partial\alpha} \frac{lc}{V} \delta(t) + C_{Z_{\alpha_t}}\left(1 - \frac{\partial\epsilon}{\partial\alpha}\right) u_s(t)$$

where $\delta(t)$ is the unit impulse function defined by

$$\delta(t) = \infty \qquad (t = 0)$$

$$\delta(t) = 0 \qquad (t \neq 0)$$

$$\int_{-\infty}^{\infty} \delta(t)\, dt = 1$$

Unsteady lift

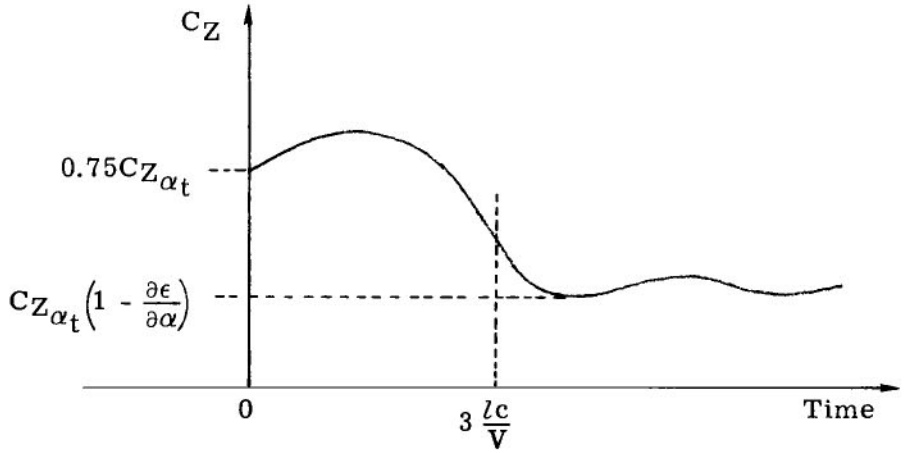

$$C_Z(t) = \left\{-A(1 - e^{-at}) + B\left[1 - \frac{1}{\sqrt{1 - \zeta^2}} e^{-\zeta\omega_n t} \sin\left(\omega_n\sqrt{1 - \zeta^2}\, t + \phi\right)\right] + C\right\} C_{Z_{\alpha_t}} u_s(t)$$

where

$$\phi = \tan^{-1} \frac{\sqrt{1 - \zeta^2}}{\zeta}$$

$$-A + B + C = 1 - \frac{\partial \epsilon}{\partial \alpha}$$

$$B = 1.25A$$

$$C = 0.75$$

$$\omega_n = 35$$

$$\zeta = 0.7$$

$$a = 40$$

$\bar{\theta}$ Terms

The $\bar{\theta}$ term in equations (1) was

$$s \frac{cl}{V} C_{Z_{\alpha_t}}$$

whereas that for the unsteady lift representation was

$$\frac{0.90 \frac{cl}{V} C_{Z_{\alpha_t}} \frac{c_t}{V} s^2 + \frac{cl}{V} C_{Z_{\alpha_t}} s}{\frac{c_t}{V} s + 1.0}$$

This term is the lift on the tail due to pitching motion of the airplane. It was assumed to be of the same form as the $C_{Z_{\alpha_w}}$ term used before because the tail can be considered to be plunging when the airplane pitches small amounts at a given pitch rate. The time constant c_t/V and the value at time equal to zero were slightly different because of the difference in the chord and aspect ratio of the tail as compared with that of the wing.

$\bar{\delta}_f$ Terms

The $\bar{\delta}_f$ terms in equations (1) were

$$\left(C_{Z_{\delta_f}}\right)_w - C_{Z_{\alpha_t}} \frac{\partial \epsilon}{\partial \delta_f}\left(1 - \frac{lc}{V} s\right)$$

whereas those for the unsteady lift representation were

$$\frac{0.64\left(C_{Z_{\delta_f}}\right)_w\left(\frac{3c}{2V}\right)s + \left(C_{Z_{\delta_f}}\right)_w}{\left(\frac{3c}{2V}\right)s + 1.0} + \frac{s^2(-Aa) + s\left(B\omega_n{}^2 - 2Aa\zeta\omega_n\right) + \left(B\omega_n{}^2a - A\omega_n{}^2a\right)}{(s + a)\left(s^2 + 2\zeta\omega_n s + \omega_n{}^2\right)}$$

The first term is lift on the wing due to flap deflection and is exactly the same form as the $C_{Z_{\alpha_w}}$ term. The second term is the lift due to the flap downwash on the tail which is also assumed to have an upwash term because of the passing of the shed vortex off the flap. However, the initial value is zero rather than a constant for the $\bar{\alpha}_o$ term. The time-domain relationships are

Equations (1)

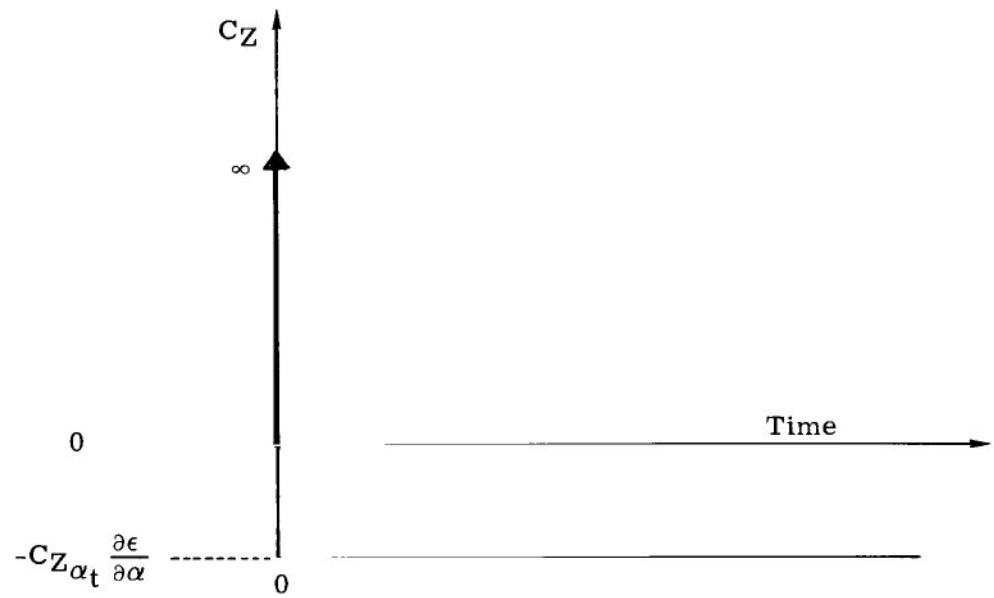

$$C_Z(t) = C_{Z_{\alpha_t}} \frac{\partial\epsilon}{\partial\delta_f} \frac{lc}{V} \delta(t) - C_{Z_{\alpha_t}} \frac{\partial\epsilon}{\partial\alpha} u_s(t)$$

APPENDIX B

Unsteady lift

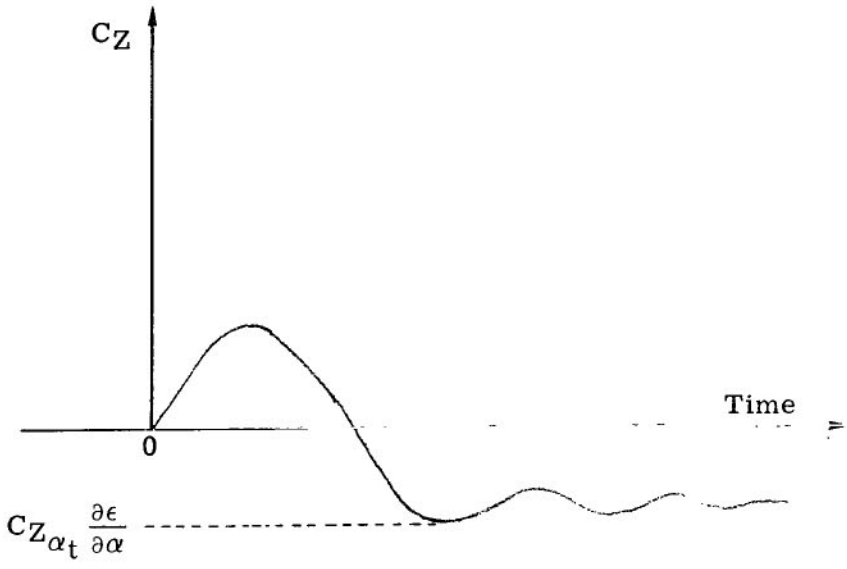

$$C_Z(t) = \left\{ -A\left(1 - e^{-at}\right) + B\left[1 - \frac{1}{\sqrt{1 - \zeta^2}} e^{-\zeta \omega_n t} \sin\left(\omega_n \sqrt{1 - \zeta^2}\, t + \phi\right)\right] \right\} \frac{\partial \epsilon}{\partial \alpha} C_{Z_{\alpha_t}}$$

where

$A = -4$

$B = -5$

$\omega_n = 35$

$\zeta = 0.7$

$a = 40$

$$\phi = \tan^{-1} \frac{\sqrt{1 - \zeta^2}}{\zeta}$$

$\bar{\alpha}_g$ Terms

The $\bar{\alpha}_g$ terms for equations (1) were

$$-C_{Z_{\alpha_w}} - C_{Z_{\alpha_t}}\left(1 - \frac{lc}{V} s\right) + C_{Z_{\alpha_t}} \frac{\partial \epsilon}{\partial \alpha}\left(1 - \frac{lc}{V} s\right)$$

whereas those for the unsteady lift representation were

$$\frac{-C_{Z_{\alpha_w}}}{\frac{3}{4}\frac{c}{V}s + 1.0} + \left(\frac{e^{-\frac{\ell c}{V}s}}{\frac{c_t}{V}s + 1.0}\right)C_{Z_{\alpha_t}} + \left[\frac{s^2(-Aa) + s\left(B\omega_n{}^2 + 2Aa\zeta\omega_n\right) + \left(B\omega_n{}^2 a - A\omega_n{}^2 a\right)}{\left(s^2 + 2\zeta\omega_n s + \omega_n{}^2\right)(s + a)}\right]\frac{\partial\epsilon}{\partial\alpha}C_{Z_{\alpha_t}}$$

The first term is the lift on wing due to penetration of the gust. The time-domain relationships for a step gust penetration are as follows:

Equations (1)

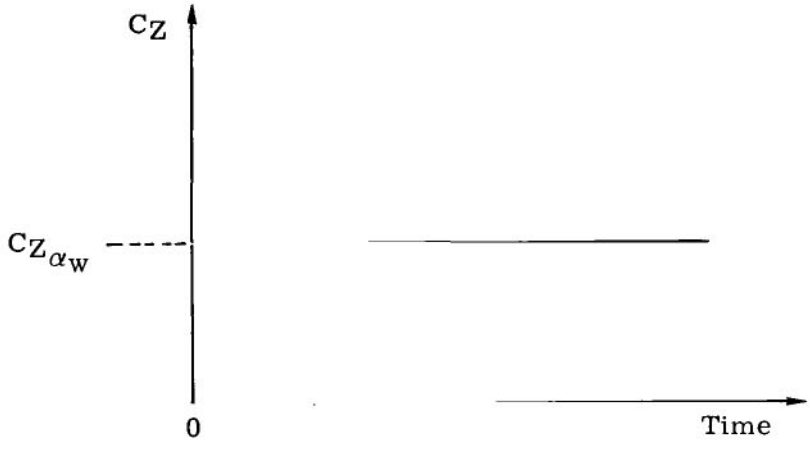

$$C_Z(t) = C_{Z_{\alpha_w}} u_s(t)$$

Unsteady lift

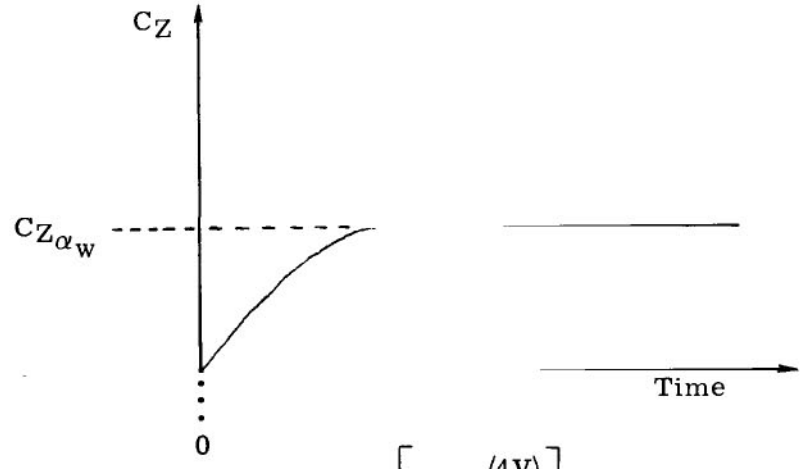

$$C_Z(t) = C_{Z_{\alpha_w}}\left[1 - e^{-\left(\frac{4V}{3c}\right)t}\right]u_s(t)$$

The second term is the transport lag term which accounts for the fact that the gust reaches the tail at a later time than it reaches the wing (which is used as the reference point). The time-domain relationships are as follows:

Equations (1)

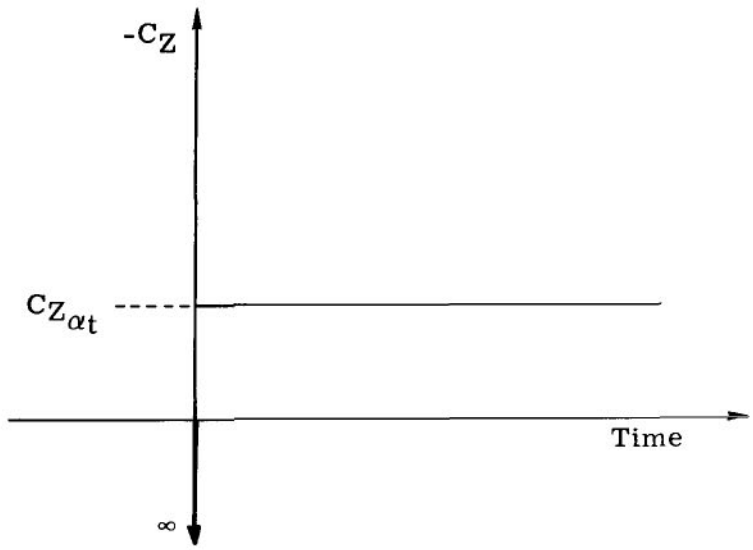

$$C_Z(t) = C_{Z_{\alpha_t}} \frac{l_c}{V} \delta(t) - C_{Z_{\alpha_t}} u_s(t)$$

Unsteady lift

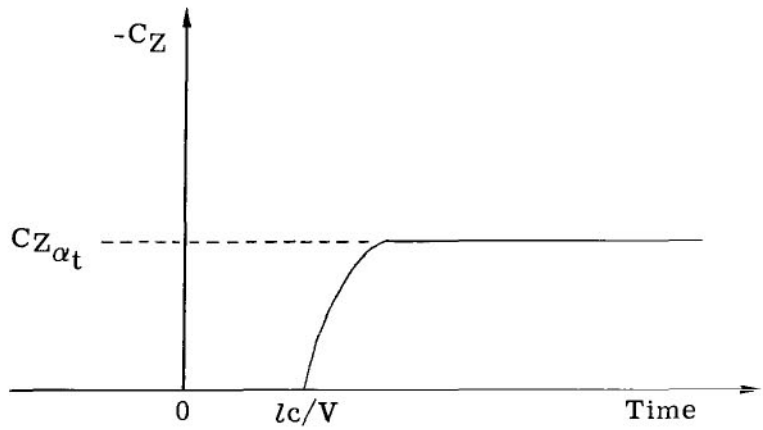

$$C_Z(t) = -C_{Z_{\alpha_t}} \left(1 - e^{-\frac{V}{c_t}t}\right) u_s\left(t - \frac{l_c}{V}\right)$$

The third term is the wing downwash term which also has a transport lag. Although it could have been represented with a transport lag term like the second term, a form like that for the second $\left(C_{Z_{\delta_f}}\right)_w$ term was used in order to account for the shed vortex. The parameters a, ω_n, and ζ were picked so that the function crossed back to the positive side at $t \approx \frac{lc}{V}$. This was done to account for the passage of the vortex shed off the wing as it penetrated the gust. The values were

$A = 4$

$B = 5$

$\omega_n = 35$

$\zeta = 0.7$

$a = 40$

The pitch equation follows a similar approach, the only change being that $C_{m_{\alpha_w}}$, $\left(C_{m_{\delta_f}}\right)_w$, and $C_{m_{\alpha_t}}$ are substituted for $C_{Z_{\alpha_w}}$, $\left(C_{Z_{\delta_f}}\right)_w$, and $C_{Z_{\alpha_t}}$. The flap equation had only two unsteady lift terms, $\bar{\alpha}_o$ and $\bar{\alpha}_g$, which had the forms of $C_{Z_{\alpha_w}}$ for plunging and penetration, respectively. The time constants and the initial value were selected for the chord and aspect ratio of the vane.

REFERENCES

1. Roskam, Jan: Opportunities for Progress in General Aviation Technology. AIAA Paper 75-292, Feb. 1975.

2. Phillips, William H.; and Kraft, Christopher C., Jr.: Theoretical Study of Some Methods for Increasing the Smoothness of Flight Through Rough Air. NACA TN 2416, 1951.

3. Hirsch, R.: L'Absorption des Rafales sur Avions et Résultats des Essais en Vol d'un Appareil Expérimental. Doc-Air-Escape, no. 105, July 1967, pp. 41-56.

4. Roesch, Phillippe; and Harlan, Raymond B.: A Passive Gust Alleviation System for a Light Aircraft. NASA CR-2605, 1975.

5. Hoak, D. E.; Finck, R. D.; et al.: USAF Stability and Control Datcom. U.S. Air Force, Oct. 1960. (Revised Feb. 1972.)

6. Stewart, Eric C.: Discussion of an Aeromechanical Gust Alleviation System To Improve the Ride Comfort of Light Airplanes. [Preprint] 750544, Soc. Automot. Eng., Apr. 1975.

7. Baird, D. C.: Experimentation: An Introduction to Measurement Theory and Experiment Design. Prentice-Hall, Inc., c.1962.

8. Ellis, David R.: Flying Qualities of Small General Aviation Airplanes. Part 4.- Review of Recent In-Flight Simulation Experiments and Some Suggested Criteria. FAA-RD-71-118, Dec. 1971. (Available from DDC as AD 739 880.)

9. Phillips, William H.: Study of a Control System To Alleviate Aircraft Response to Horizontal and Vertical Gusts. NASA TN D-7278, 1973.

10. Dommasch, Daniel O.; Sherby, Sydney S.; and Connolly, Thomas F.: Airplane Aerodynamics. Third ed., Pitman Pub. Corp., 1961.

11. Jones, Robert T.: The Unsteady Lift of a Finite Wing. NACA TN 682, 1939.

12. Jones, Robert T.; and Fehlner, Leo F.: Transient Effects of the Wing Wake on the Horizontal Tail. NACA TN 771, 1940.

TABLE I.- CHARACTERISTICS OF AIRPLANE

[Tunnel determined values are for $\alpha = 0$, $\delta_f = 0$, and center of gravity at 0.28c. Values used in ref. 4 are in parentheses.]

$C_{Z_{\alpha_w}} = -4.765 \pm 0.188$ $= (-5.07)$	$C_{m_{\alpha_w}} = 0.203 \pm 0.0209$ $= (0.203)$ [a]
$C_{Z_{\alpha_t}} = -0.664 \pm 0.029$ $= (-0.66)$	$C_{m_{\alpha_t}} = -1.948 \pm 0.015$ $= (-1.94)$ [b]
$\left(C_{Z_{\delta_f}}\right)_w = -1.073 \pm 0.076$ $= (-1.03)$	$\left(C_{m_{\delta_f}}\right)_w = -0.164 \pm 0.015$ $= (-0.352)$ [c]
$\left(C_{Z_{\delta_e}}\right)_t = -0.304 \pm 0.011$ $= (-0.429)$ [d]	$\left(C_{m_{\delta_e}}\right)_t = -0.962 \pm 0.039$ $= (-1.26)$
$\frac{\partial \epsilon}{\partial \alpha} = 0.276 \pm 0.0025$ $= (0.37)$	$\frac{\partial \epsilon}{\partial \delta_f} = 0.098 \pm 0.0086$ $= (0.15)$
$l = 2.934 \pm 0.061$	$l_n = 0$
$\rho = 1.05808$ kg/m^3	V = 59 m/sec
c = 1.48 m	S = 16.26 m^2
$k_y = 1.3$ m	$i_r = 0.063$
m = 1000 kg	

[a] Not given directly in reference 4. Calculated by using $C_{Z_{\alpha_w}}$ for present center of gravity and assuming the aerodynamic center of the wing fuselage was at 0.25c.

[b] Not given directly in reference 4. Calculated from C_{m_q} which was given, and assuming that C_{m_q} was due entirely to the tail and a tail length of 2.94c.

[c] Extrapolated to present center of gravity (0.28c).

[d] Not given directly in reference 4. Calculated from $\left(C_{m_{\delta_e}}\right)_t$ which was given, using tail length of 2.94c.

TABLE II.- OUTLINE OF TYPE OF CALCULATIONS USED AND SUBJECTS STUDIED

Subject	Type of calculation							
	Root locus	Frequency response for gust input	Frequency response for elevator input	Power spectra	Time history for step gust input	Time history for step input elevator	Static stability	Elevator position required for trimmed flight
Unsteady lift effects	X	X						
Experimental uncertainty	X			X				
Static alleviation factor	X			X	X			
Flap natural frequency and damping	X			X				
Center-of-gravity location				X				
Passenger location				X				
Flap-elevator interconnect				X				
Pitch-damper				X				
Handling characteristics			X			X	X	X

TABLE III.- VALUE OF PARAMETERS USED IN STICK-FIXED HANDLING CHARACTERISTICS CALCULATIONS

$C_{h_\alpha} = -3.0$ [a]	$C_{h_{\delta_f}} = -0.5$ [a]	$K_s = -375$ N-m/rad [a]
$C_{m_o} = 0.075429$	$\alpha_{trim} = 3.57^o$	$m' = 0.616$ [b]

K_H	K_o, N-m	i, deg (c)	α_V, deg (c)
0	0	-3.57	0
.75	260	0	3.57
1.00	347	1.19	4.76
1.50	520	3.57	7.14

[a] These values result in a static vertical alleviation factor of $K_V = 0.75$ at the trimmed flight condition $V = 59$ m/sec.

[b] This value results in the $d\delta_e/dC_L$ for steady accelerated flight being equal to that of the basic airplane.

[c] At the trimmed flight condition $V = 59$ m/sec.

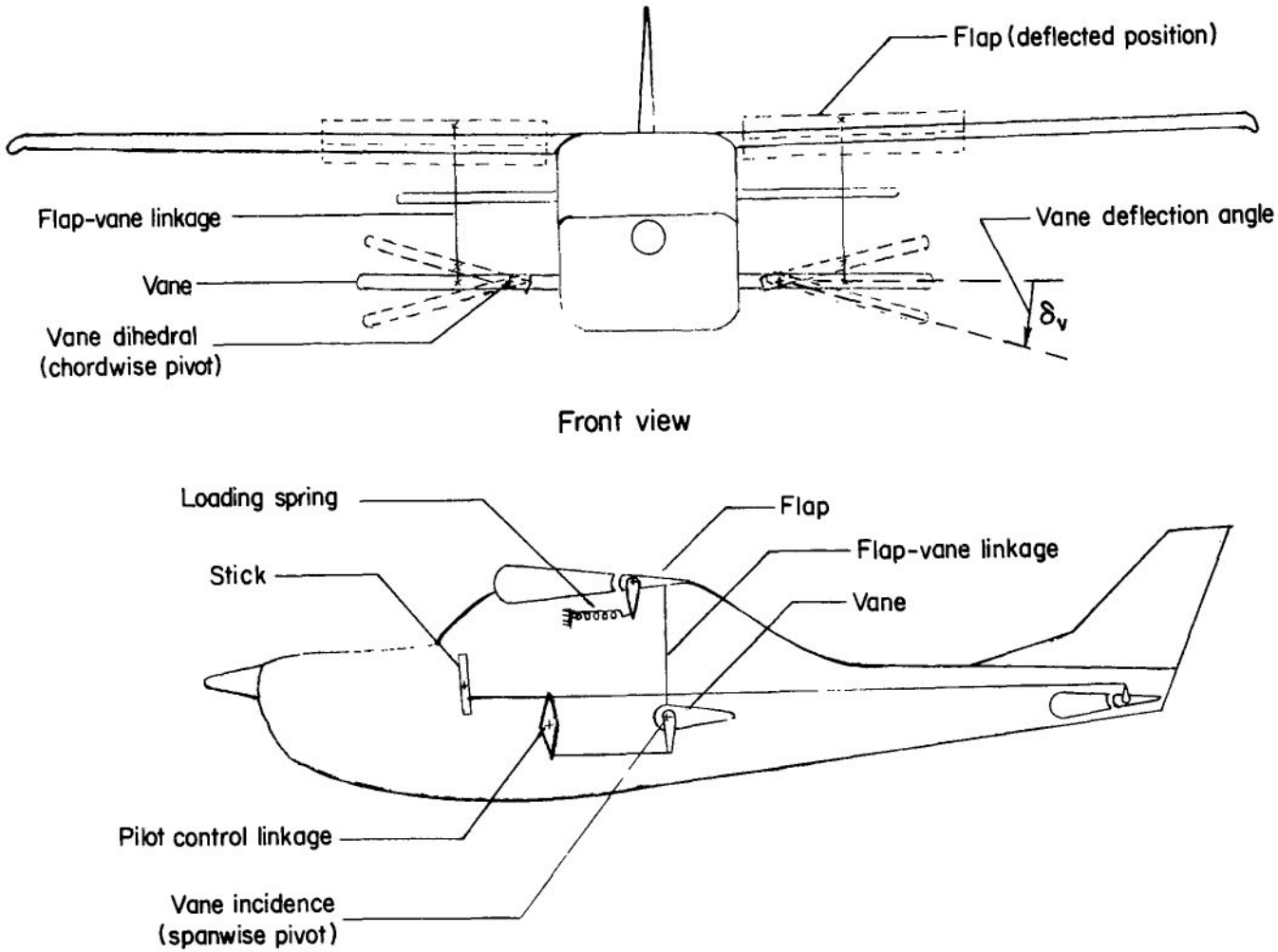

Figure 1.- Schematic representation of gust-alleviation system.

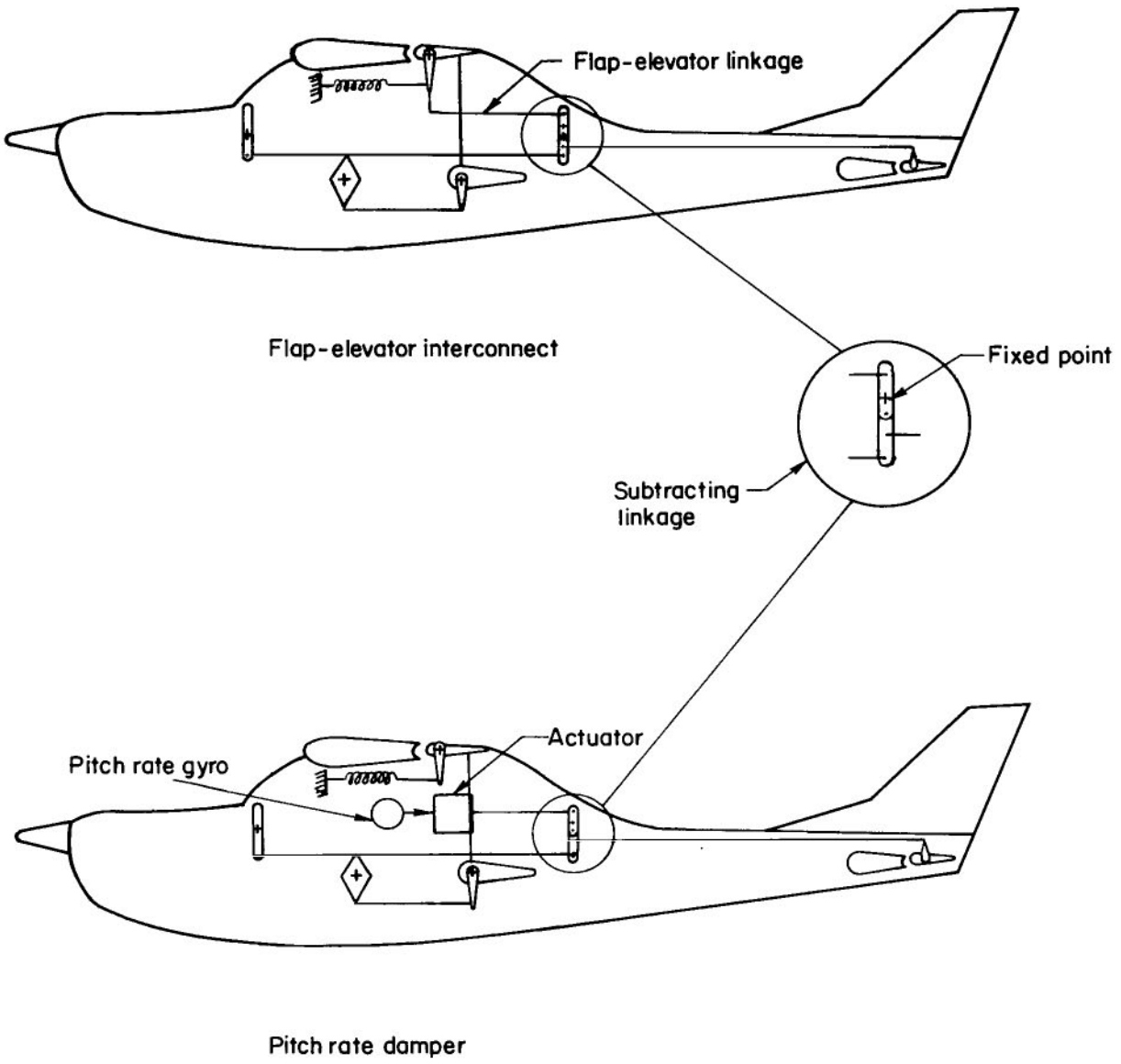

Figure 2.- Schematic representations of flap-elevator interconnect and pitch rate damper systems.

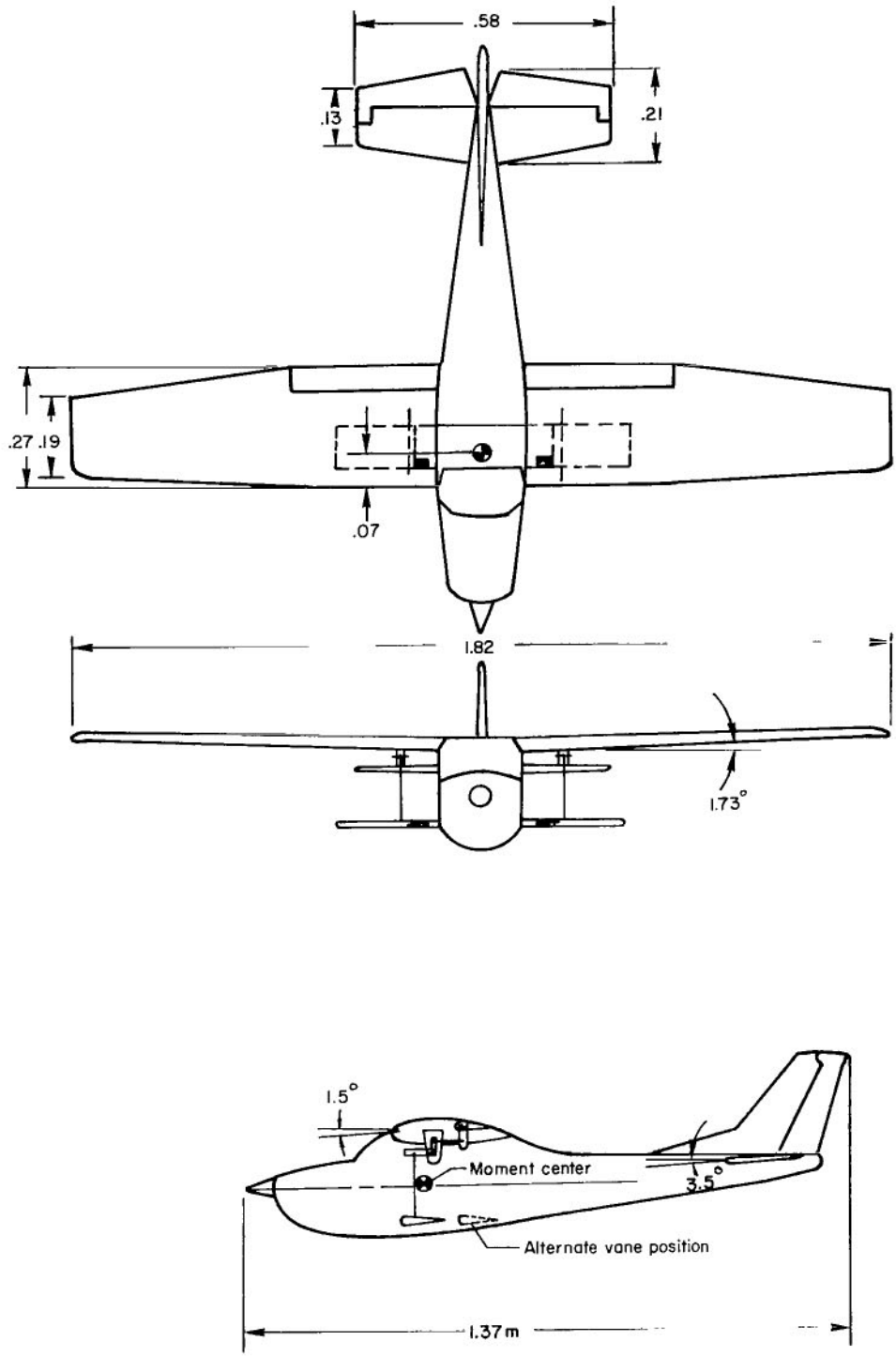

(a) Three-view drawing of model. All dimensions are in meters.

Figure 3.- Three-view drawing of model and detailed views of vane and flap.

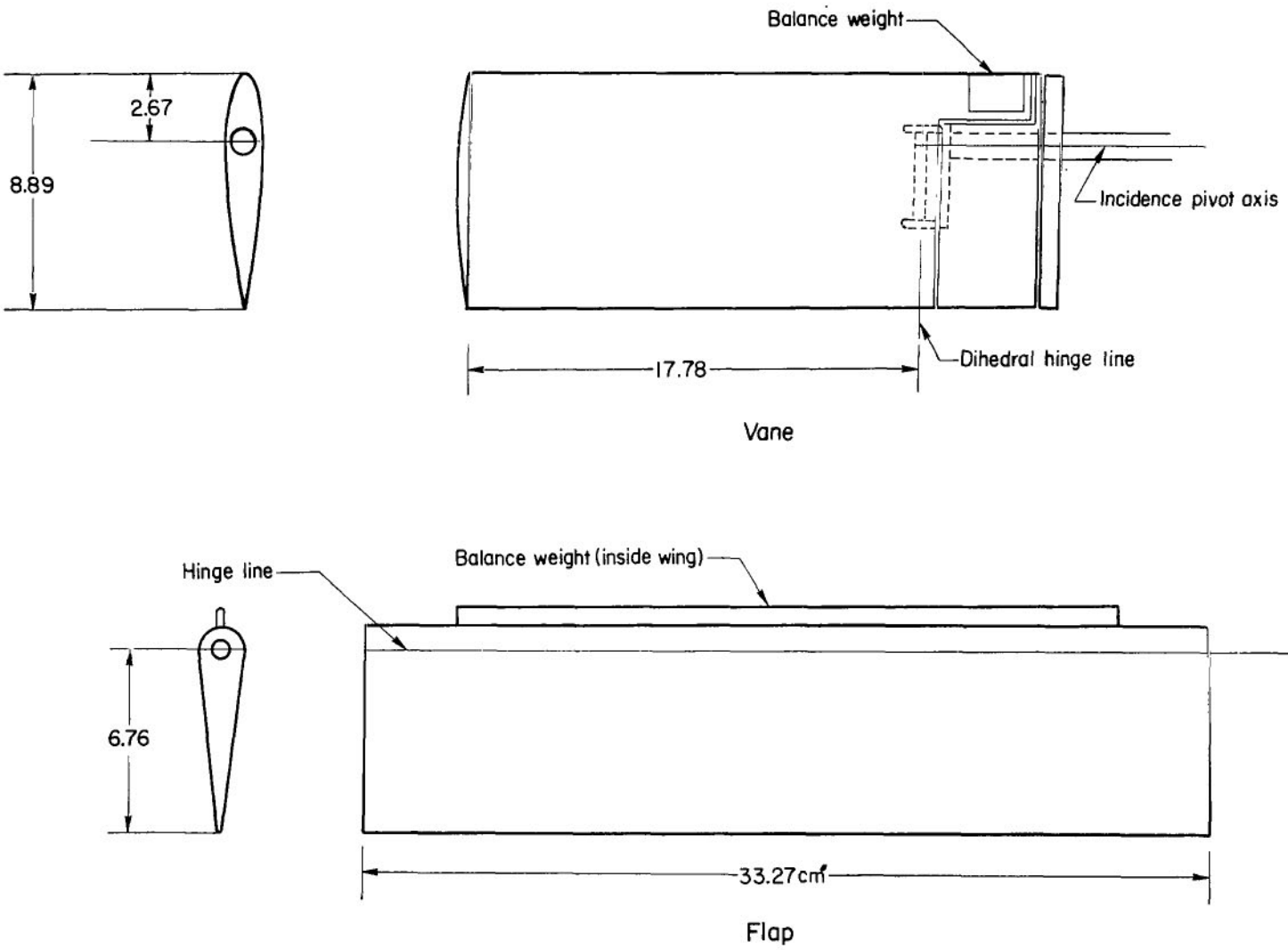

(b) Detailed views of vane and flap. All dimensions are in centimeters.

Figure 3.- Concluded.

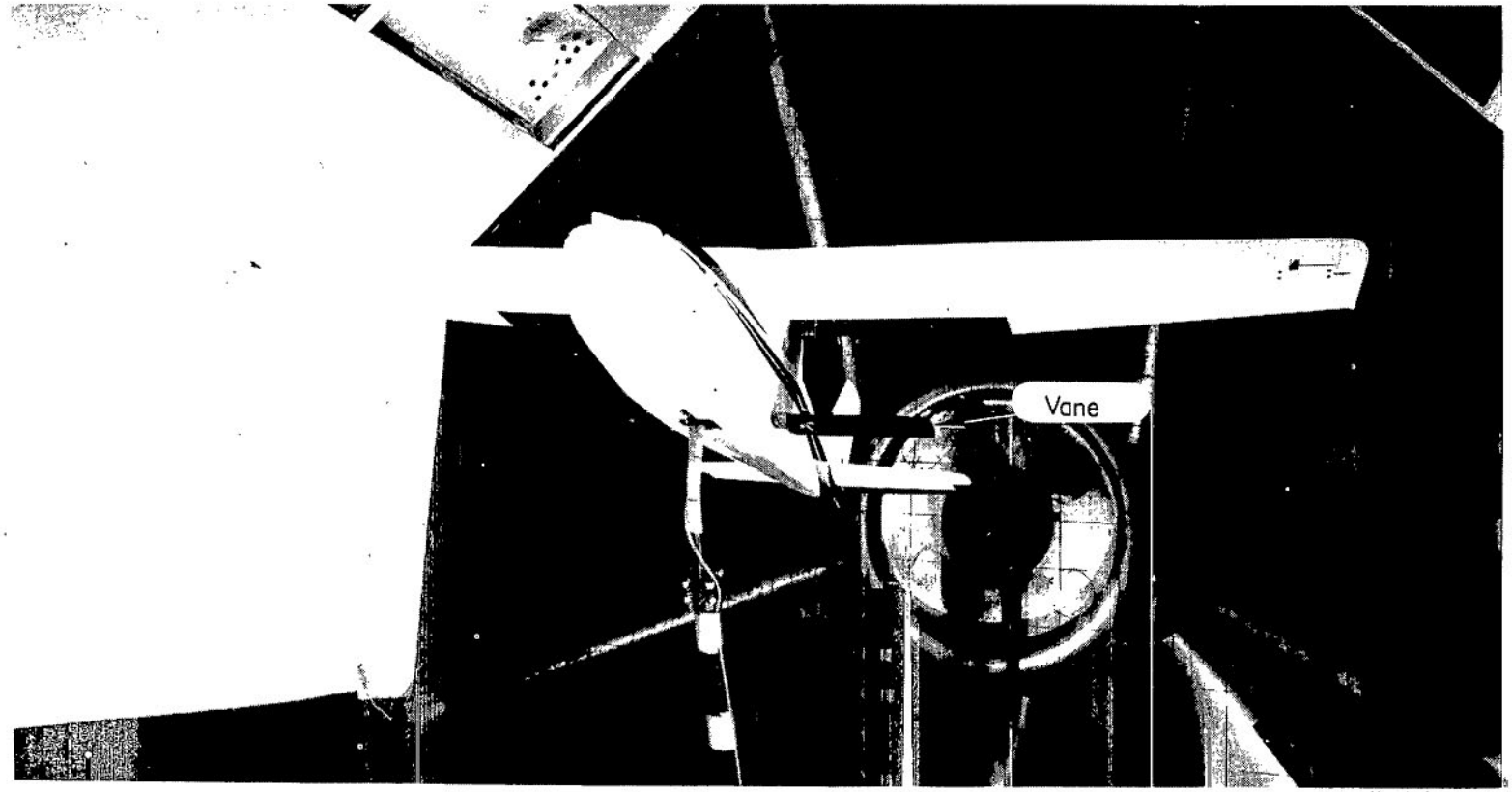

L-74-8315

Figure 4.- 1/6-scale model mounted in Langley low-speed tunnel with 12-foot (3.66-meter) octagonal test section. Vane mounted at 0.80c.

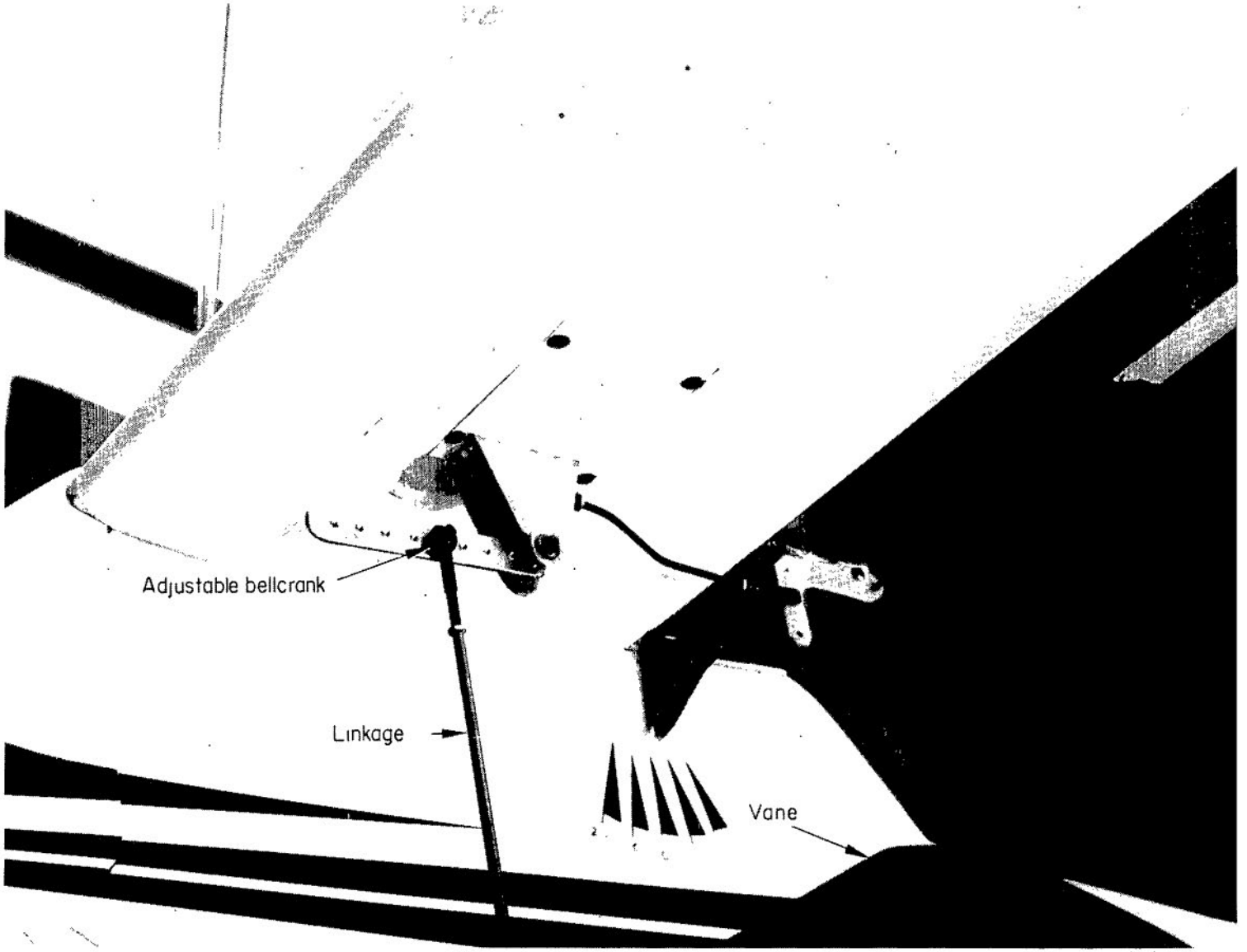

L-75-6252

Figure 5.- Mechanical linkage between vane and flap showing holes in bellcrank used to vary mechanical gain between vane and flap. Vane located at 0.26c.

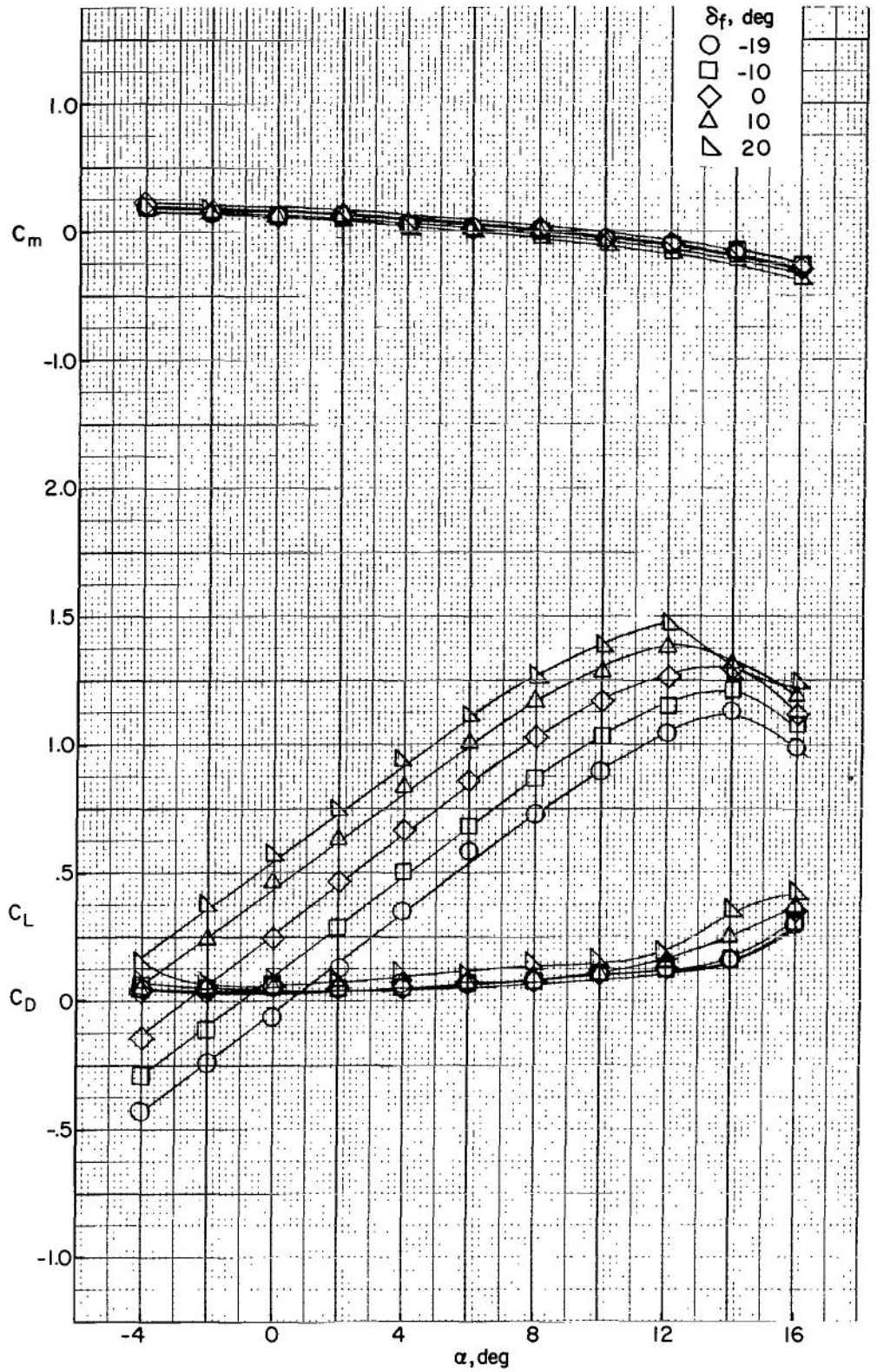

Figure 6.- Longitudinal aerodynamic characteristics of basic model for several flap deflections.

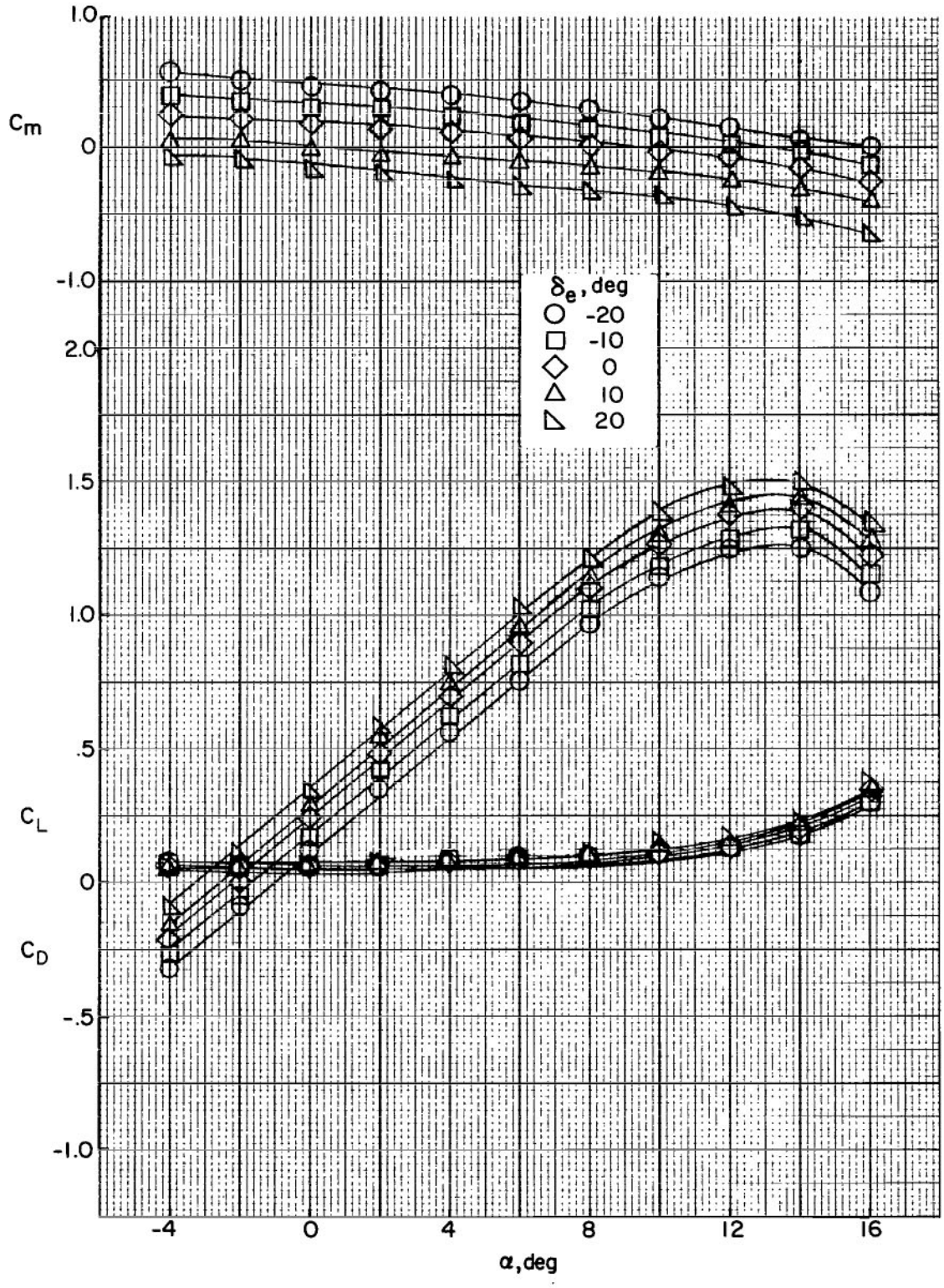

Figure 7.- Longitudinal aerodynamic characteristics of basic model for several elevator deflections.

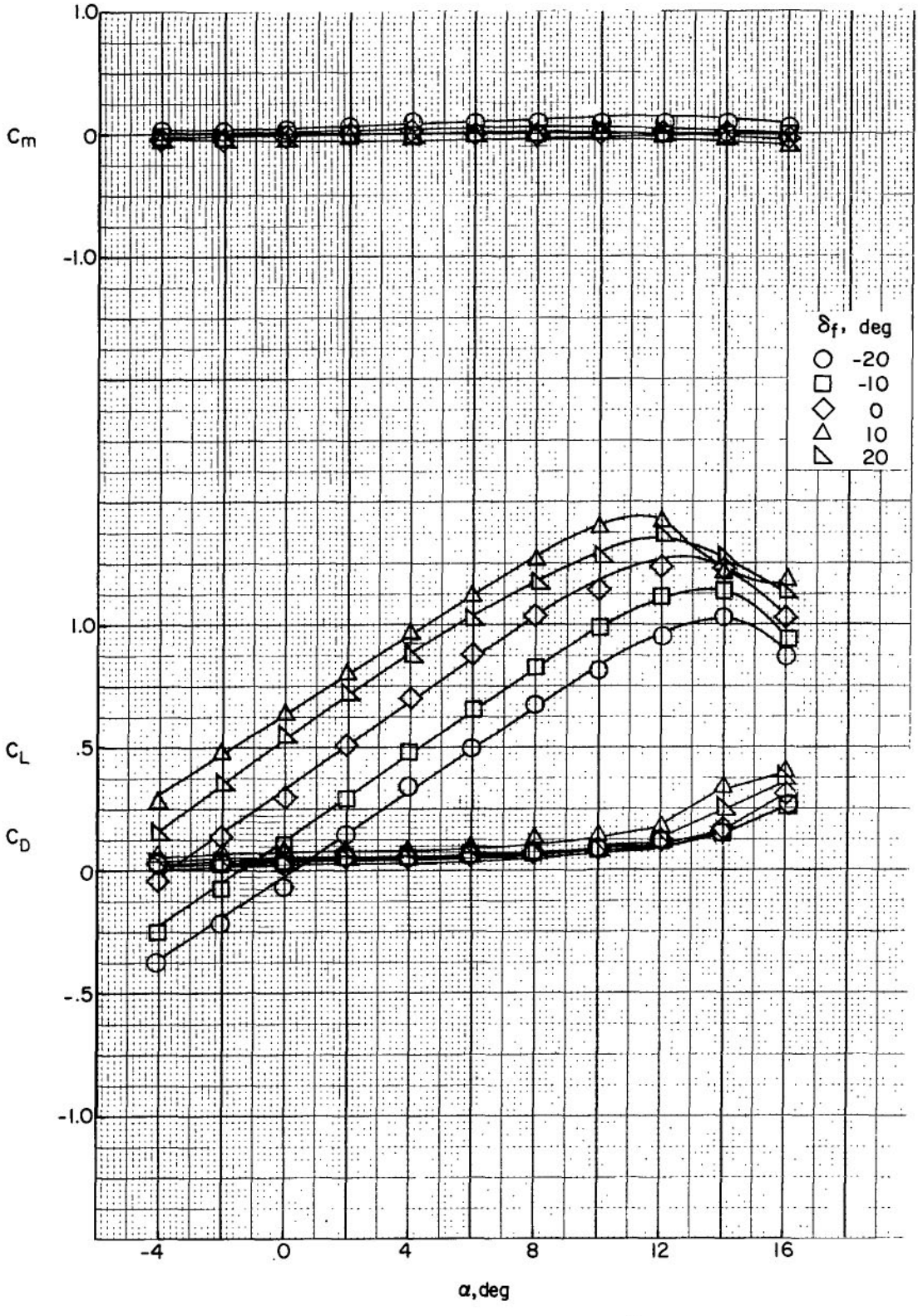

Figure 8.- Longitudinal aerodynamic characteristics of model wing-fuselage combination (horizontal tail removed) for several flap deflections.

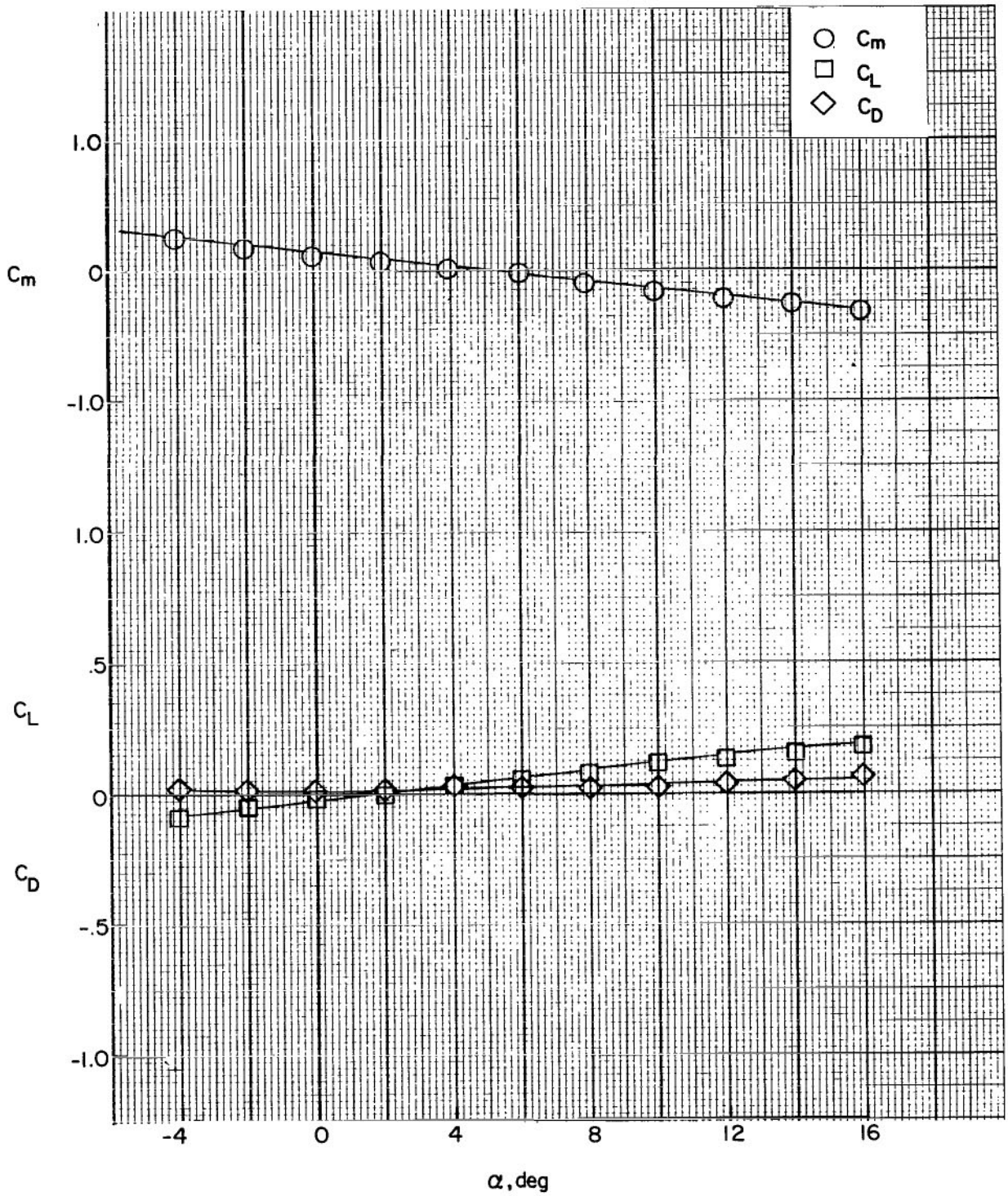

Figure 9.- Longitudinal aerodynamic characteristics of model fuselage-tail combination (wing removed).

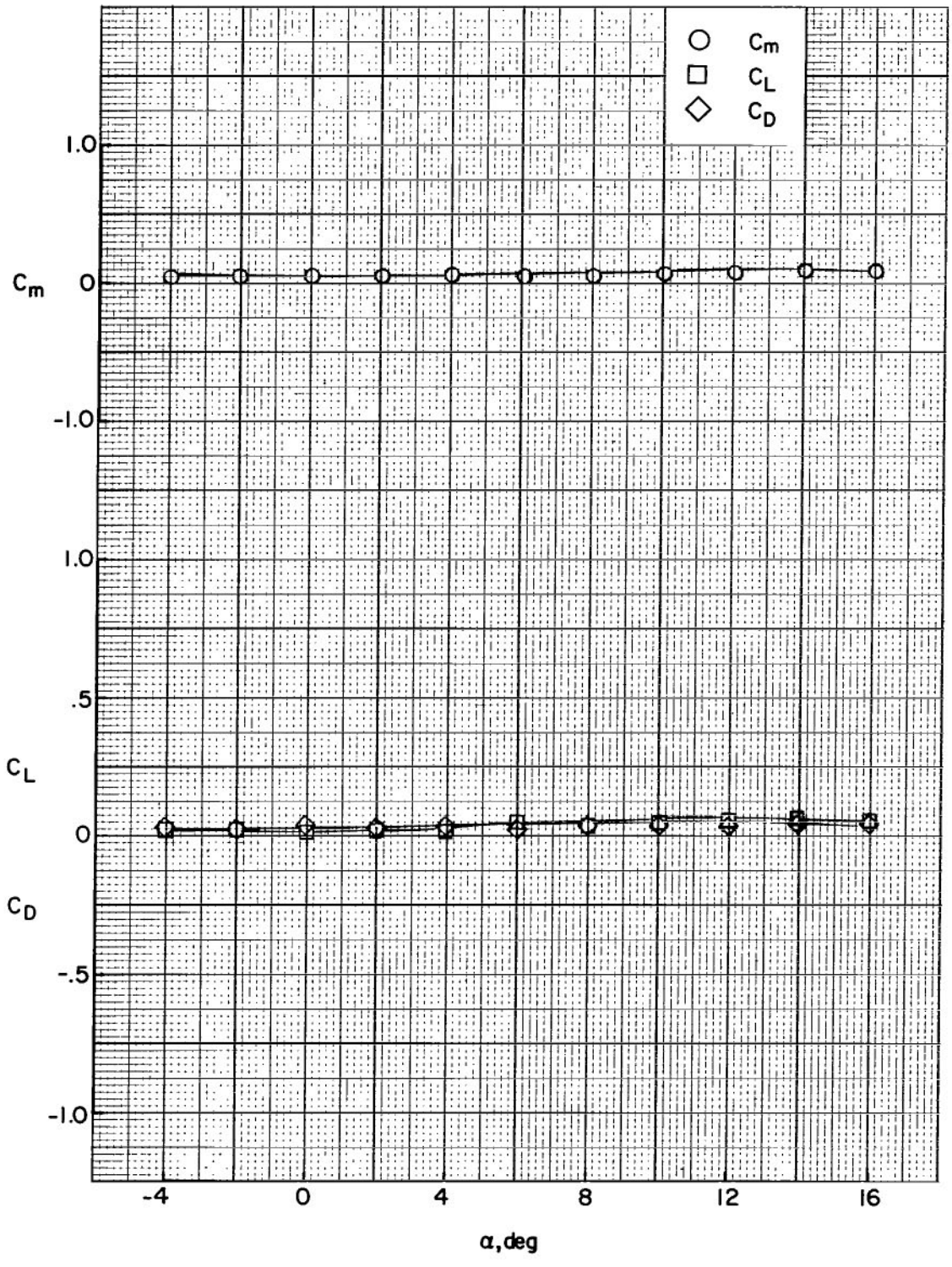

Figure 10.- Longitudinal aerodynamic characteristics for model fuselage (wing and horizontal tail removed).

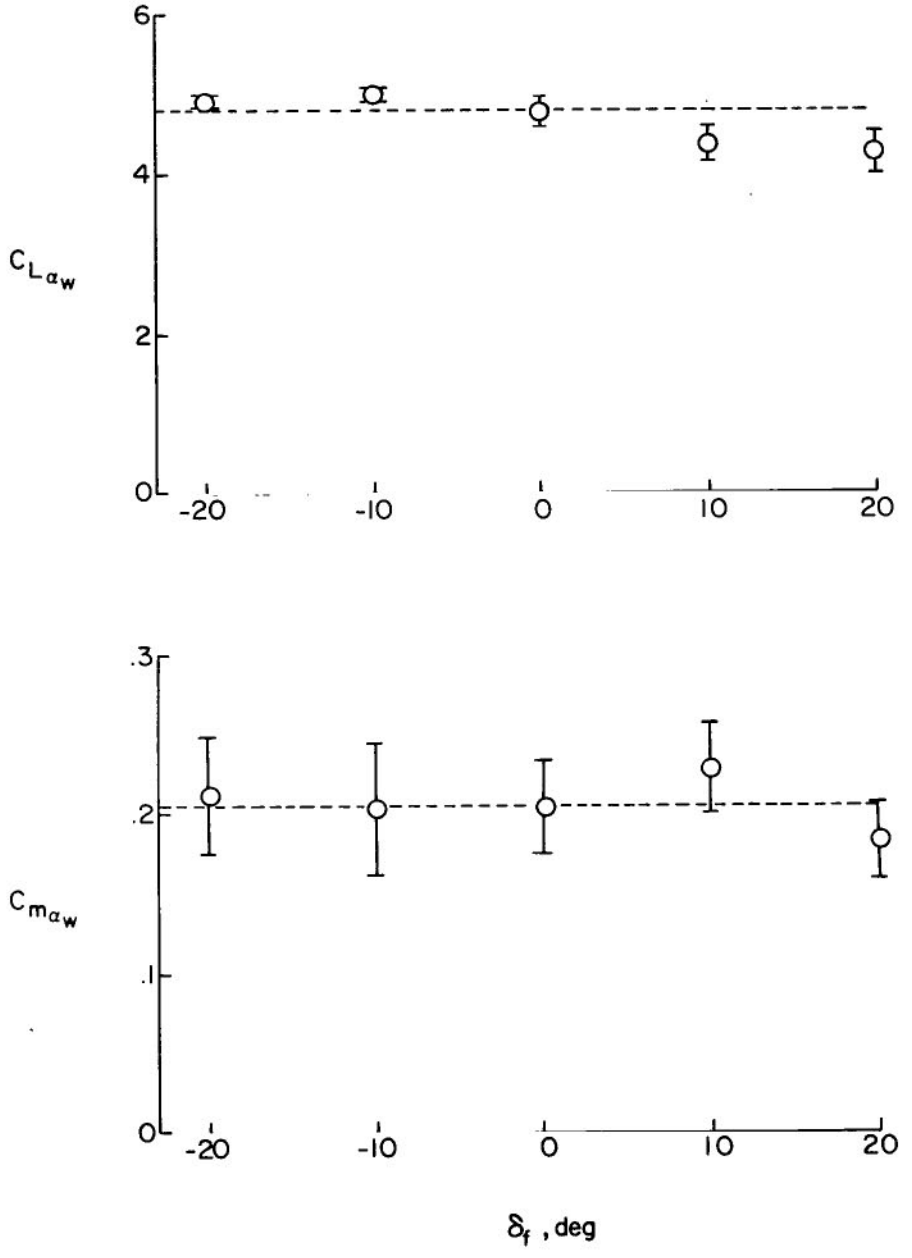

Figure 11.- Calculated lift and pitching-moment coefficient variations with angle of attack for model wing-fuselage combination for several flap deflections.

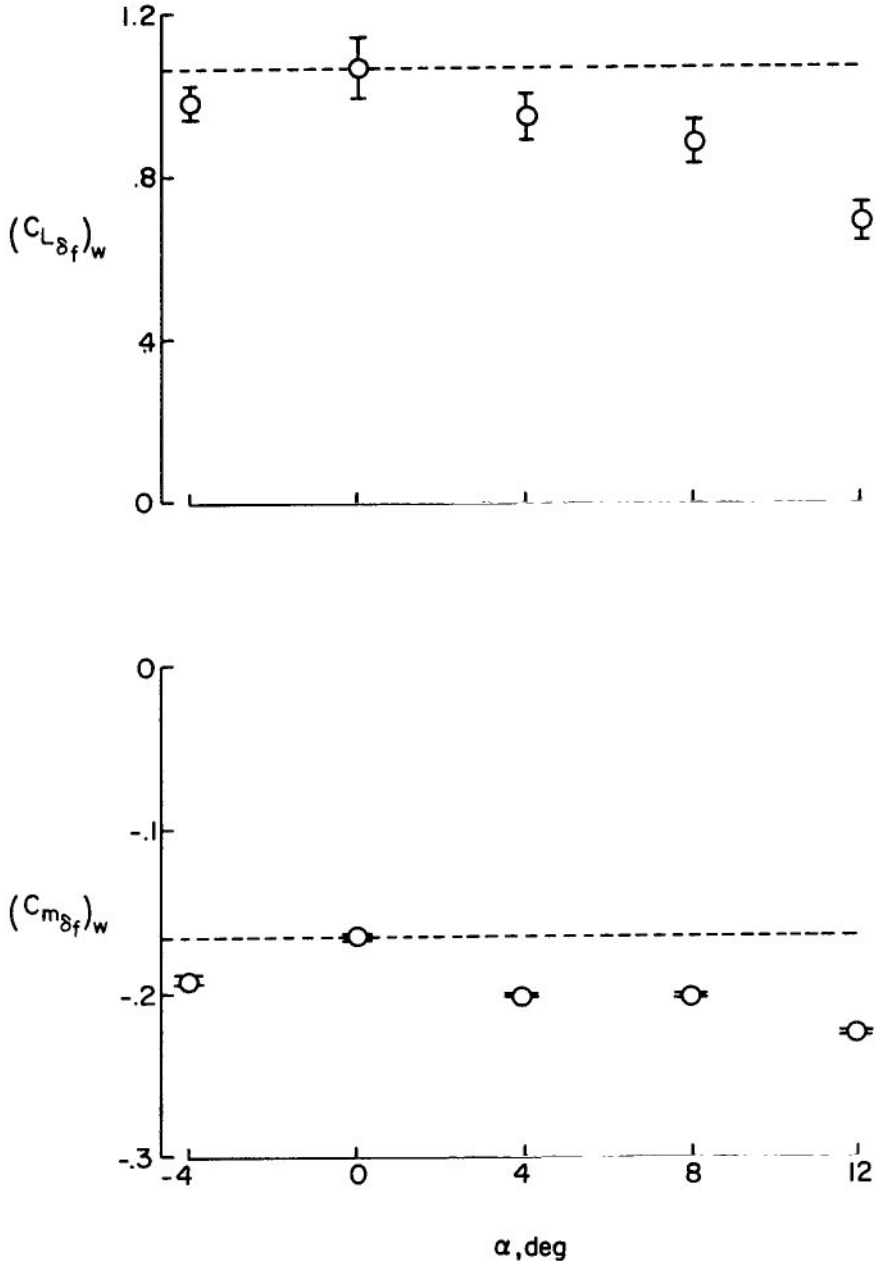

Figure 12.- Calculated lift and pitching-moment coefficient variation with flap deflection for model wing-fuselage combination for several angles of attack.

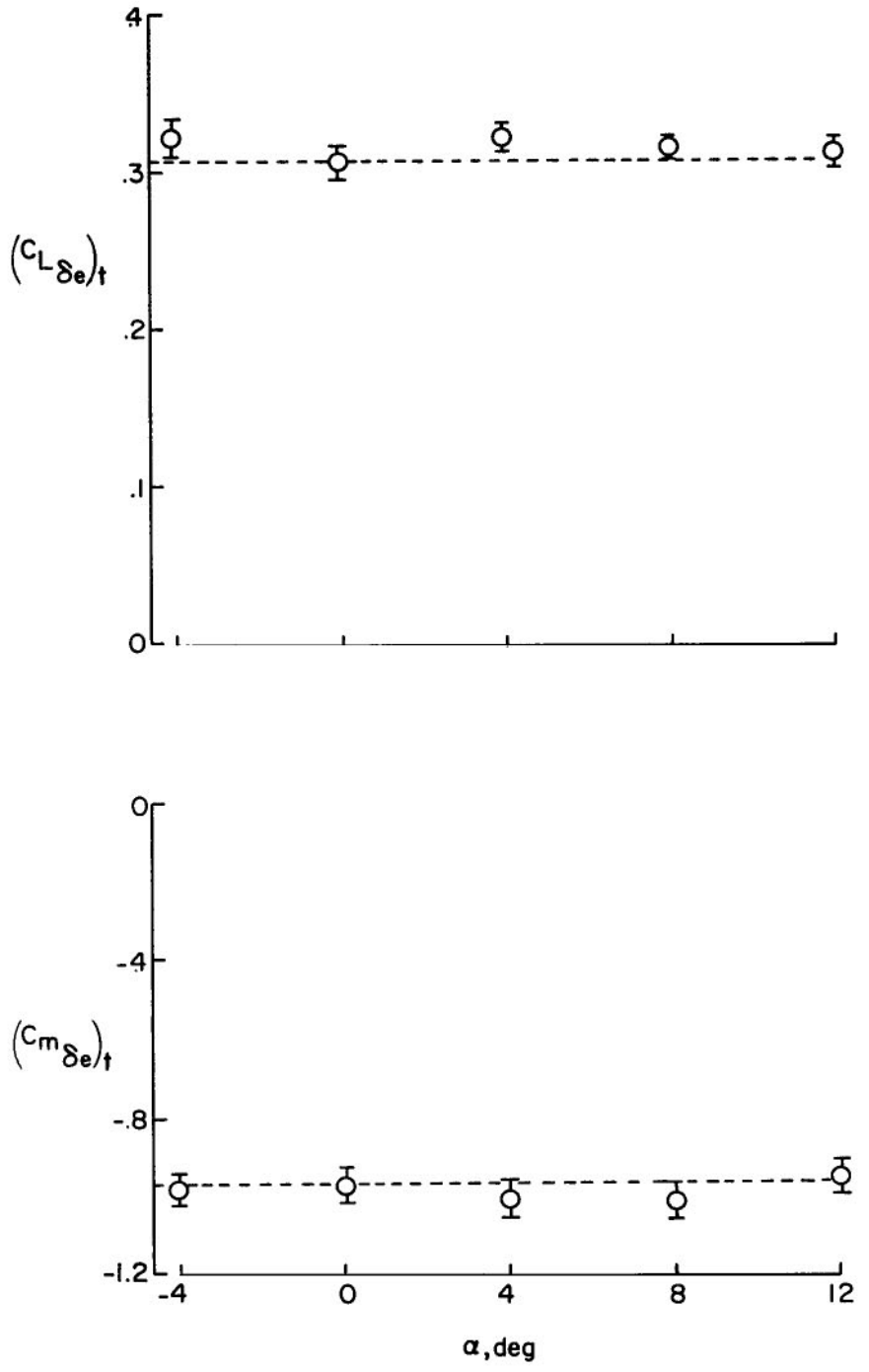

Figure 13.- Calculated variation of lift and pitching-moment coefficients with elevator deflection for basic model for several angles of attack.

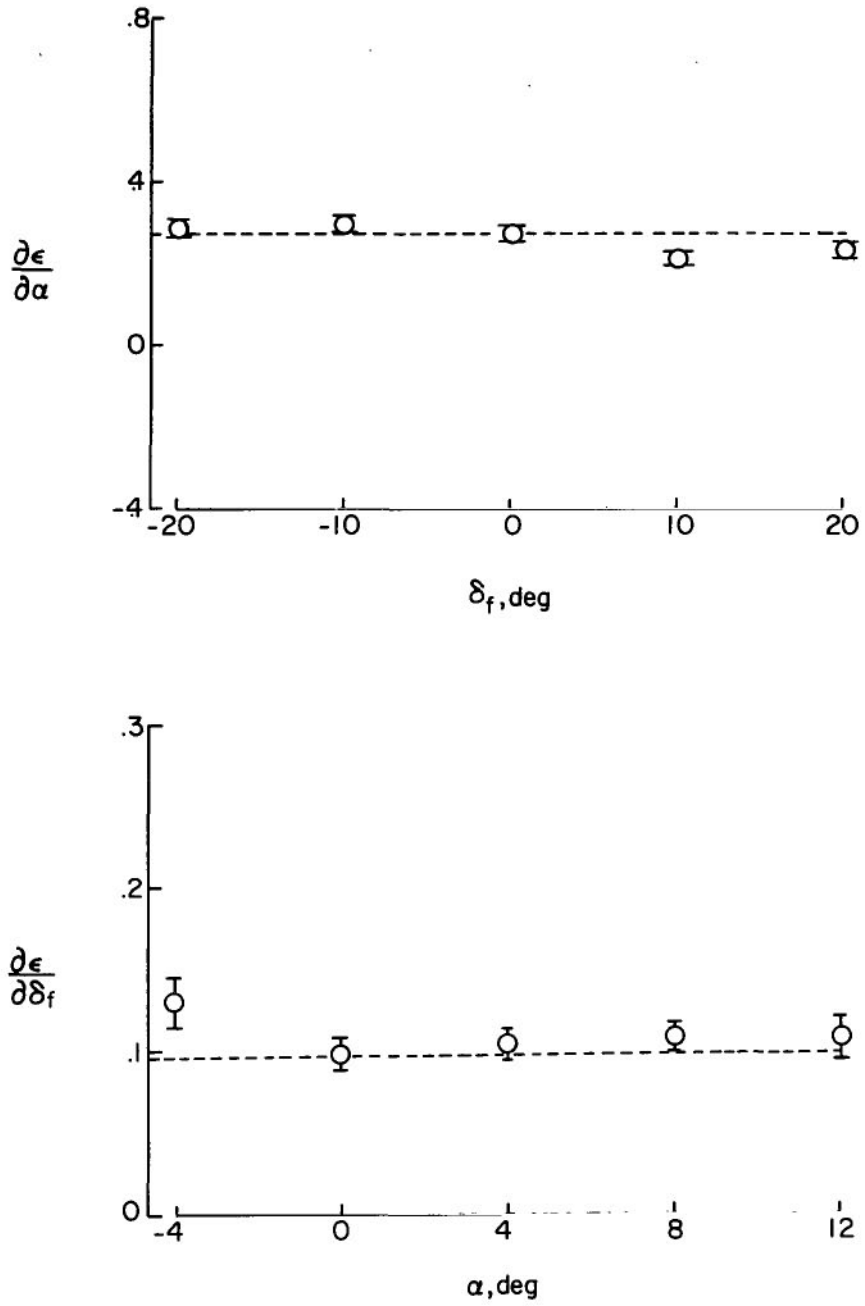

Figure 14.- Calculated variation of downwash at horizontal tail with angle of attack and flap deflection.

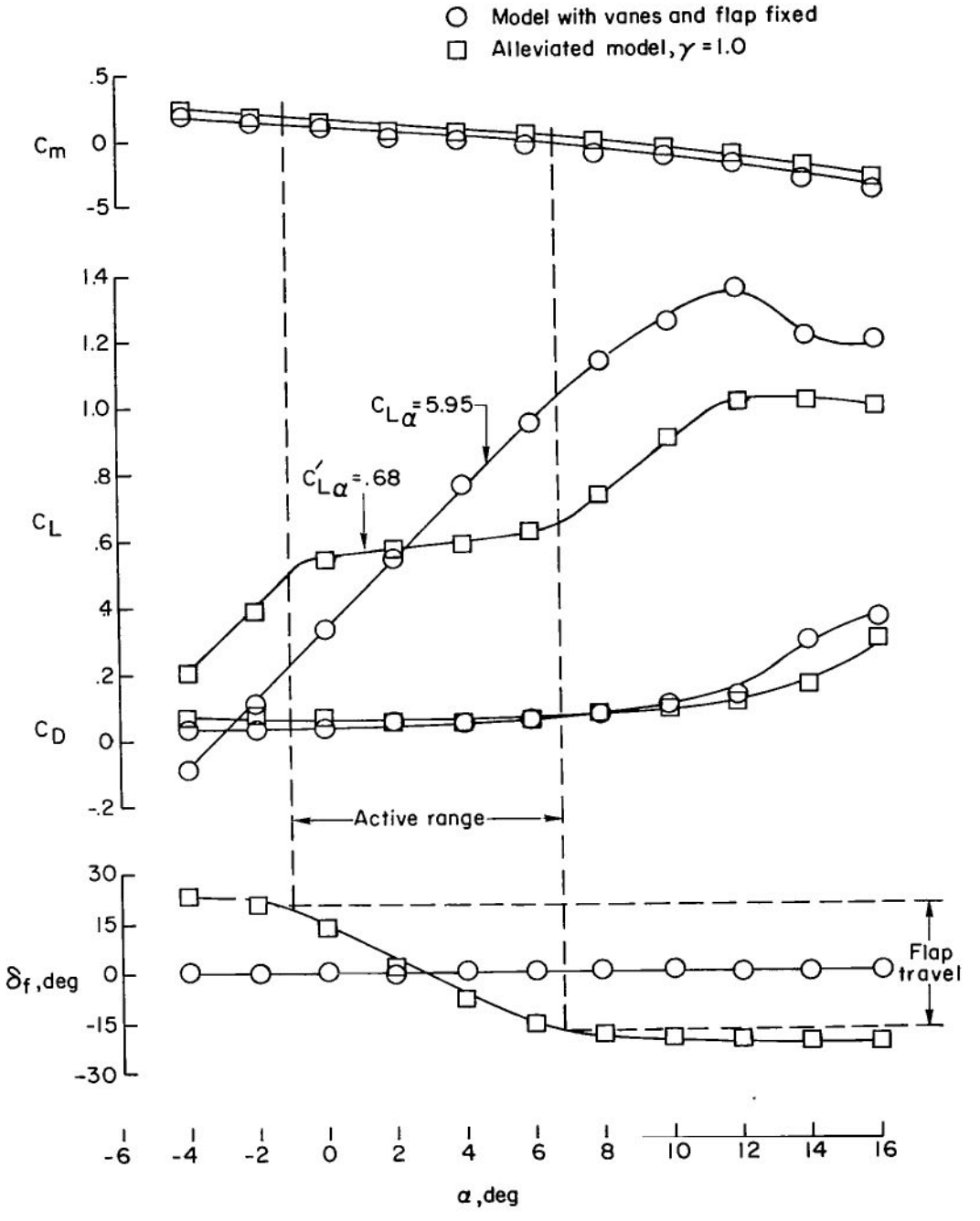

Figure 15.- Static effects of alleviation system on model characteristics.

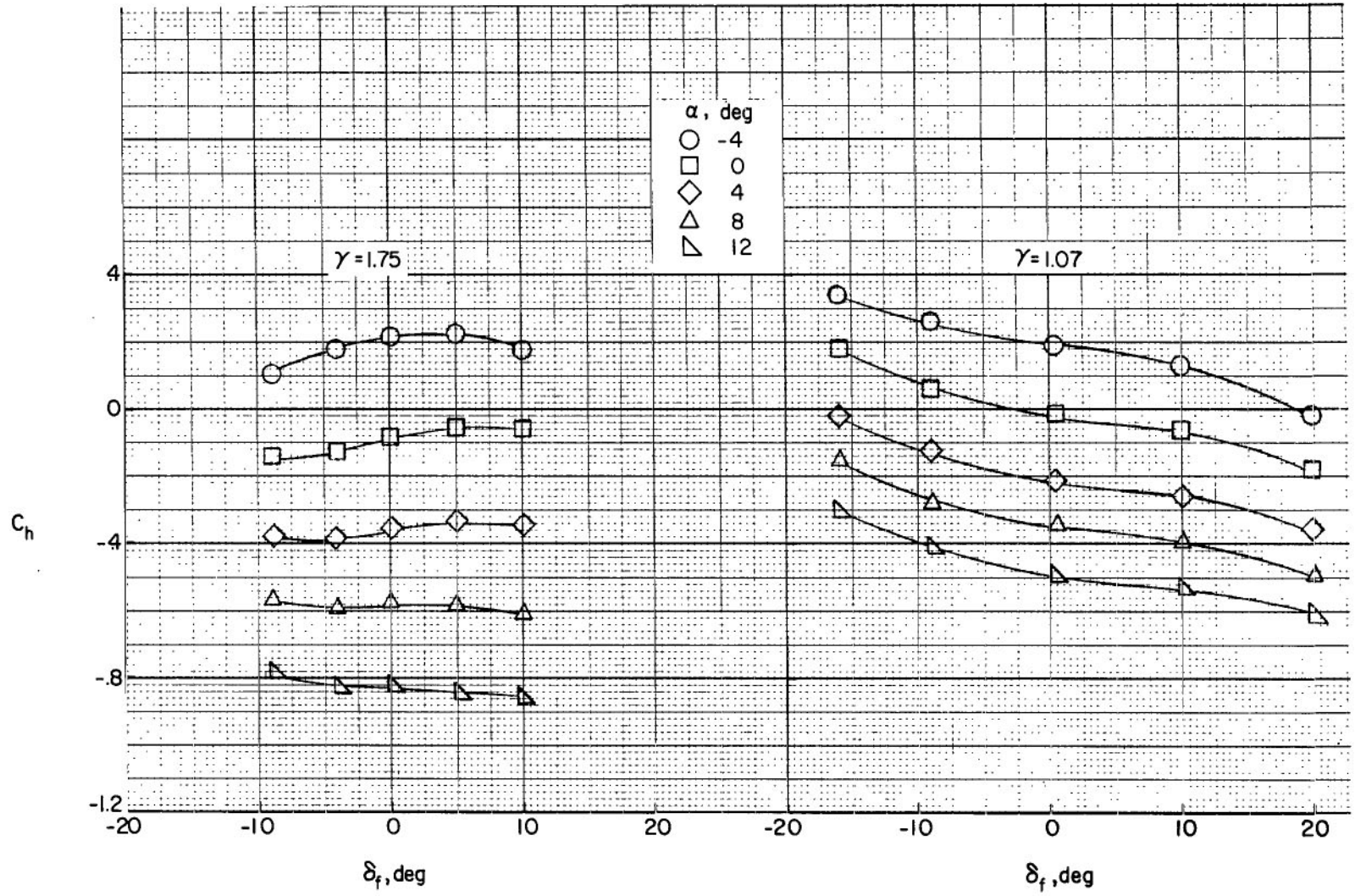

(a) Vane located at 0.80c.

(b) Vane located at 0.26c.

Figure 16.- Hinge-moment coefficients of combined flap-vane system for two longitudinal locations of vane.

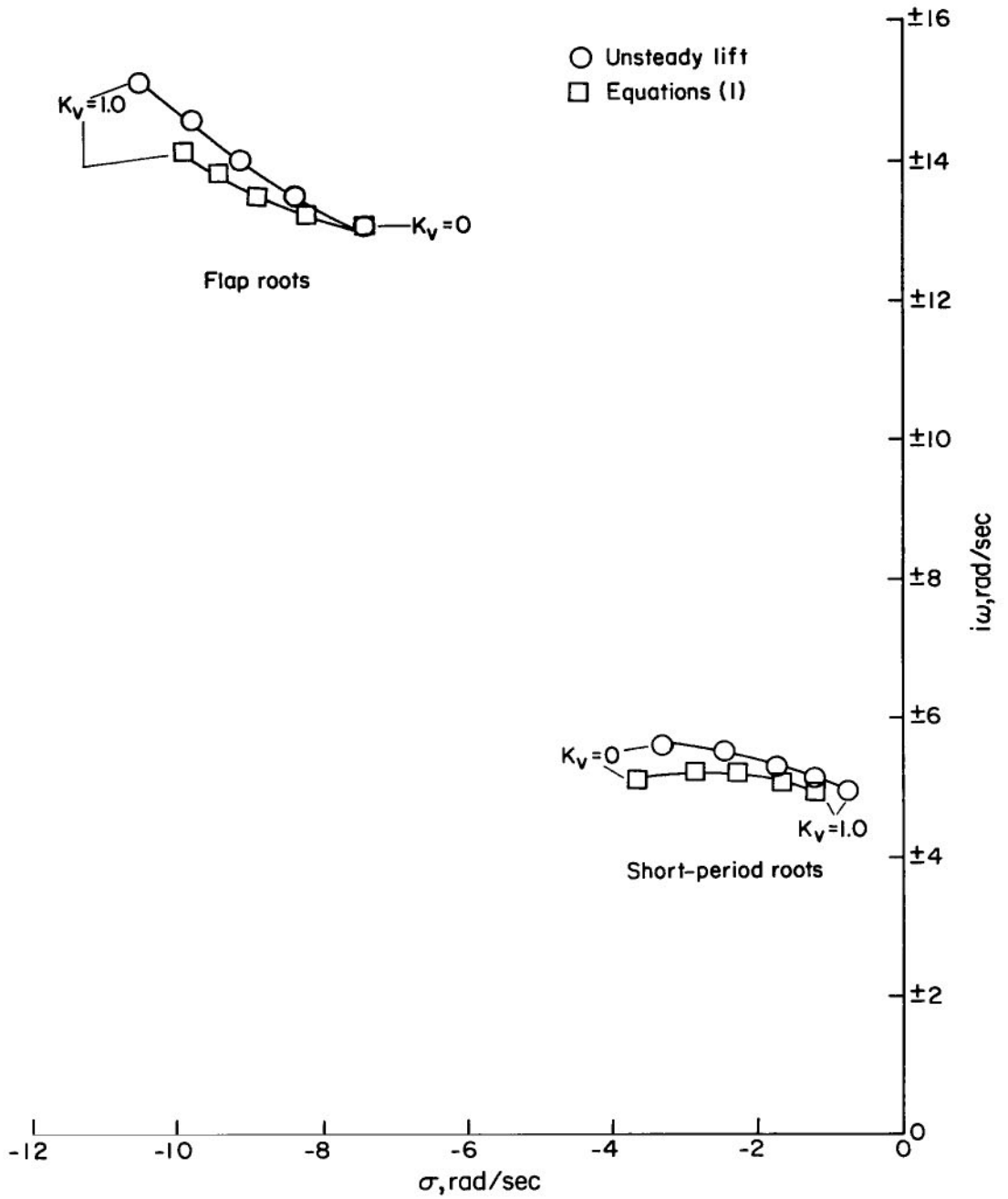

Figure 17.- Comparison of characteristic roots obtained from unsteady lift equations and from equations (1).

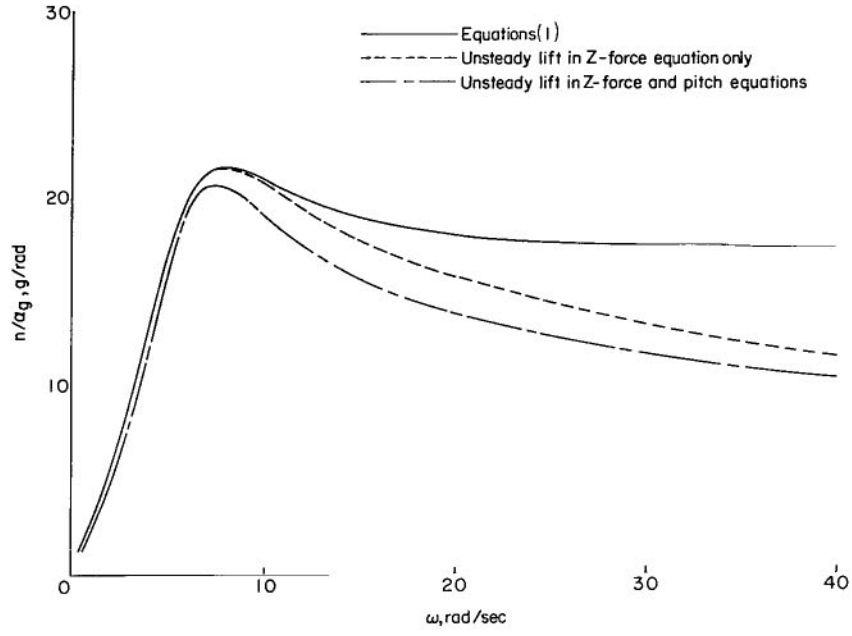

(a) Basic airplane.

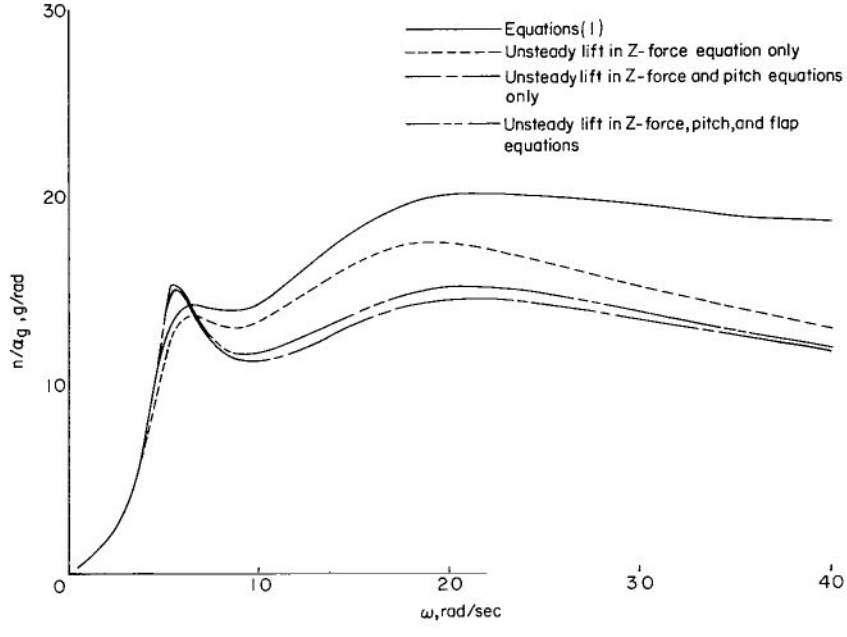

(b) Alleviated airplane. $K_V = 0.75$.

Figure 18.- Comparison of normal acceleration frequency response for different levels of unsteady lift representation with a gust forcing function.

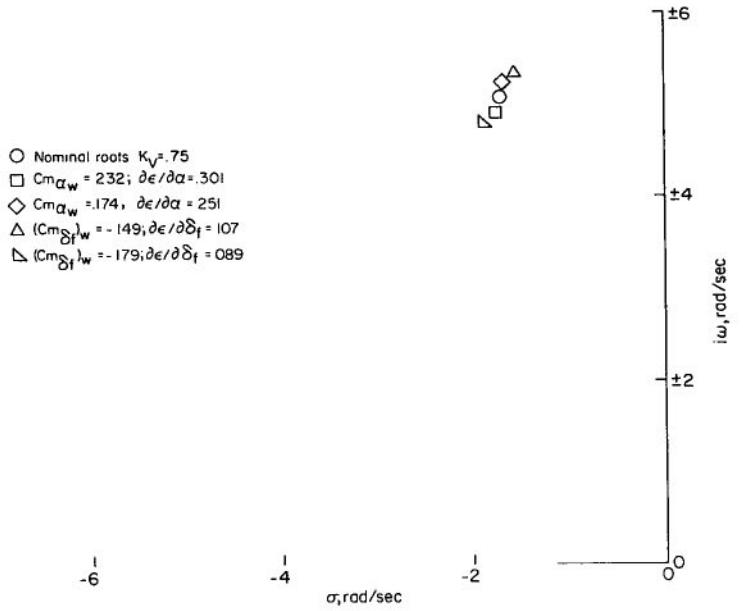

(a) Short-period roots.

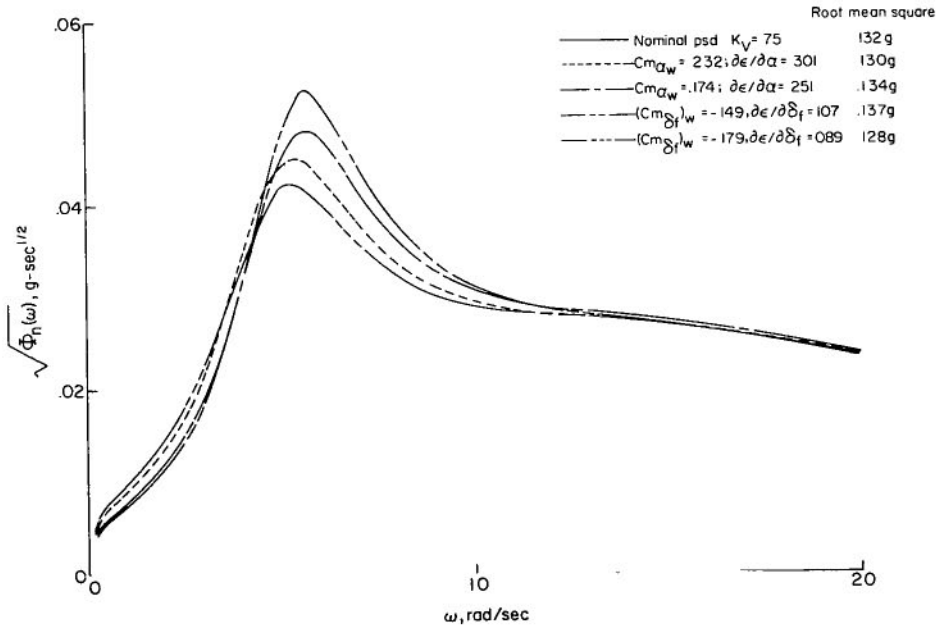

(b) Normal acceleration.

Figure 19.- Variability of results due to experimental uncertainty in tunnel-determined aerodynamic parameters.

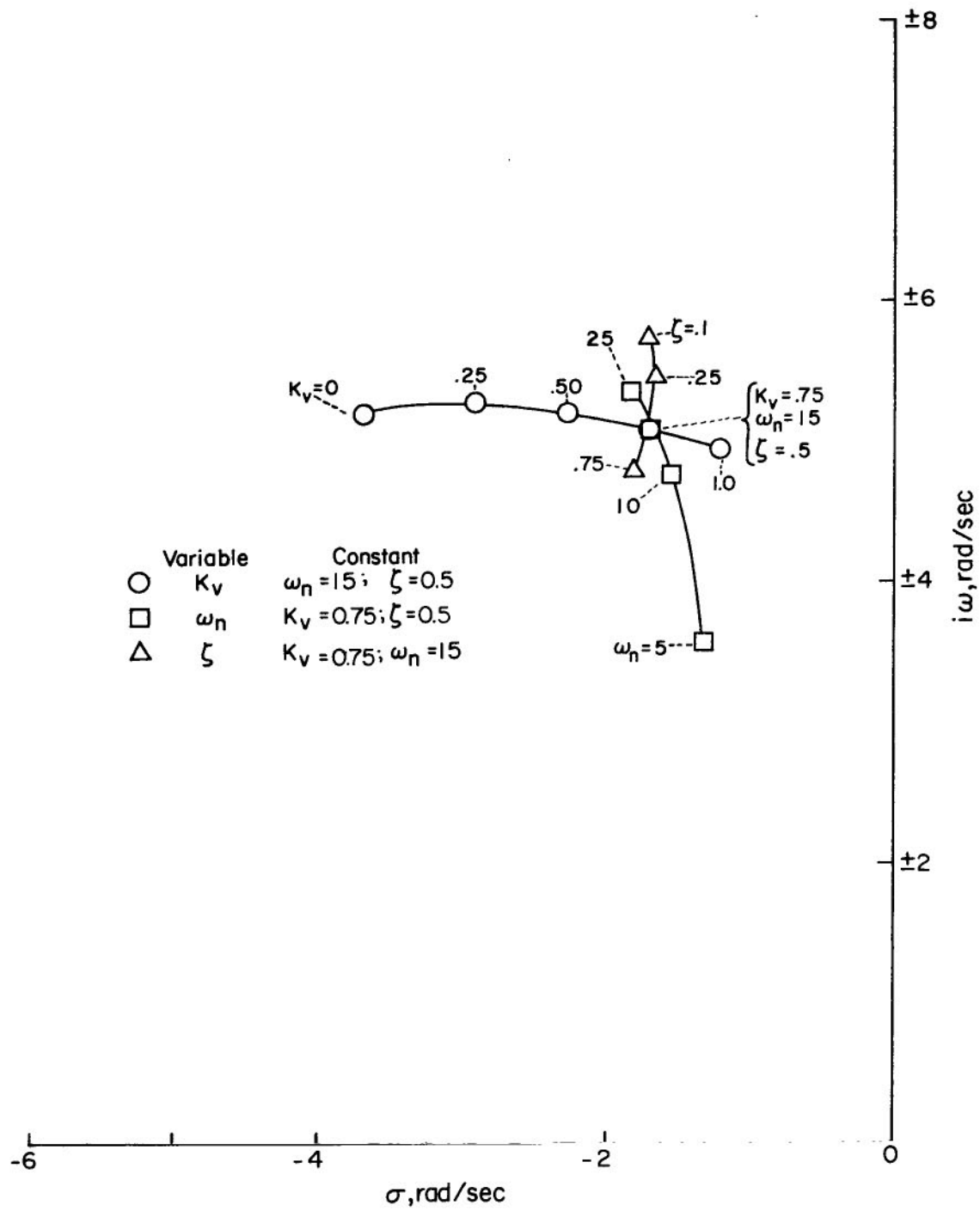

Figure 20.- Locus of short-period roots for variations of static vertical alleviation factor, flap-vane natural frequency, and damping ratio.

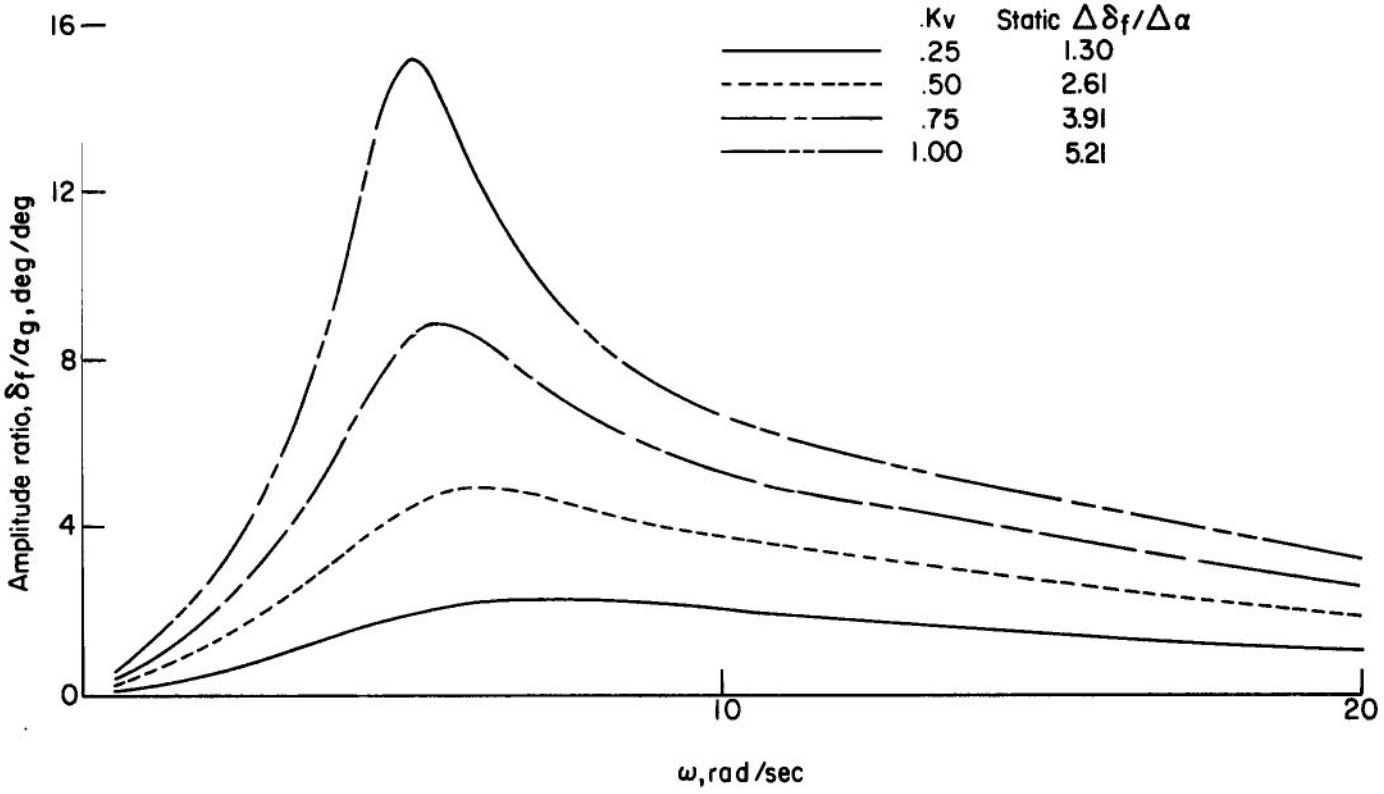

Figure 21.- Flap frequency response for different levels of static vertical alleviation factor with a gust forcing function.

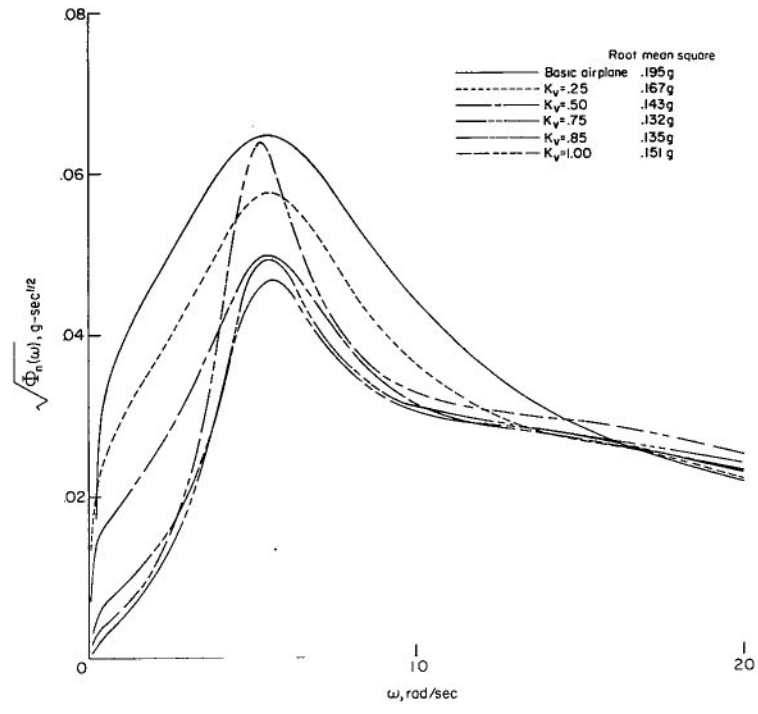

(a) Normal acceleration.

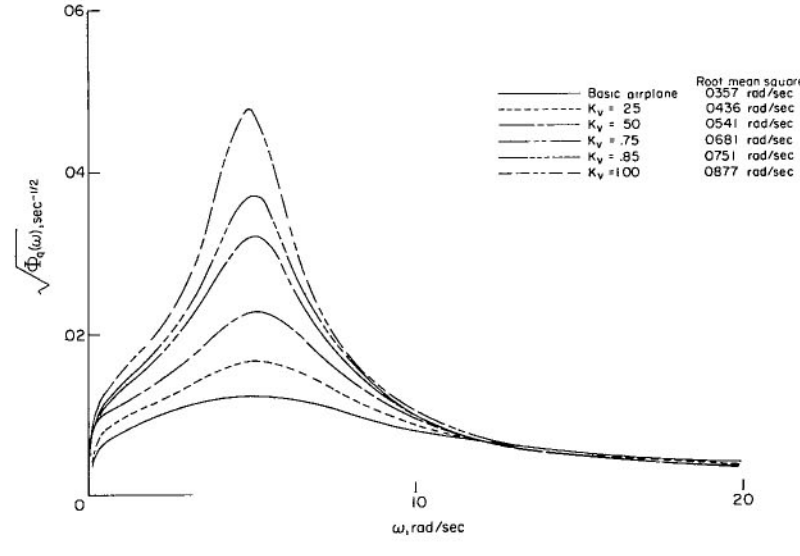

(b) Pitching rate.

Figure 22.- Power spectra of normal acceleration and pitch rate for different static vertical alleviation factors.

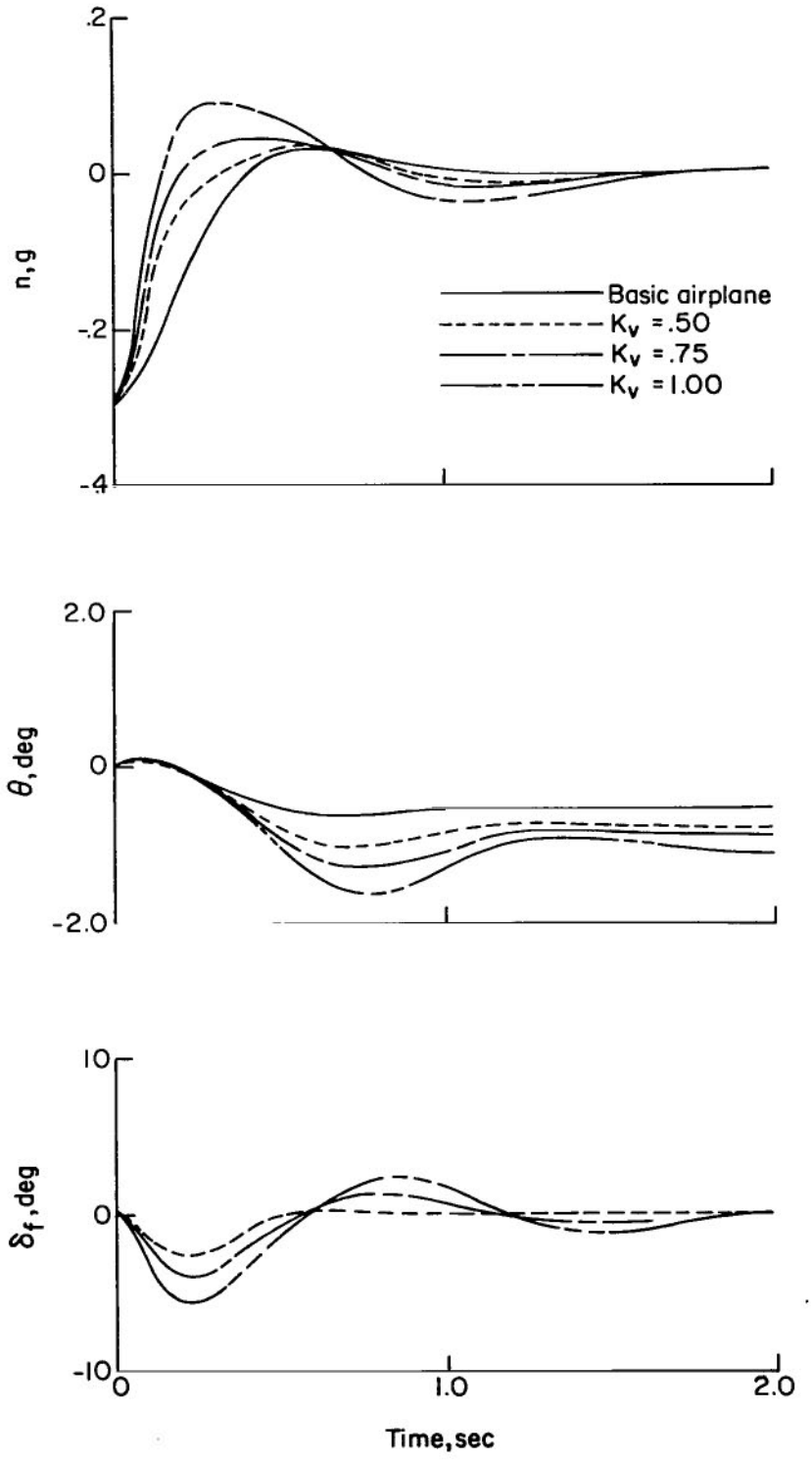

Figure 23.- Time-history responses to 1^{o} step gust inputs at time zero for different static vertical alleviation factors.

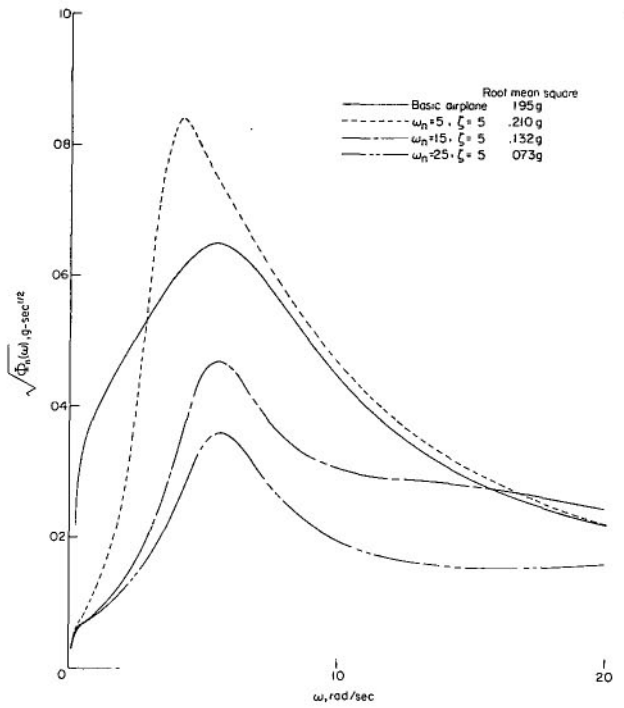

(a) Effect of flap natural frequency.

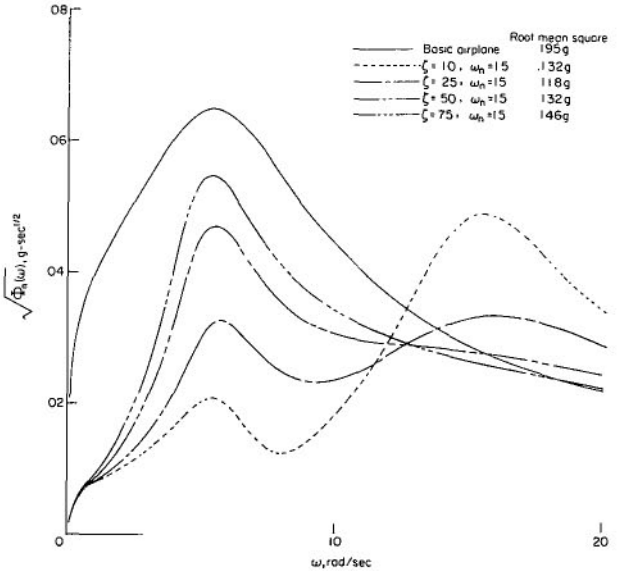

(b) Effect of flap damping ratio.

Figure 24.- Normal acceleration power spectra for different flap-vane natural frequencies and damping ratios.

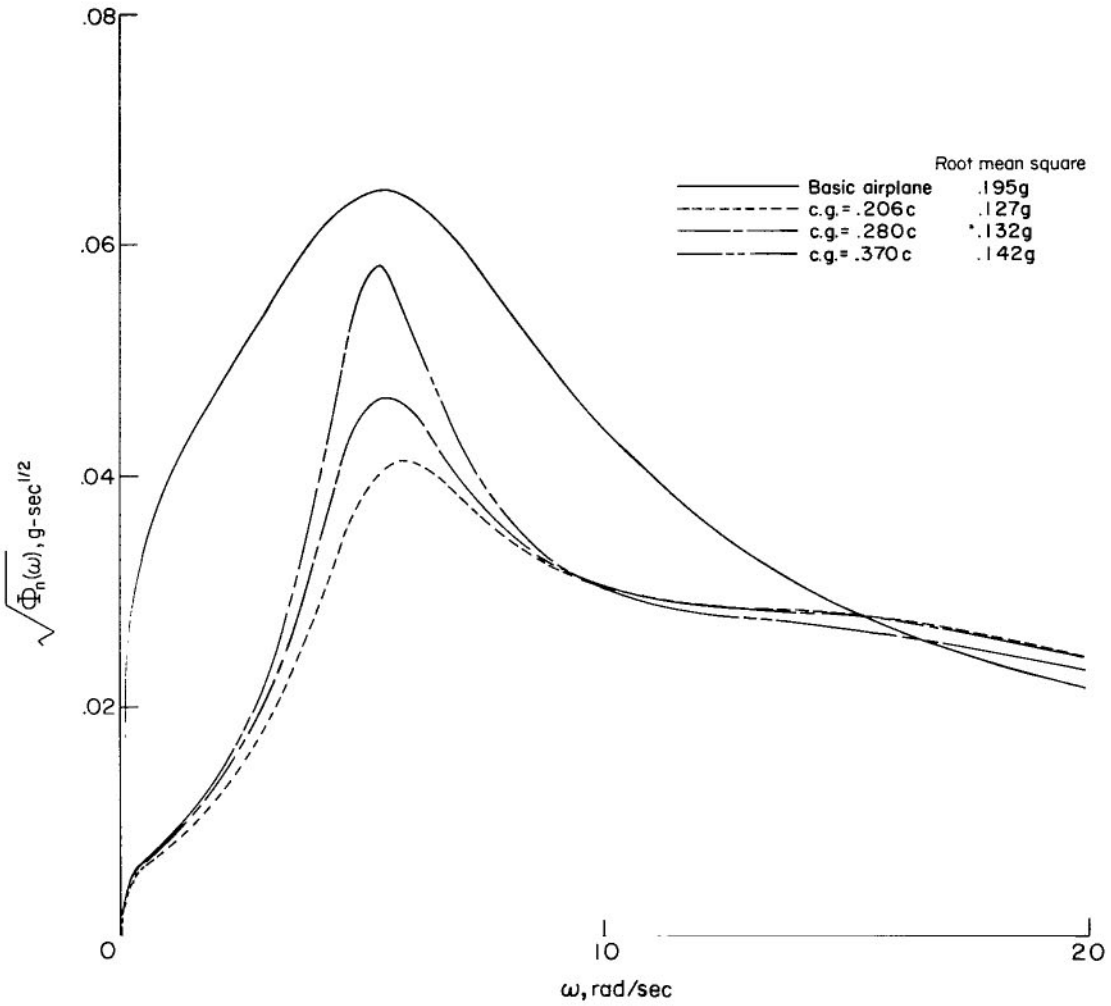

Figure 25.- Normal acceleration power spectra for different center-of-gravity (c.g.) locations with $K_V = 0.75$.

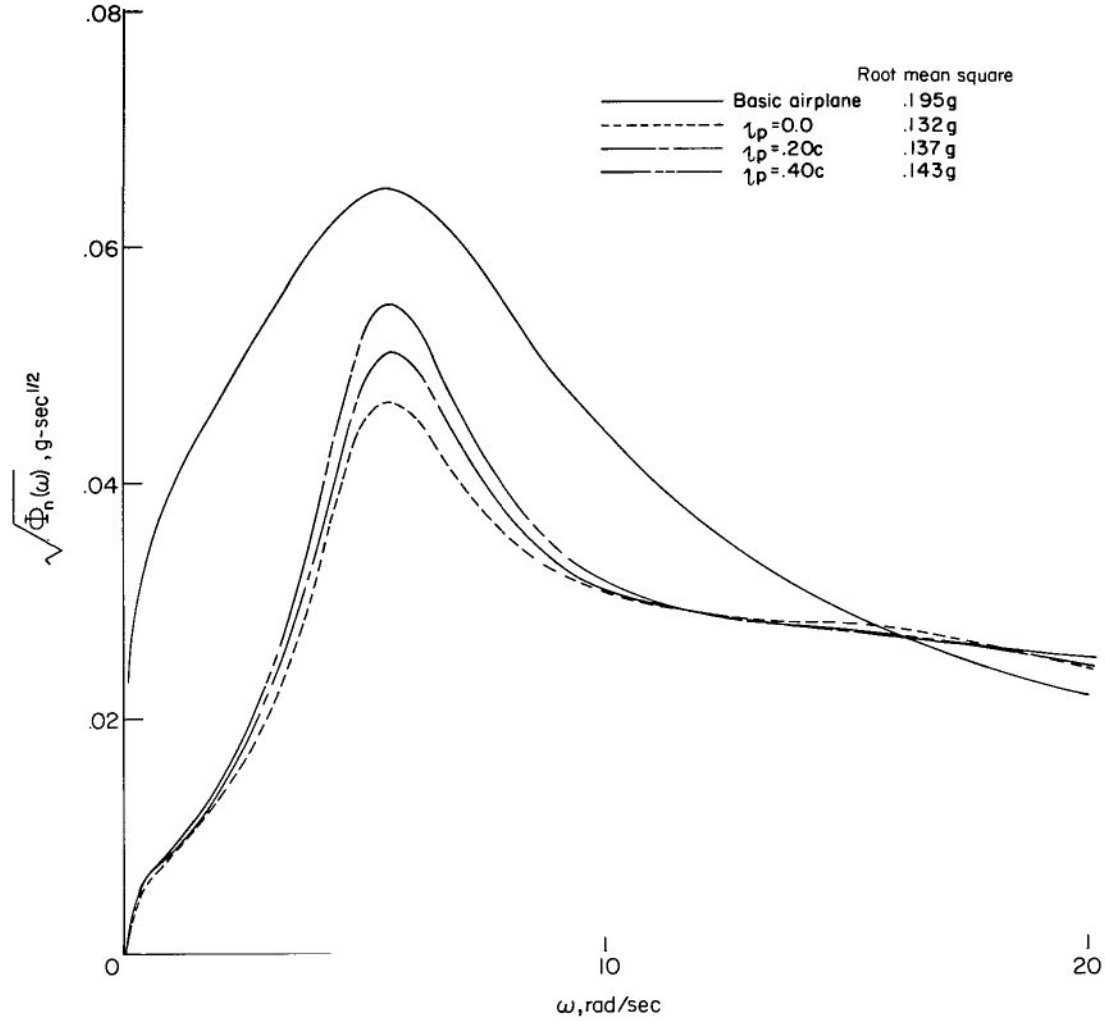

Figure 26.- Normal acceleration power spectra for different passenger locations with respect to center of gravity.

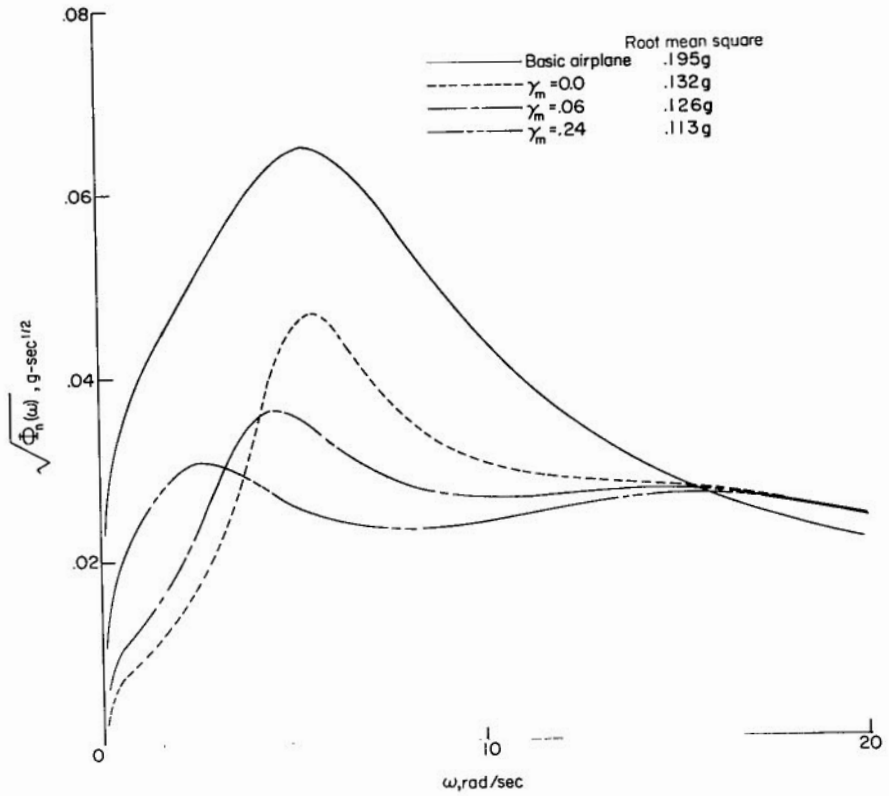

(a) Normal acceleration.

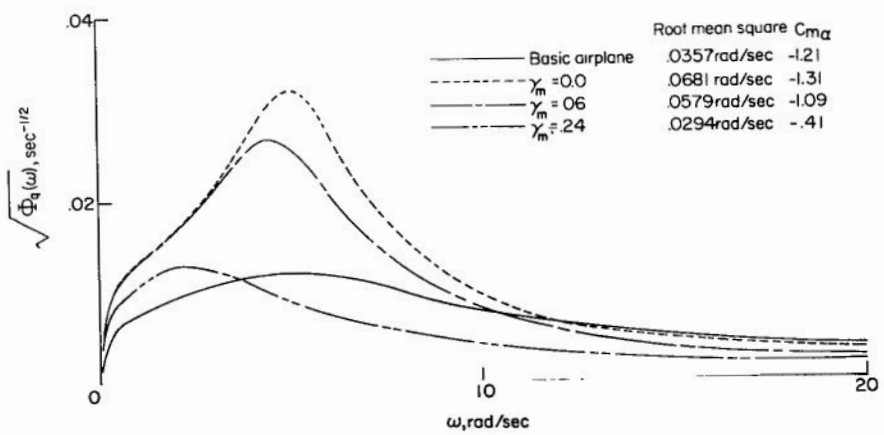

(b) Pitching rate.

Figure 27.- Power spectra for different gains of flap-elevator interconnect.

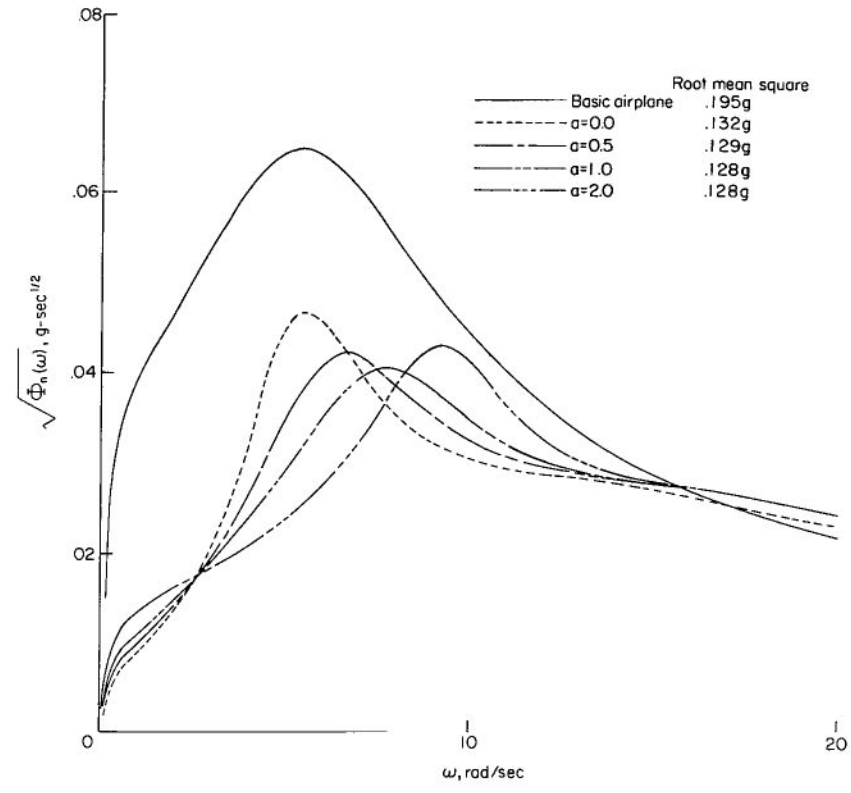

(a) Normal acceleration.

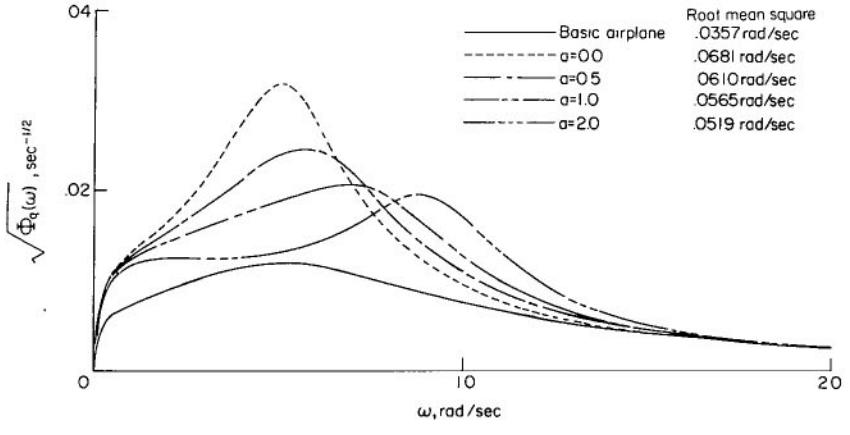

(b) Pitching rate.

Figure 28.- Power spectra for different gains of pitch-rate damper systems with a pitch damper natural frequency of 10 rad/sec.

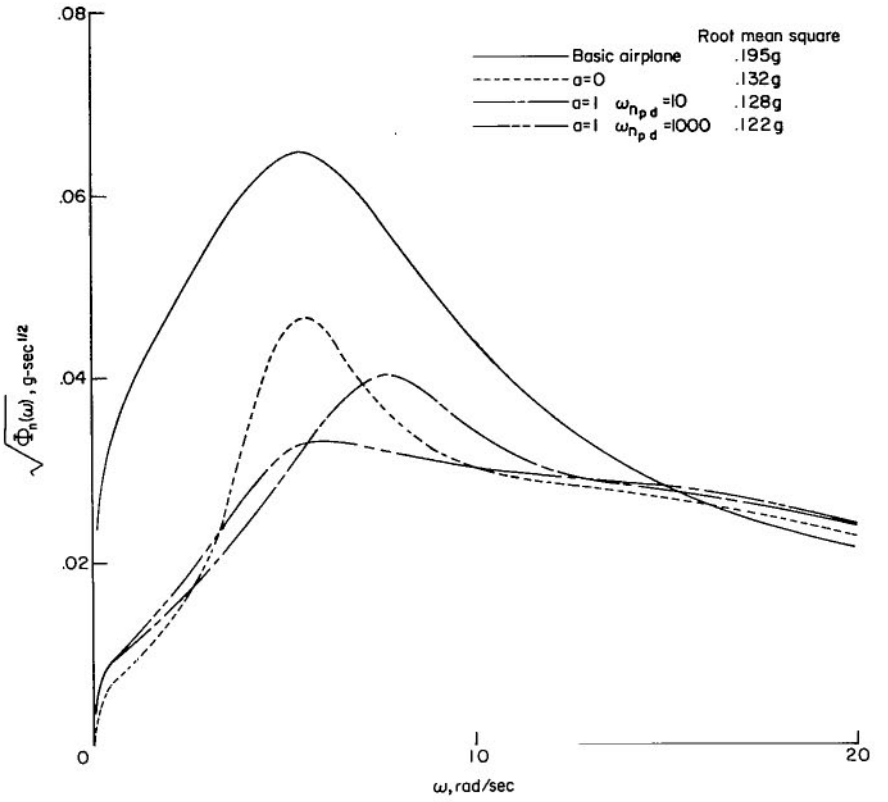

(a) Normal acceleration.

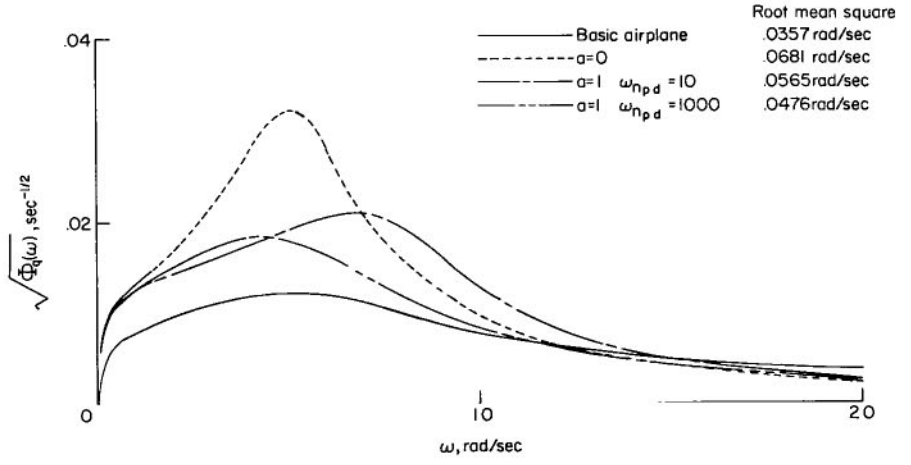

(b) Pitching rate.

Figure 29.- Power spectra for different natural frequencies of pitch-rate damper system with a pitch damper gain a equal to 1.0.

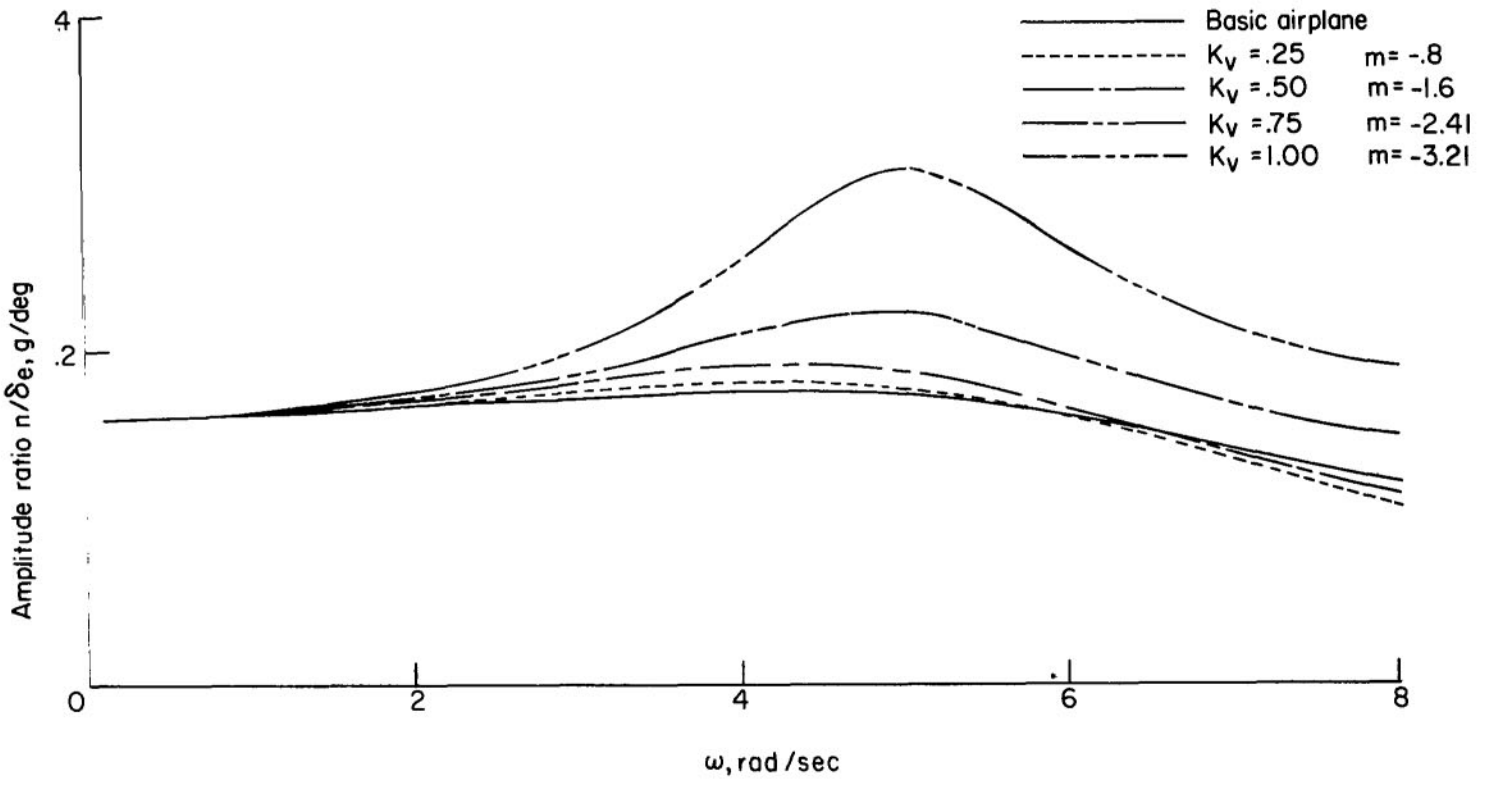

Figure 30.- Normal acceleration frequency response for different levels of static vertical alleviation factor with an elevator forcing function.

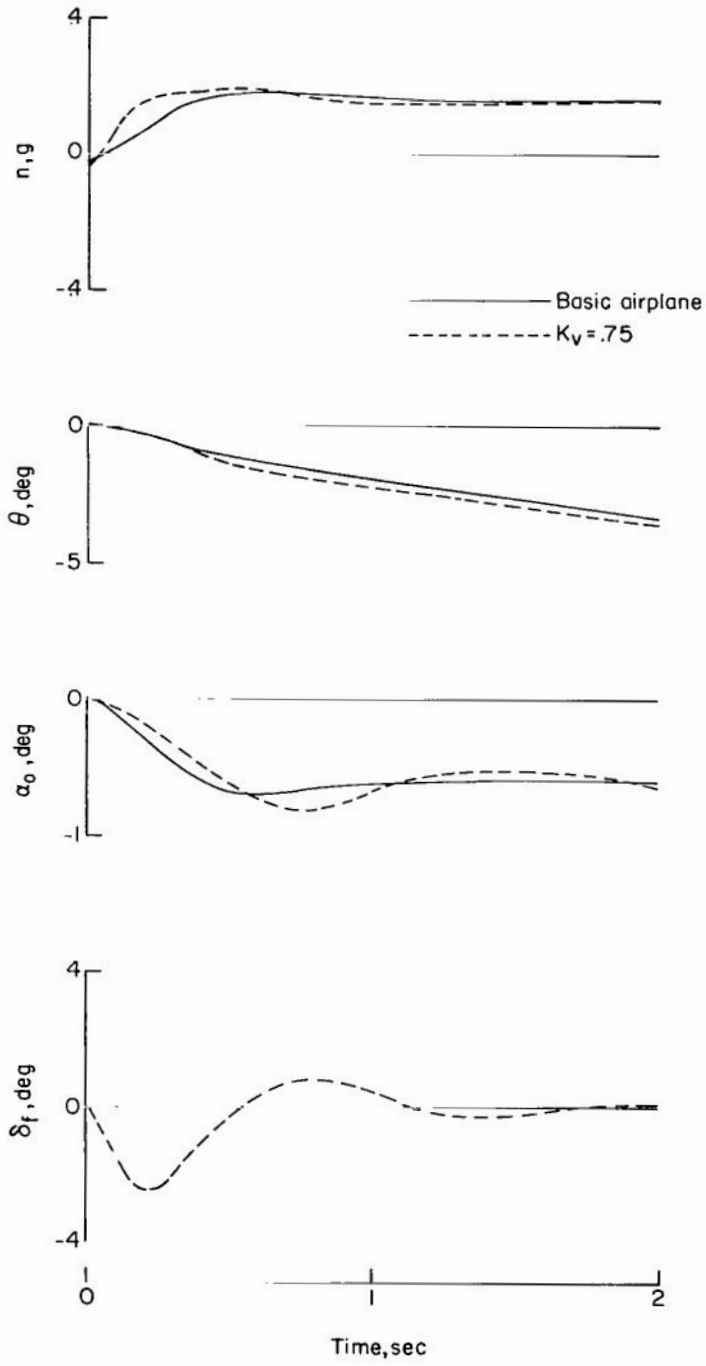

Figure 31.- Initial time history response to 1^o step elevator inputs at time zero (velocity assumed constant).

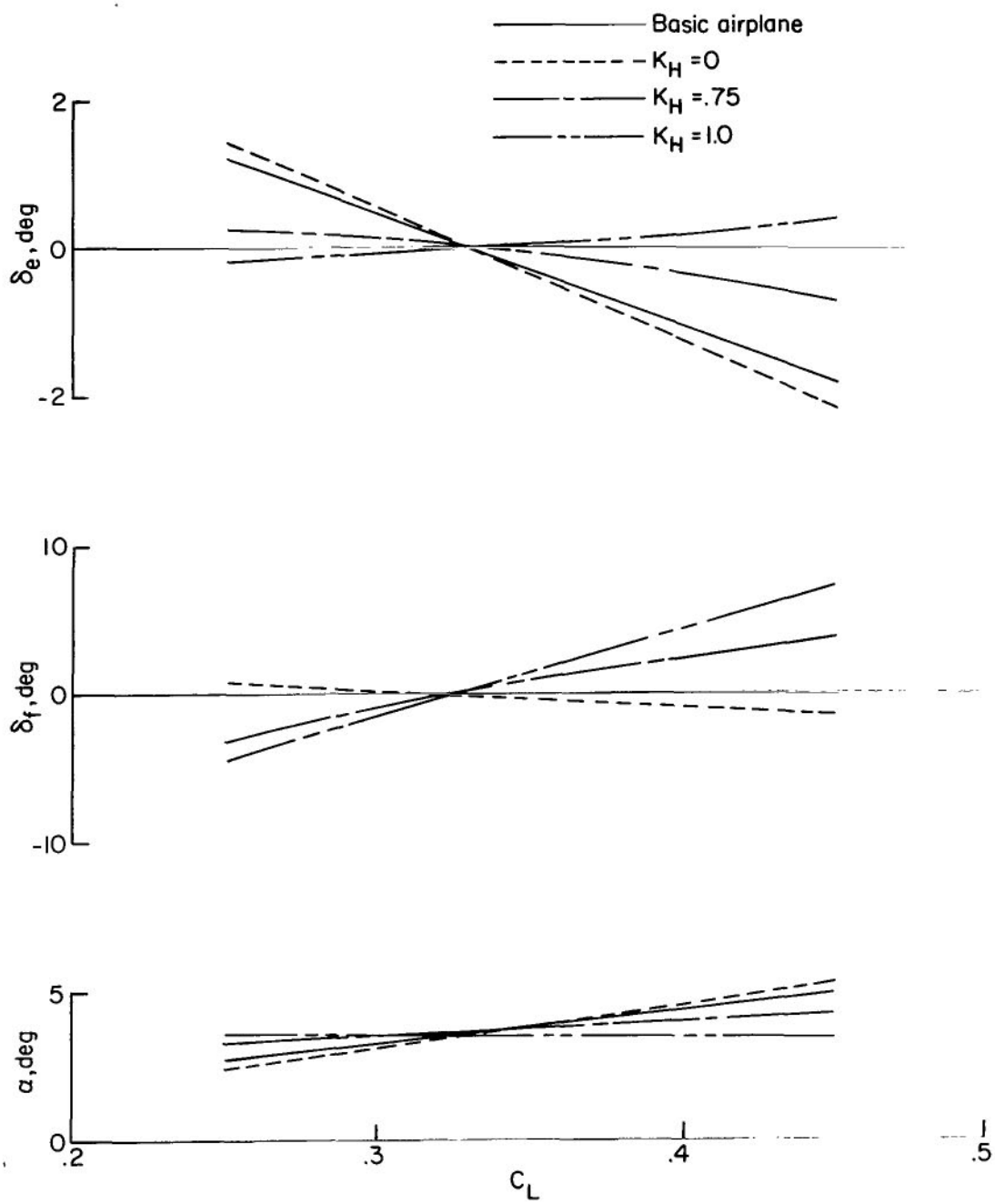

Figure 32.- Trimmed values of elevator, flap, and angle of attack for different levels of static horizontal alleviation factor K_H with $K_V = 0.75$ and $m' = 0.616$.

NATIONAL AERONAUTICS AND SPACE ADMINISTRATION
WASHINGTON, D.C. 20546

OFFICIAL BUSINESS
PENALTY FOR PRIVATE USE $300

SPECIAL FOURTH-CLASS RATE BOOK

POSTAGE AND FEES PAID
NATIONAL AERONAUTICS AND SPACE ADMINISTRATION
451

U.S.MAIL

630 001 C1 U A 760709 S00903DS
DEPT OF THE AIR FORCE
AF WEAPONS LABORATORY
ATTN: TECHNICAL LIBRARY (SUL)
KIRTLAND AFB NM 87117

POSTMASTER: If Undeliverable (Section 158 Postal Manual) Do Not Return

"The aeronautical and space activities of the United States shall be conducted so as to contribute . . . to the expansion of human knowledge of phenomena in the atmosphere and space. The Administration shall provide for the widest practicable and appropriate dissemination of information concerning its activities and the results thereof."

—NATIONAL AERONAUTICS AND SPACE ACT OF 1958

NASA SCIENTIFIC AND TECHNICAL PUBLICATIONS

TECHNICAL REPORTS: Scientific and technical information considered important, complete, and a lasting contribution to existing knowledge.

TECHNICAL NOTES: Information less broad in scope but nevertheless of importance as a contribution to existing knowledge.

TECHNICAL MEMORANDUMS: Information receiving limited distribution because of preliminary data, security classification, or other reasons. Also includes conference proceedings with either limited or unlimited distribution.

CONTRACTOR REPORTS: Scientific and technical information generated under a NASA contract or grant and considered an important contribution to existing knowledge.

TECHNICAL TRANSLATIONS: Information published in a foreign language considered to merit NASA distribution in English.

SPECIAL PUBLICATIONS: Information derived from or of value to NASA activities. Publications include final reports of major projects, monographs, data compilations, handbooks, sourcebooks, and special bibliographies.

TECHNOLOGY UTILIZATION PUBLICATIONS: Information on technology used by NASA that may be of particular interest in commercial and other non-aerospace applications. Publications include Tech Briefs, Technology Utilization Reports and Technology Surveys.

Details on the availability of these publications may be obtained from:

SCIENTIFIC AND TECHNICAL INFORMATION OFFICE

NATIONAL AERONAUTICS AND SPACE ADMINISTRATION

Washington, D.C. 20546